Elyse M Sullivan
Elyse.Sullivan@gmail.com

Degree and Date to be Conferred: PhD., 2014

Education
Miami University, B.S., 2007
Major: Zoology
University of Maryland, Baltimore, Ph.D., 2014
Program in Neuroscience

Professional Publications

1. Sullivan EM, Timi P, Hong LE, O'Donnell P. Reverse translation of clinical electrophysiological biomarkers in behaving rodents under acute and chronic NMDA receptor antagonism. *Neuropsychopharmacology* 2014 (E-pub ahead of print)
2. J.H Cabungcal , D.S Counotte , E.M Lewis, H.A Tejeda, P Piantadosi, E. M Sullivan,G.C Calhoon, E. Presgraves, M. Cuenod, K.Q Do, P. O'Donnell. Juvenile antioxidant treatment prevents adult deficits in a developmental model of schizophrenia. *Neuron* 2013 Sep 3;83(5):1073-84
3. Sullivan EM, O'Donnell P. Inhibitory interneurons, oxidative stress and schizophrenia. *Schizophrenia Bulletin* 2012 May; 38(3):373-6
4. Rademacher DJ, Rosenkranz JA, Morshedi MM, Sullivan EM, Meredith GE. Amphetamine-associated contextual learning is accompanied by structural and functional plasticity in the basolateral amygdala. *J Neurosci.* 2010 Mar 31;30(13):4676-86
5. Rademacher DJ, Sullivan EM, Figge DA. The effects of infusions of CART 55-102 into the basolateral amygdala on amphetamine-induced conditioned place preference in rats. *Psychopharmacology* (Berl). 2010 Feb;208(3):499-509

Honors/Awards

- Junior Investigator Poster Award 1st place winner, 2014 Winter Conference on Brain Research
- Early Career Policy Fellowship, Society for Neuroscience, 2013-1014
- Science Communications Internship, Office of Public Affairs (University of Maryland School of Medicine), 2013
- Program in Neuroscience Training Grant (University of Maryland School of Medicine), 2010-2011
- Summer Surgery Internship, Department of Cardiothoracic Surgery (University of Cincinnati Medical School), 2006
- Miami Medical Education Development Honorary Organization (Miami University), 2005-2007

Institutional Service

- Founder & President, Neuroscience Outreach & Volunteer Association, 2013-present
- Student Recruitment Committee, Graduate Program in Life Sciences, 2013
- Student Chair, Program in Neuroscience Annual Retreat Committee, 2012-present
- Program in Neuroscience Student Representative, Graduate Program in Life Sciences Awards, 2012
- Member, Student Training Committee, 2010-present
- Peer Mentor, Graduate Program in Life Sciences Peer Mentoring Program, 2010-present

Local & National Service

- Member of Organizing Committee, Baltimore Chapter of the Society for Neuroscience, 2013-2014
- Petition drive with the Cure Alliance for Mental Illness, 2013-2014
- Ad Hoc Reviewer, *Biological Psychiatry,* 2013
- Facilities Committee Member, Winter Conference on Brain Research, 2013
- Ad Hoc Reviewer, *Schizophrenia Bulletin,* 2011

Teaching Service

- Teaching Assistant, Proseminar in Experimental Design, 2014
- Research Supervisor and Mentor for an undergraduate student, 2012-2014

Professional Society Memberships

- Schizophrenia International Research Society, 2011-present
- Society for Neuroscience, 2008-present

Abstract:

Title of Dissertation: Neurophysiological Effects of NMDA Receptor Antagonism in Adolescence vs. Adulthood: EEG as a Translational Tool to Study Schizophrenia

Elyse M Sullivan, Doctor of Philosophy, 2014

Dissertation Directed by: Patricio O'Donnell, Professor, Program in Neuroscience

Electroencephalogram (EEG) stands out as a highly translational tool for psychiatric research, yet rodent and human EEG are not typically obtained in the same way. The first goal of this study was to develop a tool to record skull EEG in awake behaving rats in a similar manner to how human EEG are obtained. Using this novel rodent EEG technique, I tested whether acute NMDA receptor (NMDAR) antagonism replicates the effects of acute NMDAR-antagonism in humans, and found a strikingly similar shift in EEG oscillatory power from low to high frequencies in rodents, mimicking the effects reported in humans. After validating the translational potential of this approach, I paired EEG with local field recordings to investigate if a disruption to NMDAR signaling during a critical period of development caused long-lasting alterations in neural oscillations in adulthood. I found that rats exposed to an NMDAR-antagonist during adolescence, a critical period for the development of local and long-range synchrony in the brain, showed decreased gamma (30-50 Hz) synchrony between the medial prefrontal cortex (mPFC) and ventral hippocampus (HP) that was evident after NMDAR-antagonist re-exposure during adulthood. The same treatment given to adult rats did not produce this disruption to long-range synchrony, suggesting that adolescent disruption of NMDA signaling may have more robust long-term effects than a similar adult disruption. Interestingly, we did not find alterations in local oscillatory activity in

these regions, suggesting that long-range synchrony may be more sensitive than local synchrony to blockade of NMDAR signaling during adolescence. Given that deficits in long-range coherence are seen in patients with schizophrenia, this manipulation in rodents may prove useful in understanding mechanisms behind this phenomenon. Overall, the experiments presented in this Dissertation provide support for the use of EEG as a cross-species translational tool to study schizophrenia across acute and developmental animal models.

Neurophysiological Effects of NMDA Receptor Antagonism in Adolescence vs. Adulthood: EEG as a Translational Tool to Study Schizophrenia

By

Elyse M Sullivan

Dissertation submitted to the Faculty of the Graduate School of the
University of Maryland, Baltimore in partial fulfillment
Of the requirements for the degree of
Doctor of Philosophy
2014

Table of Contents

Chapter 1: General Introduction 1

A brief overview of schizophrenia 1

Schizophrenia as a disorder of dysconnectivity 2

Neural oscillations 4

NMDAR hypofunction in schizophrenia 6

Mechanisms of ketamine-induced psychosis: insights from animal work 7

Animal models of NMDAR hypofunction 9

Schizophrenia as a developmental disorder 10

Using EEG as a biomarker to study schizophrenia 12

Overall goals of research project & hypothesis 13

Chapter 2: Reverse Translation of Clinical Electrophysiological Biomarkers in Behaving Rodents under Acute and Chronic NMDA Receptor Antagonism 16

Introduction 16

Methods and Materials 18

Animals & Surgery 18

Recordings in behaving rats 20

Acute and chronic drug treatment 21

Signal processing and analysis 21

Statistical methods 23

Results 24

Oscillatory responses to auditory stimuli with acute NMDA receptor antagonism 24

Oscillatory responses to auditory stimuli with acute GABA-A receptor blockade 26

Oscillatory responses to auditory stimuli with chronic NMDA receptor antagonism 27

Gating of skull-recorded averaged evoked potentials (AEP) 29

Mismatch Negativity (MMN) 31

Discussion 32

Chapter 3. NMDA and GABA Receptor Antagonism on Auditory Steady-State Synchronization in Awake Behaving Rats 39

Introduction 39

Methods and Materials 41

Animals & Surgery 41

Recordings in behaving rats 42

Acute and chronic drug treatment 43

Signal processing 43

Statistical methods 44

Results 45

LFP intertrial coherence during auditory steady state response in A1. 45

Oscillatory power during Auditory Steady State Response in A1 46

Intertrial Coherence during Auditory Steady State Response across Recording Sites 47

Discussion 48

Chapter 4: Subchronic NMDAR-antagonist exposure in adolescence produces impaired medial prefrontal - hippocampal synchrony in adult rats 53

Introduction 53

Methods and Materials 55

Animals & drug treatment 55

Electrode implanting surgery 55

Recordings in behaving rats 56

Signal processing and analysis 58

Statistical methods 59

Results 60

mPFC-HP phase synchrony in response to auditory stimuli in adolescent-treated group: 60

mPFC-HP phase synchrony in response to auditory stimuli in adult-treated group: 62

Oscillatory responses to auditory stimuli in adolescent-treated group: 64

Oscillatory responses to auditory stimuli in adult-treated group: 67

Discussion 69

Chapter 5: General Discussion 75

Overall Summary 75

Cross-species translation of EEG 76

A. Skull-EEG Oscillatory responses 78

B. Gating of Auditory evoked potentials. 80

C. Mismatch Negativity 82

GABAergic interneuron dysfunction in schizophrenia 85

A. GABAergic interneurons and gamma oscillations: Insights from NMDAR-antagonism 86

Acute vs. chronic NMDAR-antagonist administration: Relevance to schizophrenia 89

Developmental timing of NMDAR-antagonism 91

Abnormal neural synchrony and cognitive impairments in schizophrenia 92

Overall conclusions 96

Appendix I: Juvenile antioxidant treatment prevents adult deficits in a developmental model of schizophrenia 98

Introduction 99

Results 101

Discussion 111

Experimental Procedures 116

Animals 116

Neonatal ventral hippocampal lesion surgery 116

Antioxidant pretreatment regimen 117

Immunohistochemistry 118

Slice electrophysiology 121
In Vivo intracellular recordings 123
Mismatch Negativity 124
Prepulse inhibition 125
Statistics 126
References 127

List of Figures:

Figure 1. Electrode placement diagram 19

Figure 2. Acute effect of MK-801 on sound-evoked oscillations in awake, unrestrained rats 25

Figure 3. Acute effect of picrotoxin on tone-evoked oscillations in freely moving rats . 27

Figure 4. Chronic effect of MK-801 or PTX on tone-evoked oscillations in freely moving rats 19

Figure 5. Gating of average evoked potentials in response to paired sounds 30

Figure 6. Mismatch Negativity during an auditory oddball paradigm 31

Figure 7. Effect of acute and chronic MK-801 and PTX on A1 cortex intertrial coherence during ASSR 46

Figure 8. Comparison of intertrial coherence recorded from primary auditory (A1) cortex, hippocampus (HP) and skull EEG 48

Figure 9. Schematic of experiment 57

Figure 10. Phase coherence between medial prefrontal cortex (mPFC) and hippocampus (HP) in adult rats treated during adolescence with either MK-801 or vehicle 62

Figure 11. Phase coherence between medial prefrontal cortex (mPFC) and hippocampus (HP) in adult rats treated during adulthood with either MK-801 or vehicle 63

Figure 12. Oscillatory activity in adult rats treated with MK-801 or vehicle during adolescence at baseline *(left)* and after MK-801 challenge *(right)* 66

Figure 13. Oscillatory activity in adult rats treated with MK-801 or vehicle in adulthood at baseline *(left)* and after MK-801 challenge *(right)* 68

Figure 14. Comparison of Auditory evoked oscillations in rodents (left) and humans (right) under acute NMDAR-antagonism 79

Figure 15. A NVHL blocks the adolescent increase in PV interneuron labeling in the PFC 102

Figure 16. Oxidative stress shown with 8-oxo-dG in the PFC of NVHL rats 103

Figure 17. Oxidative stress in the PFC of adult NVHL rats shown with 3-NT 104

Figure 18. The NVHL causes increased oxidative stress in PV, but not CR and CB interneurons, which is prevented by developmental NAC treatment 105

Figure 19. Perineuronal nets (PNN) are reduced in the PFC of adult NVHL rats, but rescued by juvenile NAC treatment 106

Figure 20. Electrophysiological deficits are rescued by NAC treatment in NVHL rats. 108
Figure 21. Mismatch negativity (MMN) deficits are rescued by NAC treatment 109

Chapter 1: General Introduction

A brief overview of schizophrenia

Schizophrenia is a devastating psychiatric disease with prevalence around 0.5-1% worldwide (Centers for Disease Control and Prevention, 2014). The diagnosis of schizophrenia relies on the presentation of an array of clinical symptoms that are classified into 3 types of symptom clusters: positive symptoms (delusions, hallucinations, disordered thoughts), negative symptoms (anhedonia, blunted affect, social withdrawal) and cognitive symptoms (working memory and executive function deficits) (Tamminga and Holcomb, 2005). Vulnerability for schizophrenia undoubtedly has a genetic component. The incidence of schizophrenia increases to 6-17% in first-degree relatives, and is nearly 50% in monozygotic twins (Tsuang, 2000). While schizophrenia has been shown to have a genetic component, no single gene has been strongly linked to the disorder, in fact it appears that a large number of genes may contribute to vulnerability (Schizophrenia Working Group of the Psychiatric Genomics Consortium, 2014). Rather, schizophrenia is thought to involve genetic, environmental and developmental factors (Lewis and Lieberman, 2000). Maternal infection during gestation, exposure to toxins or drugs and psychosocial stress (Jones and Cannon, 1998) have all been implicated in the development of schizophrenia along with altered maturational processes such as synaptic pruning (Feinberg, 1982) and myelination (Kochunov and Hong, 2014) during adolescence. Thus, the etiology of schizophrenia is viewed by many to be the result of multiple insults or “hits” whereby an environmental insult experienced during a critical period of development may unmask an underlying genetic vulnerability.

There are a slew of antipsychotic medications that are effective in many patients at reducing positive symptoms, and their efficacy is strongly correlated with D2 antagonism (Stone et al., 2009), although these antipsychotic medications are often coincident with many unwanted side effects such as metabolic effects (Mizuno et al., 2014) that reduce the adherence to these drugs. Additionally, many negative and cognitive symptoms are left untreated by antipsychotics (Heinrichs and Zakzanis, 1998). Furthermore, cognitive symptoms are strongly correlated with functional outcomes of patients, with measures of verbal memory and vigilance showing the strongest associations with "real-world" skills like social problem solving (Green, 1996; Green et al., 2000). Atypical or second generation antipsychotics were originally thought to be more efficacious at treating negative and cognitive symptoms than the first generation medications, however recent studies have indicated that second-generation drugs may not have superior efficacy (Tandon, 2011). Thus, despite the need for better treatment options for schizophrenia, there has been little progress made on pharmacological interventions in recent years. Furthering our understanding of the pathophysiology of the disorder is likely to result in the creation of novel therapeutic approaches in the future.

Schizophrenia as a disorder of dysconnectivity

Schizophrenia has been hypothesized to be a disorder of altered connectivity and coordination across a distributed neural network (Friston, 1998; Phillips and Silverstein, 2003; Stephan et al., 2006; Uhlhaas and Singer, 2010). Evidence for this comes from studies showing disruptions in white matter integrity (Lim et al., 1999; Burns et al., 2003; Kubicki et al., 2003; Ashtari et al., 2007b; Rotarska-Jagiela et al., 2008) and impaired neural synchrony both within and between brain regions (Kwon et al., 1999; Cho et al., 2006; Uhlhaas et al., 2006; Spencer et al., 2008; Rutter et al., 2009; Barr et al., 2010; Hong et al., 2011; Mulert et al., 2011). A well-replicated finding in schizophrenia patients using EEG is impaired auditory steady state response (ASSR) to rhythmically presented auditory stimuli. Interestingly, ASSR deficits in patients with schizophrenia are confined to the 40 Hz frequency range (Kwon et al., 1999; Brenner et al., 2003; Light et al., 2006; Spencer et al., 2009), suggesting that patients may have a specific impairment in generating and sustaining local oscillatory activity within the auditory cortex in the gamma frequency range. Although much focus recently in the literature has been on high-frequency gamma band impairments in schizophrenia, there is also considerable evidence for altered activity in low frequency bands (Moran and Hong, 2011). Increased low-frequency theta and delta power is one of the more consistent observations in schizophrenia EEG studies, and has been shown to occur in unmediated, first episode, and chronic patients (Sponheim et al., 1994; Hong et al., 2011). Additionally, it is known that high and low frequency oscillations can influence each other. For example, the amplitude of gamma oscillations can be modulated by the phase of theta-band oscillations (Canolty et al., 2006), suggesting a link between high and low frequency abnormalities in schizophrenia.

Schizophrenia patients also show impaired long-range synchronization between distant brain areas (Spencer et al., 2004; Symond et al., 2005). A study by Uhlhaas et al., found a reduction in fronto-temporal phase synchrony, specifically in the beta-band, during Gestalt perception in schizophrenia patients (Uhlhaas et al., 2006). Importantly, this study found that poor performance on the perceptual task was correlated with reduced phase synchrony, suggesting that impaired long-range synchrony may be causally related to cognitive or perceptual deficits in schizophrenia patients. Consistent with evidence of impairments in neural synchrony, there is substantial evidence of reduced white matter integrity in patients with schizophrenia. Using diffusion tensor imaging (DTI), studies have found reduced integrity of white matter tracts in many regions including the prefrontal, occipital and parietal cortices, and in the corpus collosum (Buchsbaum et al., 1998; Lim et al., 1999; Agartz et al., 2001). Proper myelination of long axonal tracts within the nervous system are essential for temporally precise communication, and reduced white matter integrity is likely to impair the timing and synchrony of long range connections (Lim et al., 1999). Indeed, white matter maturation is associated with increased cognitive abilities (Nagy et al., 2004), while poorer performance is associated with less white matter maturation (Bava et al., 2010). Although there is substantial evidence for the dysconnection hypothesis in schizophrenia, the cause of this altered neural communication is still unknown.

Neural oscillations

Information processing in the brain is thought to occur via the coordinated firing of distinct neuronal populations (Buzsáki, 2006). This coordinated activity within a large group of cells is referred to as an oscillation, and can be recorded non-invasively from the surface of the scalp using an electroencephalogram (EEG), or from extracellular electrodes within the brain itself, called a local field potential (LFP). Neural oscillations facilitate communication and interaction within and across brain regions, and in turn may be especially important in situations where it is necessary to integrate different pieces of information, such as during working memory and cognition (Uhlhaas and Singer, 2006). Fast synaptic inhibition mediated by GABAergic neurons is thought to be particularly efficient at generating synchronous firing of pyramidal neurons, and in turn at regulating network oscillatory activity. GABAergic interneurons are uniquely positioned to regulate large-scale pyramidal cell activity due to the fact that each GABA neuron can innervate numerous pyramidal cells (Gonzalez-Burgos and Lewis, 2008). Different subtypes of GABAergic interneurons are thought to regulate network oscillations at different frequencies (Tukker et al., 2007), but the exact contribution of these subtypes is relatively unknown.

Post-mortem studies in schizophrenia patients have consistently showed reductions in an enzyme responsible for synthesizing GABA, glutamic acid decarboxylase (GAD67) (Akbarian et al., 1995), which is suggestive of impaired GABAergic transmission in the disorder. Interestingly, this reduction was found predominantly in parvalbumin (PV) expressing GABAergic interneurons (Hashimoto et al., 2003). PV-expressing interneurons (PV-IN) exhibit a fast-spiking electrophysiological profile and are ubiquitously expressed in the cortex, making up 25% of all GABA neurons in the primate cortex (Condé et al., 1994) and 50% in the rodent brain (Markram et al., 2004). In contrast to other subtypes of GABAergic neurons, PV-IN's synapse onto the axon-initial segment or cell body of pyramidal cells (Kawaguchi and Kubota, 1997), thus exerting a tight control over pyramidal cell output.

Accumulating evidence has suggested that PV-IN are responsible for generation of gamma-band network oscillations. Cardin et al., showed that optogenetic stimulation of PV-IN's in the cortex increased local field power specifically in the gamma-band range, but the same stimulation to pyramidal neurons did not produce this effect, demonstrating that PV-INs can be driven to induce gamma rhythms in vivo (Cardin et al., 2009). In another study, Sohal et al., found that selectively inhibiting PV-IN's *in vivo* suppressed gamma oscillations (Sohal et al., 2009). Taken together, these studies have elegantly demonstrated that PV-IN activation is necessary and sufficient to generate gamma-band oscillatory activity, which is strongly implicated as a mechanism for efficient information processing in the brain.

NMDAR hypofunction in schizophrenia

There have been numerous theories and hypotheses about the pathophysiology of schizophrenia, but one that has become increasingly popular is the NMDA receptor (NMDAR) hypofunction hypothesis. This hypothesis primarily comes from the fact that the drugs like ketamine or PCP, which are noncompetitive NMDAR-antagonists, induce a state that resembles schizophrenia in healthy volunteers, including altered perception, impaired working memory performance and disordered thought (Luby et al., 1959; Krystal et al., 1994; Malhotra et al., 1996). Furthermore, ketamine exacerbates psychotic and cognitive symptoms when given to schizophrenia patients (Lahti et al., 1995, 2001). These findings have prompted researchers to investigate the mechanism of action behind NMDAR-antagonists in order to elucidate underlying the neuropathology in schizophrenia patients.

Magnetic resonance spectroscopy (MRS) studies in humans given acute ketamine have shown increased glutamate levels in the anterior cingulate (Rowland et al., 2005b; Stone et al., 2012), suggesting that there is a hyperglutamatergic state associated with ketamine-induced schizophrenia-related symptoms. Additionally, ketamine has been shown to elevate global connectivity measured by functional magnetic resonance imaging at rest in healthy volunteers (Driesen et al., 2013a), which is consistent with a hyperexcitable circuit. Interestingly, it was found that subjects on ketamine while performing spatial working memory task had reduced connectivity in task-related structures, which correlated with reduced task accuracy (Driesen et al., 2013b). Acute ketamine also alters EEG oscillatory activity in healthy controls. Specifically, ketamine has been shown to produce a reduction in low-frequency cortical activity and a robust increase in high-frequency activity (Hong et al., 2010). Taken together, these findings indicate that acute ketamine produces a "noisy" cortex, where higher levels of background activity may make it harder to bring on line task-related processes.

Mechanisms of ketamine-induced psychosis: insights from animal work

Extensive studies in rodents have provided insight into the how NMDAR-antagonism could produce a hyperexcitable state and schizophrenia-related symptoms, however, the exact mechanisms are still debatable (Gonzalez-Burgos and Lewis, 2012). A seminal study conducted by Bita Moghaddam served to provide a possible mechanism for how blockade of excitatory receptors would produce a seemingly paradoxical increase in cortical excitability, not a decrease, as may be expected. Moghaddam and colleagues recorded neuronal firing of both excitatory pyramidal and putative GABAergic fast-spiking interneurons in awake-behaving rodents after acute MK-801 (a selective NMDAR-antagonist) administration. They found that the firing rate of putative GABA interneurons was decreased after MK-801, while the pyramidal cells had an increased firing rate (Homayoun and Moghaddam, 2007). Consistent with this data, sub anesthetic doses of ketamine in rats increased extracellular glutamate in the PFC as measured by in vivo microdialysis (Moghaddam et al., 1997). This suggested that NMDAR-antagonists may preferentially block GABAergic interneuron activity, which would then lead to a disinhibition of pyramidal cell firing and a hyperexcitable cortex.

Additional evidence supporting the idea the fast-spiking interneurons are the primary target of NMDAR-antagonists came from data showing that repeated NMDAR-antagonist administration decreases markers of GABAergic cell activity (Keilhoff et al., 2004; Behrens et al., 2007). Both *in vivo* and *in vitro* studies have shown that NMDAR-antagonists produce a long-lasting decrease in parvalbumin and decreases in GAD67. Importantly, similar reductions in PV and GAD67 have been seen in post-mortem studies of schizophrenia patients (Akbarian et al., 1995; Lewis et al., 2005).

Furthermore, many animal models of schizophrenia show impaired interneuron function and/or loss of PV labeling in cortical regions, providing a strong agreement with observations in human subjects. These models include the neonatal ventral hippocampal lesion (NVHL) (O'Donnell et al., 2002), gestational administration of the antimitotic drug methylazoxymethanol acetate (MAM) (Lodge et al., 2009), neonatal NMDA receptor antagonist administration (Wang et al., 2008; Amitai et al., 2012) neonatal immune challenge in the hippocampus (Feleder et al., 2010), and knocking down the DISC1 gene (Niwa et al., 2010). Several of these models also reproduce the adolescent onset of symptoms, which is a crucial aspect of the disorder to study. Although acute NMDAR-antagonism has validity in the sense that it reproduces positive, negative and cognitive symptoms, it does not model the developmental nature of schizophrenia, and little is known about whether NMDAR alterations during adolescence may play a role in symptom onset. Overall, data from schizophrenia patients and animal models suggest that cortical GABAergic function, specifically due to dysfunctional parvalbumin fast-spiking interneurons, may be involved in the pathophysiology of schizophrenia; however there are still many unanswered questions as to the cause of the interneuron dysfunction.

Animal models of NMDAR hypofunction

Given the evidence supporting NMDAR and GABAergic interneuron dysfunction in schizophrenia, many studies have examined behavioral and physiological effects of manipulating these circuits in rodents using pharmacological or genetic approaches. Acute NMDAR-antagonist administration has been consistently shown to increase gamma power using *in vivo* LFP and EEG recordings in awake-behaving rodents (Pinault, 2008; Ehrlichman et al., 2009a; Hakami et al., 2009; Lazarewicz et al., 2010). This phenomenon has been demonstrated in the cortex as well as several subcortical structures including the hippocampus, amygdala and the thalamus (Ma and Leung, 2007; Hakami et al., 2009). Behaviorally, acute NMDAR-antagonism has been shown to cause locomotor hyperactivity (Hakami et al., 2009) and deficits in prepulse inhibition (Mansbach and Geyer, 1989; Ma and Leung, 2007), which is a measure of sensorimotor gating that is known to be impaired in patients with schizophrenia. Additionally, studies have found cognitive impairments after acute NMDAR-antagonism such as decreased response accuracy in the five-choice serial reaction time test (Smith et al., 2011), a measure of attention and impulsivity, as well as impaired performance on the novel object reaction test (de Lima et al., 2005), an index of recognition memory. Criticisms of these behavioral findings in rodents using acute NMDAR-antagonism comes from the fact that these drugs are known to have significant motoric effects that have the ability to confound behavioral performance.

Utilization of repeated or chronic administration of NMDAR-antagonists and then testing the animal in a drug-free state provides an alternative approach to assessing the effects of NMDAR hypofunction. This approach has advantages in that it avoids the motoric confounds of acute drug administration, however due to the variability in the duration of chronic administration, dosing, and length of abstinence before testing, these studies have provided mixed results about cognitive and physiological effects of chronic NMDAR-antagonists (Gilmour et al., 2011). For example, after chronic NMDAR-antagonist exposure performance is disrupted on the 5-choice serial reaction time task (Amitai et al., 2007) and the Morris water maze (Didriksen et al., 2007), while it is preserved in the t-maze delayed alternation (Stefani and Moghaddam, 2002) and radial arm maze reference memory tasks (Li et al., 1997). Very few studies have examined electrophysiological effects after chronic NMDAR-antagonist paradigms, however, one study has shown a decrease in hippocampal gamma and theta oscillations several weeks after subchronic ketamine exposure (Kittelberger et al., 2012), suggesting that electrophysiological effects may be long-lasting. Overall, chronic or subchronic NMDAR-antagonist regimens have some advantages over the acute models and do show impaired cognitive performance, however reproducibility between studies remains low.

Schizophrenia as a developmental disorder

An important factor in schizophrenia is the characteristic timing of disease onset, which occurs in late adolescence and early adulthood (Häfner et al., 1993), suggesting a strong developmental component to the disease. During this transition from adolescence to adulthood the brain is undergoing significant reorganization and maturation, and thus it has been hypothesized that disturbances in brain maturation at this time are involved in the pathophysiology of schizophrenia (Weinberger, 1987; Uhlhaas and Singer, 2011). Anatomically, the brain is undergoing synaptic pruning (Huttenlocher, 1979; Hoffman and Dobscha, 1989), progressive reductions in gray matter (Gogtay et al., 2004), and increases in myelination (Ashtari et al., 2007a) until early adulthood, which sparked the hypothesis that schizophrenia is caused by aberrant synaptic pruning in development (Feinberg, 1982). Cortical excitation-inhibition balance is also in flux at this time evidenced by changes in NMDA receptor expression (Wang and Gao, 2009) and GABA-A receptor subunit composition (Hashimoto et al., 2009). Additionally, the modulatory effects of dopamine on GABAergic interneurons exhibit a dramatic change from adolescence to adulthood, when dopamine D2 agonists switch from being mildly inhibitory to increasing firing in fast-spiking interneurons (Tseng and O'Donnell, 2007a). Overall, this anatomical and functional maturation during adolescence yields a circuit with more precise temporal synchrony and the capability to support more complex cognitive processes.

Adolescence is also marked by the maturation of neural oscillations and long-range synchrony during sensory processing and cognitive tasks. Auditory steady state responses (ASSR) to 40 Hz stimulation was shown to increase throughout childhood and adolescence reaching a plateau in adulthood (Rojas et al., 2006). Additionally, oscillatory phase synchrony in the beta and gamma-bands induced by perception of Mooney faces was shown to increase during childhood until age 14, undergo a reduction throughout late adolescence, and then rise sharply between the ages of 18 and 21 years (Uhlhaas et al., 2009), which is suggestive of extensive network reorganization during this time. Interestingly, increased phase synchrony was correlated with improved reaction time and detection rates on the perceptual task (Uhlhaas et al., 2009). Taken together, this data suggests that cortical networks exhibit increased high-frequency oscillations along with enhanced long-range synchrony during the transition from adolescence to adulthood, which enables more precise temporal coding and communication necessary to support complex cognitive processes.

Given that adolescence is a critical period for normal development, it has been hypothesized that environmental insults during this time could be particularly deleterious. Indeed, studies in rodents utilizing adolescent exposure to NMDAR-antagonists (Thomases et al., 2013) or THC (Raver et al., 2013) found long-lasting electrophysiological deficits once the animals reached adulthood. Importantly, MK-801 and THC exposure in adult animals did not show these effects, highlighting the importance of the disruption during this critical period of development. As full-blown schizophrenia emerges during this transition from adolescence to adulthood, it is possible that symptom onset is driven by factors that affect periadolescent development.

Using EEG as a biomarker to study schizophrenia

A significant hurdle to progress in psychiatric disease research lies in the fact that these disorders are difficult to model in animals. It is unknown if naturally occurring homologues of these disorders occur in non-human species, and due to the difficulty of detecting many of the hallmark symptoms of psychotic diseases such as hallucinations or disordered thought, animal models of schizophrenia cannot recapitulate the full spectrum of symptoms. In order to work around this issue, the field has begun to separate the disorder into different symptom clusters or phenotypes that themselves are more readily modeled in rodents. Neurophysiological phenotypes such as altered EEG signals represent an attractive phenotype for studying schizophrenia pathophysiology and have recently received increased attention in the literature (Luck et al., 2010; Gandal et al., 2011). EEG recordings are relatively inexpensive, non-invasive and quick procedures that make them well suited to use in large screening studies. Additionally, EEG characteristics have the potential to be able to define a subgroup of patients within schizophrenia who may respond better to a certain type of treatment. For example, the amplitude of EEG response during a auditory odd-ball task (called mismatch negativity) predicts the patient's response to the antipsychotic clozapine (Schall et al., 1999). Furthermore, some EEG measures have a strong component of heritability (Hong et al., 2008b), making them useful for assessing candidate genes implicated in schizophrenia. Another important feature of EEG is that it has the potential to be recorded in humans and in animals in a very similar manner, allowing for cross-species translational approaches. For instance if an EEG or ERP abnormality characteristic of schizophrenia could be induced in a rodent model, this model could then be used as an assay for the effectiveness of potential therapeutic compounds. Homologues of several EEG and ERP measures have already been demonstrated in rodents and non-human primates, such as P50 sensory gating (Swerdlow et al., 2006) and mismatch negativity (Javitt et al., 1996), using LFPs or electrocorticograms (EcoG) as a proxy for EEG recordings in humans. However, due to the methodological differences in the acquisition, the translatability of these neural signals to that of scalp-recorded EEG's in humans remains questionable.

Overall goals of research project & hypothesis

Given the potential utility of using EEG as a cross-species translational tool to study the pathophysiology of schizophrenia, the first goal of my research was to create a novel method for recording EEG signals in freely-moving rodents that is more similar to the way EEG is acquired in humans than methods currently in use. In order to assess the translational potential of this novel method, I adapted several different EEG and ERP paradigms commonly used in human studies for use in rodents, and tested whether rodents show similar profiles to human subjects when given NMDAR-antagonists acutely. Second, I examined how these translationally relevant neurophysiological measures are affected under chronic pharmacological NMDA and GABA-A receptor manipulations, and explored the mechanisms contributing to these EEG signals using simultaneous multi-site local field recordings. Third, given that schizophrenia is a developmental disorder, I tested whether pharmacologically decreasing NMDA receptor signaling during adolescence causes long-term neurophysiological changes that are distinct from changes observed following chronic reductions in NMDA receptor signaling during adulthood.

My overall hypothesis is that exposure to NMDA antagonists in rats recapitulates EEG deficits observed in response to NMDA antagonists in humans, and that the period of adolescence renders the brain particularly vulnerable to effects of these drugs. From this hypothesis stems two specific aims that are tested in the chapters of this dissertation.

- ***Specific Aim 1:*** Rodent skull surface EEG can replicate human EEG signals and human and rodent EEG will be similarly altered in response to acute NMDAR antagonism.

- ***Specific Aim 2:*** Given that adolescence is a critical period for cortical development, disruption of NMDA receptor function during this time, but not in adulthood, will produce long lasting alterations in neural activity.

Chapter 2: Reverse Translation of Clinical Electrophysiological Biomarkers in Behaving Rodents under Acute and Chronic NMDA Receptor Antagonism[1]

Introduction

A significant hurdle to research on the pathophysiology and treatment of major psychiatric disorders is that these conditions are difficult to model in animals. While much effort has been put into establishing useful rodent models, it is essential to identify aspects of rodent brain physiology that are analogous and, when possible, homologous to human brain physiology, through validated cross-species biomarkers. Electroencephalogram (EEG) is one of the few techniques for measuring neural activity during resting, sensory, and cognitive tasks that can be recorded in rodents and humans alike. EEG is therefore a candidate translational biomarker that may allow us to conduct parallel studies across species (Luck et al., 2010). EEG abnormalities are well characterized in schizophrenia (Cho et al., 2006; Rutter et al., 2009; Uhlhaas and Singer, 2010; Hong et al., 2012), bipolar disorder (Clementz et al., 1994), alcohol dependence (Costa and Bauer, 1997), and other psychiatric conditions. Previous studies have assessed EEG and evoked potentials in rodent models (Bickel et al., 2008; Brenner et al., 2009; Dissanayake et al., 2009; Ehrlichman et al., 2009a; Hakami et al., 2009; Broberg et al., 2010), and recent evidence suggests surface EEG is correlated with neural synchrony among local field potential (LFP) sites (Musall et al., 2014). However, the results are

[1] Sullivan EM, Timi P, Hong LE, O'Donnell P.
As published in Neuropsychopharmacology, 2014

difficult to compare with human data due to very different approaches in how the signals are acquired and processed. Animal EEG recordings are routinely conducted with electrodes in direct contact with brain tissue with field electrodes or screws driven through the skull. A direct contact with brain tissue captures strong local signals that mask EEG data, while human EEG signals are greatly attenuated by non-conductive tissue (i.e., the skull and skin). Therefore, questions remain on how well low-powered high frequency components are represented in scalp EEG.

The first goal of this study was to create a tool to record skull EEG in awake behaving rats in a similar manner to how human EEG are obtained and then test whether rodent EEG signals are altered similarly to human EEG under acute NMDA receptor antagonism. We chose NMDA receptor blockade because of its well-characterized effects on human EEG (Hong et al., 2010) and extensive use in human research to model aspects of schizophrenia (Krystal et al., 1994; Malhotra et al., 1996; Rowland et al., 2005a). To further minimize methodological differences between human and rodent EEG, we used an auditory evoked potential paradigm and processed rodent EEG data using the wavelet-based signal processing we previously used in human studies (Hong et al., 2008a, 2010). We analyzed evoked power by presenting both pre- and post-stimulus data instead of their ratio, in order to avoid assumptions as to whether pre and post stimulus oscillations interact. In all, we are applying our established analytical tools in human neurophysiology studies to rodent EEG data.

The intent of reverse translational studies is not simply to replicate human observations, but to also explore mechanism behind these phenomena by utilizing experimental approaches in animals that cannot be carried out in humans. Thus, in addition to recording skull EEG, we simultaneously obtained LFP from the primary auditory cortex (A1) and hippocampus (HP) to explore regional specificity of oscillatory signals. Furthermore, given the strong evidence for GABAergic abnormalities in psychiatric disorders and the dependence of NMDA antagonism on inhibitory interneuron suppression, we expanded our pharmacological manipulations to study oscillatory effects of GABA-A antagonism. Finally, we examined the consequences of chronic treatment with NMDA receptor and GABA-A antagonists on EEG and LFP signals.

Methods and Materials

Animals & Surgery

All procedures were conducted according to the USPHS *Guide for the Care and Use of Laboratory Animals*, and were approved by the University of Maryland School of Medicine Institutional Animal Care and Use Committee. Adult male Sprague-Dawley rats (n=18) were purchased from Charles River Laboratories (Wilmington, MA) and group-housed (3 per cage) upon arrival in a room maintained at 23º C with a 12 hr light/dark cycle (lights on at 7 PM) with *ad libitum* access to food and water. Rats were allowed 2 weeks of acclimation to the animal facility before electrode implantation. Electrode arrays (Innovative Neurophysiology, Durham, NC) consisting of skull EEG electrodes and microwires for deep recordings (35 µm in diameter; Figure 1) were implanted in rats (400-450 g) under isoflurane anesthesia (5% in oxygen for induction and 2-3% for maintenance). Skull EEG electrodes consisted of 2 mm diameter Ag/AgCl disks that were cemented onto the skull surface at bregma, equivalent to the human vertex EEG site. Deep electrodes were implanted in A1 (5.2 mm caudal from bregma, 6.5

mm lateral to midline, 2.2 mm ventral to dura) and the CA1 region of the HP (5.2 mm caudal from bregma, 5.5 mm lateral, 3.8 mm from dura) and secured with dental cement. Carprofen (5 mg/kg i.p.) was given once daily for 72 hours post-surgery. Rats were allowed 3 weeks recovery before recordings. At the end of the study, rats were anesthetized with chloral hydrate and transcardially perfused with 0.9% saline followed by 4% paraformaldehyde. Brains were removed and sectioned at 50 μm on a freezing microtome. Electrode tracts were identified as small lesions in the tissue using a rat brain atlas (Paxinos and Watson, 1998). Only animals with appropriate electrode placement in A1 and HP were used for analyses.

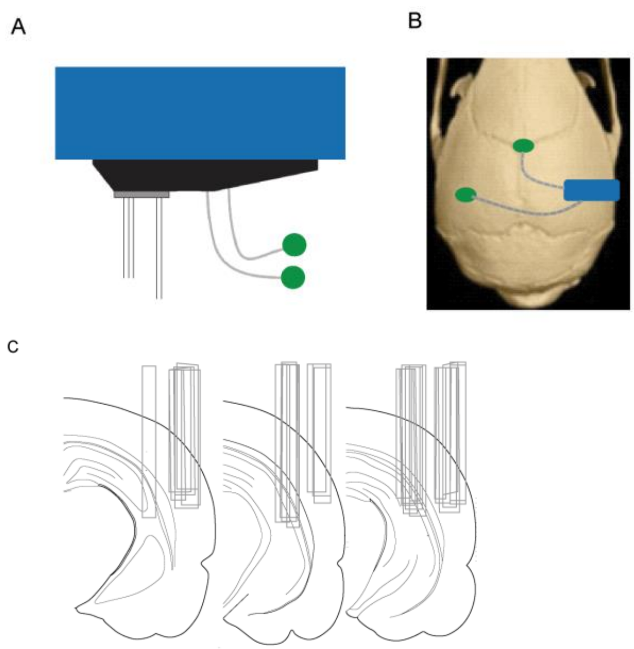

Figure 1. Electrode placement diagram 1

A) Schematic of electrodes used with EEG disc electrodes illustrated in green and LFP electrodes in gray. B) Illustration of skull surface EEG placement (green discs). C) Placement of LFP electrodes in A1 cortex and HP. Each bar represents the placement of electrode arrays as verified by histology. Data from animals with improper placement were excluded from the analysis.

Recordings in behaving rats

Recording sessions were conducted in clear 12” x 12” plexiglass boxes (Med Associates, St. Albans VT) housed within a sound-attenuated chamber. Rats were given 3 sessions of 30 minutes each to habituate to the recording box and to being plugged in and tethered to the commutator (Plexon, Dallas, TX). Electrophysiological signals were sampled at 1 kHz using a 32-channel Omniplex system (Plexon). Tones were driven by an RZ6 system (Tucker Davis Technologies, Alachua, FL) and delivered via speakers mounted in the recording chambers. After 10 minutes of habituation, rats were presented with 200 pairs of single white-noise sounds (1 ms, 75 dB clicks) with 500 ms intervals with a jittered time interval between click pairs (2 ± 0.5 sec). Sound parameters were the same as those used in humans (Hong *et al*, 2010; Hong *et al*, 2008b). We assessed oscillations during presentation of the first click (S1) and gating of evoked oscillations by calculating the ratio of the amplitudes of responses to the second click (S2) divided by the response to the first click (S1). We also assessed mismatch negativity (MMN) using an auditory oddball paradigm where tones of a “standard” frequency were presented repetitively with a “deviant” tone of a different frequency presented 5% of the time. The tones (7 or 9 kHz) were presented for a duration of 30ms with an ISI of 400ms, and were counterbalanced so that half of the time 7 kHz tone was the standard and half of the time it was the deviant tone.

Acute and chronic drug treatment

After 3 baseline recording sessions on consecutive days with no drug or vehicle injection, all rats were recorded under acute (+)-MK-801 hydrogen maleate (0.1 mg/kg, i.p.; Sigma, St. Louis, MO), picrotoxin (0.5 mg/kg, i.p.; Sigma), or saline. MK-801 was chosen as opposed to ketamine for this study due to its substantially longer action in rodents (Pinault, 2008; Hakami et al., 2009) and increased specificity for NMDA receptors (Miyamoto et al., 2000). Additionally, previous studies using LFP recordings found similar effects of ketamine and MK-801 on oscillatory activity (Hakami *et* al, 2009; Pinault, 2008). Rats were given i.p. injections and placed in the recording chamber to habituate for 15 minutes prior to recording. After the acute recording day, each animal was subsequently injected daily in their home cage for 21 days. This study was conducted in a counterbalanced crossover design. Animals were randomly assigned into 1 of 3 groups: MK-801-picrotoxin, picrotoxin-MK-801, or saline-saline. Baseline recordings were followed by acute drug administration and testing, daily injection for 21 days, and finally chronic testing in the drug-free state 1 day after the last injection. All rats had a 3 week washout period during which they remained in their home cage. Following this washout period, the group that previously received acute and chronic MK-801 was switched to acute and chronic picrotoxin and vice versa.

Signal processing and analysis

We used Neuroscan v5.4 (Compumedics, El Paso, TX) to analyze sound-evoked oscillations. EEG signals from the S1 response obtained during the paired-sound task were filtered at 1-180 Hz, and sorted into 300 ms post-stimulus epochs. An automated artifact rejection using an amplitude filter at ±300 µV was used for all data to reject contaminated trials. This was followed by visual inspection of EMG and EEG data for movement-contaminated trials. The average number of trials used for each animal was 144.6 ± 23.5. We employed data analysis methods identical to those used in human studies (Hong et al., 2008a, 2010) to maximize comparability between species. To evaluate evoked power at different frequency bands of each single trial, we used an 8-level discrete biorthogonal wavelet (Matlab bio5.5, Wavelet Toolbox, MathWorks, Inc.) to separate evoked responses into 8 details representing 8 frequency bands. By simulation, we estimated the frequency bands of each detail: D1-D3 correspond to very high gamma frequencies >85 Hz, D4: 40-85 Hz (gamma), D5: 20-40 Hz (low gamma), D6: 12-20 Hz (beta), D7: 5-12 Hz (theta-alpha), D8: 1-5 Hz (delta). This method measured oscillations in single trials that include both stationary and non-stationary oscillatory responses associated with the stimulus, rather than only the stationary, time-locked component as in averaged evoked potentials. Energy within each frequency band was measured by power spectrum density (PSD) using a Welch method. The PSD in each frequency range from the accepted trials were then averaged. We converted the PSD data from each subject into relative power by normalizing the power in each frequency band to the total power in the 1-180 Hz range.

We also calculated the averaged auditory evoked potentials (AEP) in response to S1 and S2 to measure sensory gating. We filtered the EEG signals from individual animals using a 1-180 Hz bandpass filter, normalized to a 100 ms prestimulus interval, epoched, and averaged across trials. The P1 and N1 components were identified from the averaged AEP. We defined P1 as the first positive-going wave occurring between 10-45 ms post-stimulus, and the N1 component as the first negative-going component directly following P1 between 20-70 ms post-stimulus. N1 and P1 were automatically identified for S1 and S2, which were then visually verified. We calculated sensory gating as the S2/S1 ratio for N1 and P1.

For MMN analysis, 300 ms epochs around the tone were selected, filtered at 1-30 Hz, baseline-corrected to the 100 ms prior to the stimulus, and averaged separately for standard and deviant tones. A difference wave was constructed by subtracting the standard wave from the deviant wave, and MMN was quantified by measuring the area under the curve in the period between 35 and 100 ms after the stimulus.

Statistical methods

SPSS and Graphpad programs were used for statistical analyses. For sound-evoked oscillations, we used a two-way repeated measures ANOVA to compare power in 5 frequency bands (gamma, high beta, low beta, theta-alpha, delta) across recording sessions. All data passed the Shapiro-Wilks test of normality and violations of sphericity were subjected to Greenhouse-Geisser correction when necessary. For auditory gating and MMN, we used one-way repeated measures ANOVAs to compare across recording sessions. Bonferroni post-hoc tests were used for multiple comparisons following significant ANOVA.

Results

Oscillatory responses to auditory stimuli with acute NMDA receptor antagonism

Acute MK-801 (0.1 mg/kg, i.p.) altered oscillatory power recorded with skull surface EEG. Repeated measures ANOVA on 5 frequency bands during baseline (pre-drug) and acute MK-801 showed a significant frequency by session interaction ($F_{(4,40)}$=5.560, p=0.001) without affecting total broadband power (1-180 Hz; $t_{(10)}$=0.731, p=0.482). Post-hoc tests revealed a significant increase in gamma (40-85 Hz; $t_{(10)}$=3.956, p=0.003) and a significant decrease in beta (12-20 Hz; $t_{(10)}$=4.551, p=0.001) power with acute MK-801 (Figure 2). Thus, NMDA receptor blockade causes a shift from low to high evoked EEG frequencies in rats. When analyzing the pre-stimulus period, we found a similar frequency by session interaction ($F_{(4,40)}$=6.400, p<0.001), with a significant elevation of gamma power (40-85 Hz; $t_{(10)}$=3.900, p=0.003) and a decrease in beta power (12-20 Hz; $t_{(10)}$=3.269, p=0.008), suggesting that acute MK-801 has a similar effect on EEG oscillations at rest and during auditory sensory processing.

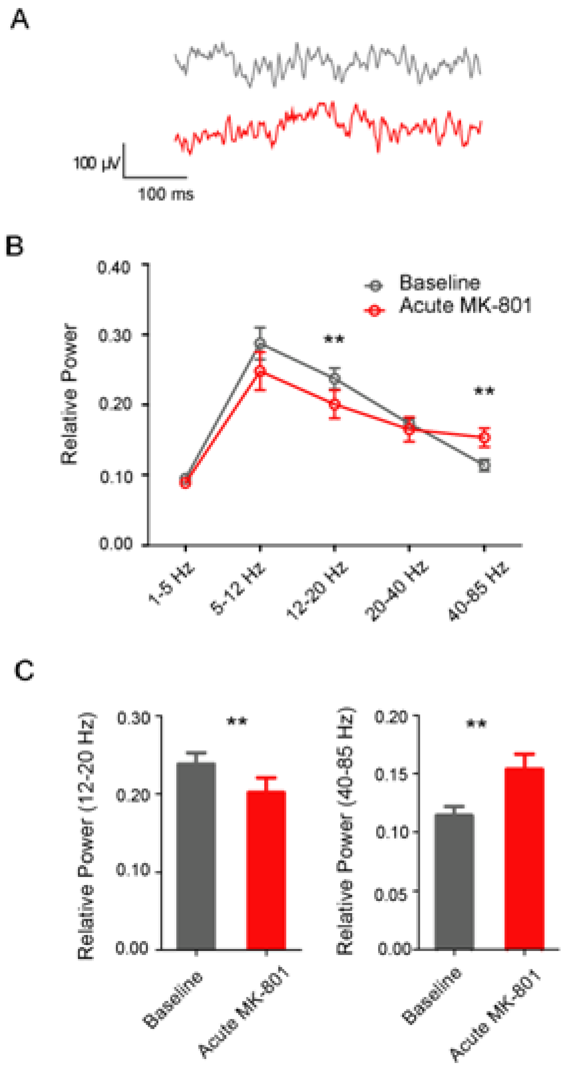

Figure 2. Acute effect of MK-801 on sound-evoked oscillations in awake, unrestrained rats. A) Representative EEG traces at baseline (gray) and after acute MK-801 (red). B) Power spectrum density (PSD) plot of vertex EEG signal from 12 rats during a 300 ms post-stimulation epoch across 5 frequency bands at baseline and after MK-801 (0.1 mg/kg i.p.). Baseline data shown are average values of the three baseline sessions for each animal. Acute MK-801 data is from a single session after acute MK-801 injection. We normalized the evoked power in each of the 5 frequency bands to the total power for each subject, represented here as relative power. Acute MK-801 significantly increased tone-evoked gamma power (40-85 Hz), while decreasing beta power (12-20 Hz) compared to baseline. C) Bar graphs show enlarged relative power in the gamma band *(right)* and decreased relative power in the beta band *(left)*. In this and subsequent figures, all data are plotted as mean ± SEM. (**p<0.01)

In order to establish correlates of activity in brain regions important for processing sensory information thought to be disrupted in schizophrenia, we simultaneously recorded LFP responses from the A1 cortex and the CA1 region of the HP, observing a pattern similar to skull surface EEG. In the HP, we found a significant frequency by session interaction ($F_{(4,32)}$=3.674, p=0.014), and post-hoc tests revealed that acute MK-801 increased gamma power ($t_{(8)}$=3.590, p=0.007) and decreased beta power from baseline ($t_{(8)}$=2.743, p=0.025). In the A1 cortex, the frequency by session interaction

($F_{(4,40)}$=2.291, p=0.076) did not reach statistical significance. There was no change in total broadband power in the HP ($t_{(8)}$=1.873, p=0.098) or the A1 cortex ($t_{(10)}$=1.599, p=0.141) after acute MK-801 administration. Thus, HP activity may correlate more closely with surface evoked EEG oscillations than A1 cortex under this paradigm.

Oscillatory responses to auditory stimuli with acute GABA-A receptor blockade

As NMDA blockade has been proposed to exert its effects by selectively inactivating NMDA receptors in cortical GABA interneurons (Homayoun and Moghaddam, 2007), we next explored whether GABA-A blockade reproduced the effects of NMDAR antagonists. The GABA-A channel blocker picrotoxin (PTX) also affected oscillations. We found a significant frequency by session interaction ($F_{(4,40)}$=5.543, p=0.001), and post-hoc tests showed that acute PTX (0.5 mg/kg) reduced beta band power from baseline ($t_{(10)}$=4.557, p=0.001), similar to the effect of acute MK-801, but there was no significant difference in gamma band power. As with acute MK-801, total broadband power was not altered with acute PTX ($t_{(10)}$=1.382, p=0.197; Figure 3). In contrast to what we observed with acute MK-801, we found no significant frequency by session interaction in the pre-stimulus epoch, suggesting that the reduction in beta power by GABA-A blockade may only be evident during auditory sensory processing. To ensure the lack of response to PTX was not due to insufficient dosing, we tested a subset of rats (n=4) with a higher dose (1.0 mg/kg) and found that 3 out of the 4 rats developed seizures within 20 minutes of injection. Therefore, the 0.5 mg/kg PTX dose was likely close to a maximal dose without epileptogenic activity. The data suggest that MK-801-induced reduction in beta, but not increased gamma, oscillations could be mediated by an attenuation of local inhibitory processes. We also analyzed oscillations in the HP and A1 cortex and did not find a significant frequency by session interaction at either location (HP; $F_{(4,32)}$=1.072, p=0.382, A1 $F_{(4,32)}$=1.087, p=0.376).

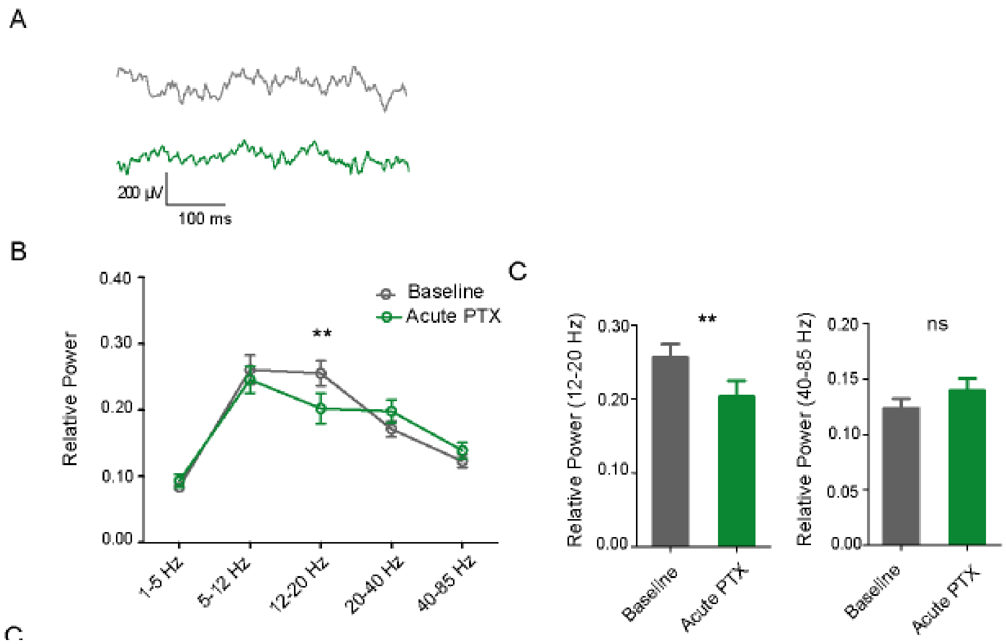

Figure 3. Acute effect of picrotoxin on tone-evoked oscillations in freely moving rats. A) Representative EEG traces at baseline (gray) and after acute PTX (green). B) Power spectrum density (PSD) plot of vertex EEG signal from 12 rats during a 300 ms post-stimulation epoch across 5 frequency bands at baseline and after PTX (0.5 mg/kg i.p.). Baseline data shown are average values of the three baseline sessions for each animal. Acute PTX data is from a single session after acute PTX injection. We normalized the evoked power in each of the 5 frequency bands to the total power for each subject, represented here as relative power. Acute PTX significantly decreased tone-evoked beta power (12-20 Hz) compared to baseline, but had no significant effect on gamma band power. C) Bar graphs shows decreased relative power in the beta band *(left)* and no difference in the gamma band *(right).*

Oscillatory responses to auditory stimuli with chronic NMDA receptor antagonism

Acute NMDAR blockade may be insufficient to model long-lasting electrophysiological changes associated with psychiatric disorders. To explore the consequences of sustained NMDAR blockade, we treated rats with MK-801 (0.1 mg/kg) for 21 days. EEG was recorded prior to treatment and again on day 22 (one day after drug cessation) to determine whether chronic exposure would lead to changes in oscillations even when the animal no longer had the drug in their system (half-life of MK-801 is 2 hours) (Vezzani *et al*, 1989). When comparing oscillatory power after 21 days of chronic MK-801 with power at baseline, we found no session by frequency interaction ($F_{(4,40)}$=0.503, p=0.733), suggesting chronic NMDA antagonism did not change power when MK-801 was absent (Figure 4). We did find a decrease in total broadband power after chronic MK-801 ($t_{(10)}$=2.941, p=0.015) in the absence of any significant changes in a given bandwidth. This suggests that prolonged exposure to MK-801 may function to dampen EEG oscillatory power across all frequency bands. However, we did not find a significant decrease in total power in the HP ($t_{(8)}$=1.162, p=0.279) or A1 ($t_{(10)}$=1.599, p=0.141). As a control for possible effects of injection procedures in EEG responses, 6 rats were exposed to saline acutely or chronically for 21 days. No effects were detected on oscillatory power after acute and chronic exposures (frequency by session interaction: $F_{(8,40)}$=1.483, p=0.194). We also failed to observe significant changes in power following chronic PTX ($F_{(4,40)}$=0.908, p=0.469; Figure 4B) with no change in total broadband power in the EEG ($t_{(10)}$=0.112, p=0.913), HP ($t_{(8)}$=1.794, p=0.111), or A1 ($t_{(10)}$=1.650, p=0.130).

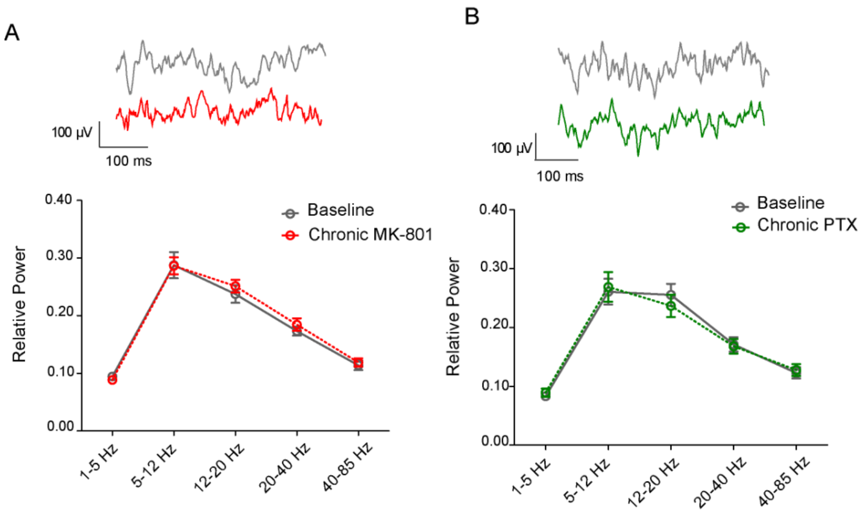

Figure 4. Chronic effect of MK-801 or PTX on tone-evoked oscillations in freely moving rats. A-B) Power spectrum density (PSD) plot of vertex EEG signal from 12 rats during a 300 ms post-stimulation epoch across 5 frequency bands at baseline and after 21-days of MK-801 (0.1 mg/kg i.p.) or PTX (0.5 mg/kg i.p). Baseline data shown are average values of the three baseline sessions for each animal. Chronic data is recorded 24 hrs after the last chronic injection in the drug-free state. We normalized the evoked power in each of the 5 frequency bands to the total power for each subject, represented here as relative power. Neither chronic MK801 nor PTX significantly altered tone-evoked oscillations compared to baseline.

Gating of skull-recorded averaged evoked potentials (AEP)

A common feature of schizophrenia is the inability to ignore irrelevant external information, evidenced by impairments in sensory gating (Adler *et al*, 1982; Freedman *et al*, 1983). In the same experiments, we assessed AEP gating and their modulation by MK-801, PTX, or saline. P1 amplitude at S1 showed an overall significant effect when comparing baseline, acute MK-801, and chronic MK-801 ($F_{(2,18)}$=7.210, p=0.005), although post-hoc tests only revealed a significantly higher P1 amplitude in acute compared with chronic MK-801 ($t_{(9)}$=3.032, p=0.014), and no differences between baseline and acute or chronic MK-801 (p>0.05; Figure 5). When comparing baseline, acute PTX, and chronic PTX, there was no significant effect of P1 amplitude at S1 ($F_{(2,20)}$=0.607, p=0.554). We also tested if there were changes in N1 amplitude, and found that at S1 there was no significant effect when comparing baseline, acute MK-801, and chronic MK-801 ($F_{(2,18)}$=2.281, p=0.131) or PTX ($F_{(2,20)}$=0.449, p=0.644). Neither P1

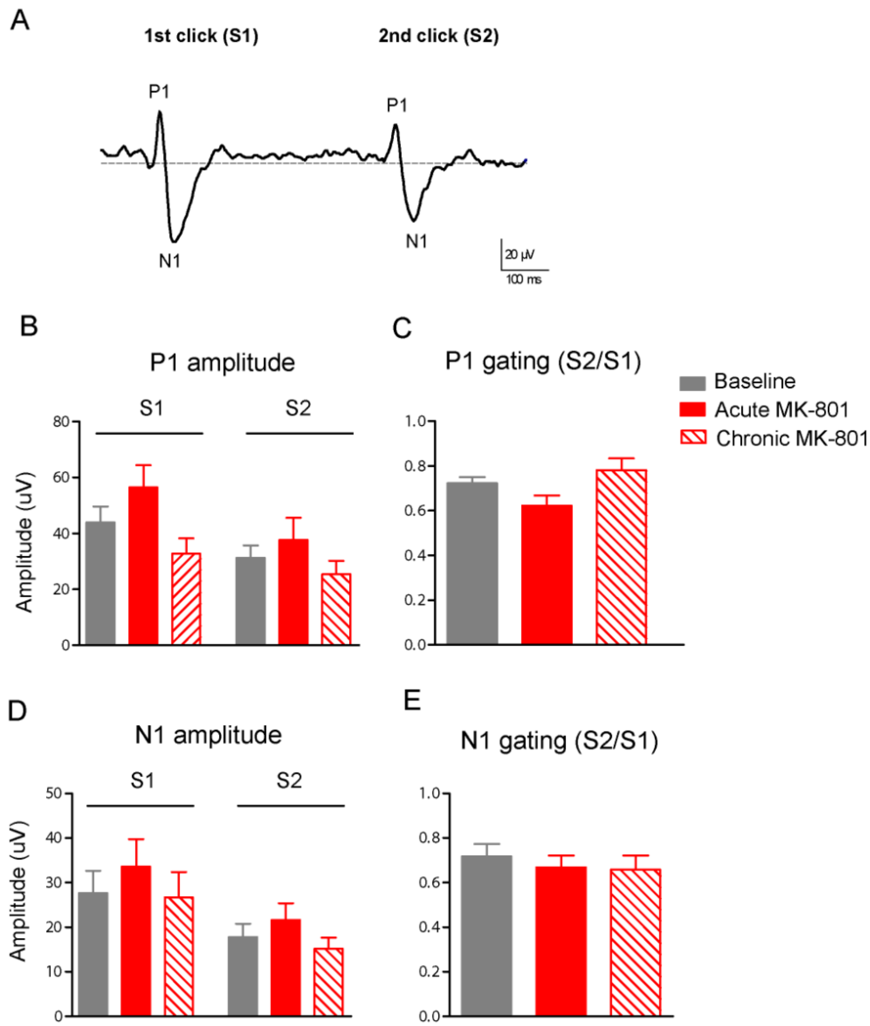

Figure 5. Gating of average evoked potentials in response to paired sounds. A) Representative auditory evoked potential during the paired-click paradigm, illustrating a reduction of P1 and N1 amplitudes in response to the second tone (S2) compared to the first (S1). B,D) Bar graph representation of P1 and N1 peak amplitudes in response to the first click (S1) and the second click (S2) at baseline (gray), with acute MK-801 (red), and with chronic MK-801 (red-striped). No significant differences in peak amplitudes were found with acute or chronic MK-801 compared to baseline. C,E) Auditory sensory gating of P1 and N1 components obtained by dividing the peak amplitude evoked by S2 by the peak amplitude evoked by S1. All groups demonstrated gating of the response of S2 relative to S1, however acute or chronic MK-801 treatment did not alter this gating from baseline.

gating nor N1 gating showed differences when comparing baseline, acute MK-801, and chronic MK-801 (P1 gating: $F_{(2,18)}$=3.124, p=0.069, N1 gating: $F_{(2,18)}$=0.3382, p=0.718) or PTX (P1 gating: $F_{(2,20)}$=0.995, p=0.386, N1 gating $F_{(2,20)}$=0.204, p=0.817).

Mismatch Negativity (MMN)

We also assessed if mismatch negativity (MMN) was altered by acute of chronic MK-801 or PTX. MMN is a measure of pre-attentive deviance detection and is known to be consistently decreased in patients with schizophrenia (Javitt et al., 1993). We were able to obtain a consistent MMN as measured from the skull-EEG at baseline, however the magnitude of the difference wave was not significantly affected by acute or chronic MK-801 ($F_{(2,22)}$=0.506, p=0.610), or acute or chronic PTX ($F_{(2,20)}$=0.024, p=0.976) (Figure 6).

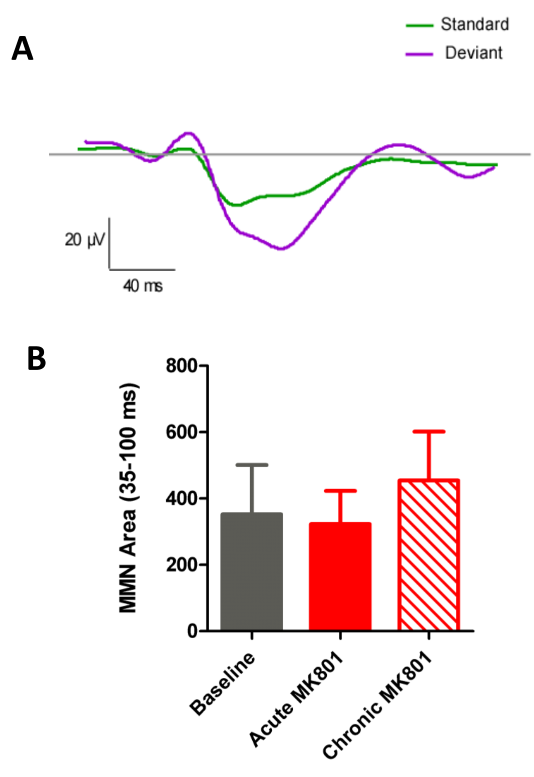

Figure 6. Mismatch Negativity during an auditory oddball paradigm. A) Representative auditory evoked potential illustrating the larger response to the deviant (purple) compared to the standard (green) tone. B) Bar graph representation of MMN at baseline, and after acute or chronic MK-801 administration. There is no significant effect of acute or chronic MK-801 on MMN magnitude as recorded from the skull-EEG. MMN is quantified by measuring the area under the curve of the difference wave.

Discussion

In an effort to optimize EEG as a translational tool, we developed a method of acquiring skull surface EEG in awake-behaving rats that resembles how EEG is acquired in humans. Acute NMDAR antagonism using MK-801 significantly increased vertex EEG gamma power and reduced beta frequency power in behaving rats during an auditory-evoked paradigm. To explore the mechanisms behind altered oscillations we used the GABA-A receptor antagonist PTX, which reduced vertex EEG beta power similarly to acute MK-801, but did not affect gamma band power. These effects suggest that the increase in gamma power induced by NMDAR antagonism may be due to actions on a specific subtype of GABAergic interneurons and not on an overall reduction in interneuron activity. The lack of effect on gamma band by PTX does not appear to be due to low dose because we used a dose close to what is required to induce seizures. Acute MK-801 also increased gamma and reduced beta power in the HP, but not A1. We also examined the effects of chronic NMDAR antagonist or GABA-A blockade on oscillations, but did not find any frequency specific effect of 21-day MK801 or PTX treatment on auditory-evoked EEG oscillations. We did, however, find a significant decrease in total EEG broadband power after chronic MK-801, suggesting there may be a general blunting of oscillatory activity.

EEG oscillations are useful tools to assess neural excitability and correlates of cortical disinhibition in a translational manner. These oscillations are thought to facilitate communication within and across brain regions (Uhlhaas and Singer, 2006). In schizophrenia patients, neural oscillations are altered and may contribute to abnormal sensory and cognitive performance (Kwon et al., 1999; Cho et al., 2006; Uhlhaas et al., 2006; Spencer et al., 2009; Barr et al., 2010; Mulert et al., 2011). Supporting rodent skull EEG as a useful translational tool, we found that acute MK-801 in rodents closely mirrors ketamine effects in healthy human volunteers (Hong et al., 2010). In a previous study, the same auditory paradigm and wavelet signal extraction used here revealed that acute ketamine significantly elevated gamma band oscillations at 40-85 Hz and reduced low frequency oscillations at delta and theta-alpha bands (1-12 Hz) compared to placebo in humans (Hong et al., 2010). Although low frequency decreases induced by ketamine in humans (1-12 Hz) and by MK-801 in rodents (12-20 Hz) slightly differ in the bandwidth involved, there is an overall similar pattern of shifting power from low to high frequencies with acute NMDAR antagonism in both humans and rodents. While not identical, these comparable results suggest that evoked EEG oscillations are highly translatable across species when recorded in a similar manner.

We also examined if AEP gating was affected by NMDAR antagonists in rodents and humans in a similar manner. Although AEP gating is impaired in schizophrenia patients (Adler et al., 1982; Freedman et al., 1983), it is not affected by ketamine when tested in healthy controls (van Berckel et al., 1998; Oranje et al., 2002; Hong et al., 2010), suggesting that NMDA receptors may not be critically involved in this auditory evoked potential. Here, we found that neither acute nor chronic MK-801 treatment significantly altered the amplitude of the rat P1 or N1 components or the gating of P1 or N1 amplitudes. This lack of effect of MK801 on AEP gating is consistent with what has been found with humans on ketamine, further supporting our ability to replicate human EEG findings in rodents. However, our finding that MMN is not affected by NMDAR antagonism differs from what has been reported in humans given ketamine (Umbricht et al., 2000). It is known that patients with schizophrenia show deficits in auditory sensory ("echoic") memory, which encodes representations of the features of an auditory stimulus, such as pitch or intensity, for a short duration of time after presentation. This deficit has been demonstrated behaviorally in tasks where the subject is asked to determine if a tone matches a previously presented tone after a short delay (Strous et al., 1995), and additionally in the reduced generation of an AEP component termed MMN (Javitt et al., 1995) ,which is thought to represent an index of echoic memory. In light of evidence showing that MMN is reduced after NMDAR-antagonism in both humans (Umbricht et al., 2000) and non-human primates (Javitt et al., 1996), many hypothesize that NMDA receptors play a crucial role in MMN generation. However, investigation of this phenomenon in awake-behaving rodents has proved difficult. This demonstration of an MMN-like phenomenon in freely moving rodents is one of the first reports in the literature, and although we were able to generate an exaggerated response to the deviant tone that is similar to what is seen in human EEG recordings, NMDAR-antagonism did not disrupt this response. There was a large amount of variability in this response both between animals and within the same animal across different recording sessions, bringing up the possibility that the high variability masked a true NMDAR-antagonism effect. Future studies using much larger numbers of animals would need to be done to further examine this possibility.

NMDAR antagonists have been used extensively to probe questions related to the neurobiology of schizophrenia. Indeed, NMDAR antagonists such as ketamine consistently induce a schizophrenia-like psychotic state in healthy volunteers (Luby et al., 1959; Krystal et al., 1994; Malhotra et al., 1996), worsen psychosis in schizophrenia patients (Lahti et al., 1995), and improve depression (Berman et al., 2000; Zarate et al., 2006). These drugs are hypothesized to produce psychotomimetic effects by creating a hyperexcitable state in the brain as evidenced by increased glutamate levels (Rowland et al., 2005b; Stone et al., 2012) and an elevation in global connectivity (Driesen et al., 2013b). Furthermore, EEG studies have revealed alterations in excitation-inhibition balance following acute ketamine such as increased high frequency and decreased low-frequency activity (Hong et al., 2010). Non-competing NMDAR antagonists are thought to preferentially act on GABAergic interneurons, perhaps due to their depolarized membrane potential or selective expression of NMDAR subunits with greater sensitivity to non-competing blockade such as GluN2C (Monyer et al., 1994). This selective action would reduce inhibitory influence on pyramidal cells and cause a net hyperexcitable circuit (O'Donnell, 2011). Consistent with this scenario, MK-801 has been shown to increase glutamate levels in the prefrontal cortex (PFC) of rats (Moghaddam et al., 1997), while decreasing GABA levels (Yonezawa et al., 1998). The data we report here along with others (Pinault, 2008; Ehrlichman et al., 2009a; Hakami et al., 2009; Lazarewicz et al., 2010) indicate that acute NMDAR antagonists produce robust elevations in gamma band activity. It is hypothesized that NMDAR antagonists may preferentially act at certain subtypes of GABAergic neurons to produce alterations in gamma activity. Indeed, optogenetic studies have shown that parvalbumin-expressing interneurons (PV-IN) are involved in the generation of gamma band oscillations (Cardin et al., 2009; Sohal et al., 2009). Thus, it is possible that alterations in PV-IN activity may underlie oscillatory changes driven by NMDAR antagonists. However, we did not observe any significant change in gamma band activity following acute GABA-A blockade. One possible explanation for the differential effects of PTX and MK-801 on gamma oscillations is that MK-801 could be acting on somatostatin-expressing interneurons, which inhibit both pyramidal cells and PV-IN, while PTX inhibits all GABAergic activity. On the other hand, the effect of MK801 on beta oscillations was mimicked by GABA-A antagonism, suggesting that beta band activity may be driven by a different cellular mechanism than gamma oscillations. Our findings suggest that NMDA blockade effects on beta oscillations may be driven by overall loss of GABA-A activity, but the effects on gamma oscillations could be due to complex actions that may be limited to a subset of neurons.

We also assessed EEG effects of chronic administration of NMDAR and GABA-A antagonists. Previous studies have shown that while acute ketamine increases frontal cortical blood flow (Lahti et al., 1995; Breier et al., 1997; Vollenweider et al., 1997), long-term ketamine or PCP use is associated with reduced frontal lobe blood flow and glucose utilization (Hertzmann et al., 1990). These data suggest that acute NMDAR antagonist administration may produce a hyperactive cortical state, but repeated or chronic NMDAR antagonist exposure may produce the opposite. Behavioral effects of chronic NMDAR antagonists in rodents have yielded mixed results, with some tasks showing impairments (Hanania et al., 1999; Lee et al., 2005; Abdul-Monim et al., 2007; Broberg et al., 2009) while others are intact (Egerton et al., 2008). Very little is known about long-lasting neurophysiologic effects of chronic NMDAR antagonism. Our data show that, in contrast to the robust effects of acute MK-801 and PTX, chronic administration did not alter auditory evoked oscillatory activity when tested in a drug-free state. However, we did find a significant decrease in total broadband power after chronic

MK-801, but not PTX, suggesting that chronic MK-801 may produce a blunting of oscillatory power in a non-frequency specific manner. This is in line with previous studies showing reduced theta and gamma power after chronic or subchronic NMDAR antagonism (Featherstone et al., 2012; Kittelberger et al., 2012). Interestingly, these studies detected oscillatory effects several weeks or months after cessation of chronic NMDAR antagonism, suggesting that effects of chronic NMDAR antagonism may be long lasting. Our current study only tested the rats after 24 h of abstinence, and thus it is possible that we would have found stronger or more frequency-specific effects after a longer duration of abstinence.

We have implemented a practical technique for recording skull surface EEG in awake-behaving rodents that resembles human EEG recording, while allowing for simultaneous intra-cortical recording. The majority of neurophysiological studies in rodents have used LFP recordings, which can provide more spatially localized oscillatory information. However, data acquired this way is less directly translatable to human EEG given the significant differences in signal attenuation and filtering and the masking effect of local neural activity on a true EEG signal. The fact that our EEG findings in rodents with acute MK-801 closely mirror EEG data from humans on ketamine further supports the validity of this platform for translating between rodent and human EEG studies. Our approach also allowed us to directly compare skull EEG and intracortical signals within the same animals. We found that even though high frequency oscillations comprise a small percentage of the total EEG signal, we were able to detect significant changes in these oscillations with acute NMDAR antagonists. This finding supports the legitimacy of high frequency oscillatory data in human EEG studies. In fact, although we observed parallel oscillatory changes in the HP and skull-surface EEG with NMDAR blockade, the pharmacological effect was actually stronger in the EEG signal. Overall, skull EEG electrodes have the potential to be a powerful translational tool for elucidating mechanisms behind altered oscillations in psychiatric disorders, and hold promise for future studies into mechanisms underlying oscillatory abnormalities across multiple disorders.

Chapter 3. NMDA and GABA Receptor Antagonism on Auditory Steady-State Synchronization in Awake Behaving Rats[2]

Introduction

Sensory processing deficits are commonly observed in schizophrenia (SZ) and are thought to play a role in a variety of symptoms, including perceptual distortions and impaired language processing (Javitt, 2009; Turetsky et al., 2009). These deficits have been associated with reduced gray matter volume in the superior temporal gyrus (McCarley et al., 1999) and a reduction in dendritic spines in the auditory cortex in schizophrenia patients (Sweet et al. 2009). These observations suggest that the auditory cortex may be part of the neural substrates contributing to these deficits. However, the underlying neurobiological basis of these cortical and perceptual abnormalities in schizophrenia is currently not fully understood. Several studies have used auditory steady state responses (ASSR) of the electroencephalogram (EEG) to probe neural network function in schizophrenia. ASSR measures the intrinsic ability of auditory neuronal ensembles to entrain to rhythmically presented stimuli and can be assessed using EEG in humans and intracranial recordings in animals (Brenner et al., 2009). Human studies have consistently shown a 40 Hz deficit in ASSR, both in phase locking and evoked power, in patients with schizophrenia (Kwon et al., 1999; Brenner et al., 2003; Light et al., 2006; Krishnan et al., 2009; Spencer et al., 2009) and in family members with increased risk for schizophrenia (Hong et al., 2004), while other frequencies appeared relatively intact. While animal models could allow further exploration of mechanisms underlying ASSR

[2] Sullivan EM, Timi P, Hong LE, O'Donnell P
Under review at International Journal of Neuropsychopharmacology

deficits, very few studies have looked at ASSR in animal models involving putative pathophysiological mechanisms that have been associated with schizophrenia. Here, we tested ASSR in rats treated with a non-competing NMDA and a GABA-A antagonist.

The NMDAR antagonist ketamine induces a transient state in healthy human subjects that resembles some aspects of schizophrenia (Luby et al., 1959; Krystal et al., 1994; Malhotra et al., 1996) and is widely used to study underlying mechanisms of the disorder in both human and animal studies. NMDAR antagonists are hypothesized to produce psychotomimetic effects by altering excitation-inhibition balance in cortical circuits, yielding alterations in oscillatory activity (Braun et al., 2007; Homayoun and Moghaddam, 2007; Pinault, 2008; Hakami et al., 2009; Hong et al., 2010). Cortical GABAergic interneurons strongly regulate network oscillations, particularly in the gamma band (Cardin et al., 2009; Sohal et al., 2009), and dysfunction in these cells are commonly implicated in mechanism of schizophrenia through postmortem and clinical studies (Akbarian et al., 1995; Hashimoto et al., 2003). Thus, alterations in cortical GABAergic neurotransmission may underlie abnormal oscillations in schizophrenia patients and could be involved in the effects of NMDAR antagonists.

Here, we examined the effects of NMDA or GABA-A receptor blockade on ASSR in awake-behaving rodents. Specifically, we recorded ASSR at 4 different stimulation frequencies from the A1 cortex and hippocampus using chronically implanted local field electrodes, while simultaneously recording from a vertex skull EEG electrode which approximates human scalp EEG recordings. To test whether pharmacological alterations of excitatory or inhibitory neurotransmission mimic ASSR abnormalities in schizophrenia, we assessed changes in ASSR by acute and chronic administration of MK-801, an NMDAR antagonist known to produce oscillatory changes in rodents (Pinault, 2008), and the GABA-A receptor antagonist picrotoxin (PTX).

Methods and Materials

Animals & Surgery

All procedures were conducted according to the USPHS *Guide for the Care and Use of Laboratory Animals*, and were approved by the University of Maryland School of Medicine Institutional Animal Care and Use Committee. Adult male Sprague-Dawley rats (300 g upon arrival) were purchased from Charles River Laboratories (Wilmington, MA). Rats (n=18) were group-housed (3 per cage) upon arrival in a room maintained at 23º C with a 12 hr light/dark cycle (lights on at 7 PM) with *ad libitum* access to food and water. Rats were allowed 2 weeks of acclimation to the animal facility before electrode implantation. Prior to implantation of custom-made electrode arrays (Innovative Neurophysiology, Durham, NC) consisting of skull EEG electrodes and microwires for deep recordings (35 µm in diameter), rats (400-450 g) were anesthetized with isoflurane (5% in oxygen for induction and 2-3% for maintenance). Skull EEG electrodes consisted of 2 mm diameter Ag/AgCl disks that were cemented onto the skull surface at bregma, mimicking the human vertex EEG site where the most robust ASSR is typically recorded (Kwon et al 1999). Depth electrodes were implanted in the primary auditory (A1) cortex (5.2 mm caudal from bregma, 6.5 mm lateral to midline, 2.2 mm ventral to dura) and hippocampal (HP) CA1 region (5.2 mm caudal from bregma, 5.5 mm lateral, 3.8 mm from dura). Arrays were secured to the skull with dental cement. Carprofen (5 mg/kg i.p.)

was given once daily for 72 hours post-surgery, along with topical antibiotic ointment. All animals were allowed 3 weeks recovery before the recordings. At the end of the study, rats were anesthetized with chloral hydrate and transcardially perfused with 0.9% saline followed by 4% paraformaldehyde. Brains were removed and sectioned at 50 µm on a freezing microtome. Electrode tracts were identified as small lesions in the tissue using a rat brain atlas (Paxinos and Watson, 1998). Only animals with appropriate electrode placement in the A1 cortex and hippocampus were used for analyses.

Recordings in behaving rats

Recording sessions were conducted in clear 12” x 12” plexiglass boxes (Med Associates, St. Albans VT) housed within a sound-attenuated chamber. Rats were given 3 sessions of 30 minutes each to habituate to the recording box and to being plugged in and tethered to the commutator (Plexon, Dallas, TX). Electrophysiological signals were acquired at 1 kHz sampling rate using a 32-channel Omniplex system (Plexon). Tones were driven by an RZ6 system (Tucker Davis Technologies, Alachua, FL) and delivered via speakers mounted in the recording chambers. After 10 minutes of habituation, rats were presented with trains of 15 clicks (1 ms 80 dB clicks) at 10, 20 ,40 and 80 Hz. 150 click trains were presented at each of the 4 frequencies with 2.5 s interstimulus interval as done in humans, with the exceptions of including a higher frequency at 80 Hz, more click trains per frequency, and longer interstimulus interval (Hong et al., 2004).

Acute and chronic drug treatment

Rats underwent 3 baseline recording sessions on consecutive days with no drug or vehicle injection, followed by an acute (+)-MK-801 hydrogen maleate (0.1 mg/kg, i.p.; Sigma, St. Louis, MO), or picrotoxin (0.5 mg/kg, i.p.; Sigma) session. For NMDAR antagonism, MK-801 was chosen as opposed to ketamine for this study due to its substantially longer duration of action (Pinault, 2008; Hakami et al., 2009) and increased specificity for NMDA receptors (Miyamoto et al., 2000). Rats were given i.p. injections and placed in the recording chamber to habituate for 15 minutes prior to recording. After the acute recording day, each animal received daily injections in their home cage for 21 more days, then were recorded from again 1 day after the last injection of the 21 day regimen.

This study was conducted using a counterbalanced crossover design. Animals were randomly assigned into one of two groups: MK-801-picrotoxin or picrotoxin-MK-801. All rats had a 3 week washout period between the different drug treatments during which they remained in their home cage. Following this washout period, the group that previously received acute and chronic MK-801 was switched to acute and chronic picrotoxin and vice versa.

Signal processing

We used Neuroscan v5.4 (Compumedics, El Paso, TX) to analyze sound-evoked oscillations. EEG signals were filtered at 1-180 Hz, and sorted into epochs post-stimulus. An automated artifact rejection using an amplitude filter at ±300 μV was used for all data to reject contaminated trials. The mean number of trials accepted was 134 ± 18. Single trial data was filtered at 1-180 Hz, and cut into epochs corresponding to the stimulation duration (1200 ms for 10 Hz, 800 ms for 20 Hz, 400 ms for 40 Hz, 200 ms for 80 Hz). The primary variable used to assess ASSR was intertrial coherence (ITC), which measures the trial to trial phase synchronization for each stimulation frequency across its stimulation duration on a single trial. ITC was calculated using a Matlab script implemented in EEGLab toolbox. The ITC was averaged across the accepted single trials. Oscillatory power during the stimulation period was also calculated using a fast Fourier transform (Neuroexplorer, Plexon). These steps, including software, closely followed what we use to process human ASSR data (Hong et al 2004).

Statistical methods

The MK-801/PTX and PTX/MK-801 groups were combined in all statistical analyses. SPSS and Graphpad programs were used for statistical analyses. A repeated measures ANOVA with stimulation frequency (10, 20, 40, 80 Hz), drug (MK-801, PTX) and session (baseline, acute, chronic) all as within-subjects factors was used to test for frequency by drug, frequency by session, or 3-way interactions. A significant frequency x drug interaction was followed by post-hoc repeated measures ANOVAs at each of the 4 stimulation frequencies and post-hoc comparisons with Bonferroni correction for multiple comparisons. These analyses were conducted first using the A1 cortex site, and if a significant effect was identified, we conducted similar analysis for the hippocampus and skull EEG recordings. ITC and power were separately calculated.

Results

LFP intertrial coherence during auditory steady state response in A1.

We investigated ITC during ASSR at 4 stimulation frequencies (10, 20, 40 and 80 Hz) across 3 recording sessions (baseline, acute, and chronic treatment) with both MK-801 and PTX. A repeated measures ANOVA revealed a stimulation frequency x drug interaction ($F_{(3,30)}$=4.540, p=0.010), and a significant main effect of session ($F_{(2,20)}$=9.843, p=0.001). When we analyzed individual stimulation frequencies, there was a significant drug x session effect at 20 Hz ($F_{(2,20)}$=4.513, p=0.024) and 40 Hz stimulation ($F_{(2,20)}$=3.816, p=0.039), but not at 10 Hz (p=0.817) and 80 Hz (p=0.180). At 20 Hz stimulation there was a significant main effect of session when comparing baseline, acute, and chronic MK-801 ($F_{(2,20)}$=7.528, p=0.004), with post-hoc tests showing that ITC after acute MK-801 was significantly greater than at baseline ($t_{(10)}$=3.427, p=0.007) (Figure 7b). However, chronic MK-801 was not significantly different from baseline ($t_{(10)}$=0.137, p=0.893). Similarly, at 40 Hz stimulation we found a significant main effect of session ($F_{(2,20)}$=3.542, p=0.049). Post-hoc tests showed that ITC was significantly elevated after acute MK-801 ($t_{(10)}$=2.653, p=0.024) but not chronic MK-801 ($t_{(10)}$=1.237, p=0.244) compared with baseline. Repeating the above analysis for PTX, we found no significant effect of session at 20 Hz ($F_{(2,20)}$=2.149, p=0.143) or 40 Hz stimulation ($F_{(2,20)}$=2.046, p=0.155) (Figure 7c). Overall, the data indicate that acute MK-801 augments ITC in a frequency-dependent manner, exhibiting effects at 20 and 40 Hz stimulation frequencies. Chronic MK-801, or acute and chronic PTX, did not have significant effects on auditory cortex ASSR compared to baseline at the chosen dose and duration.

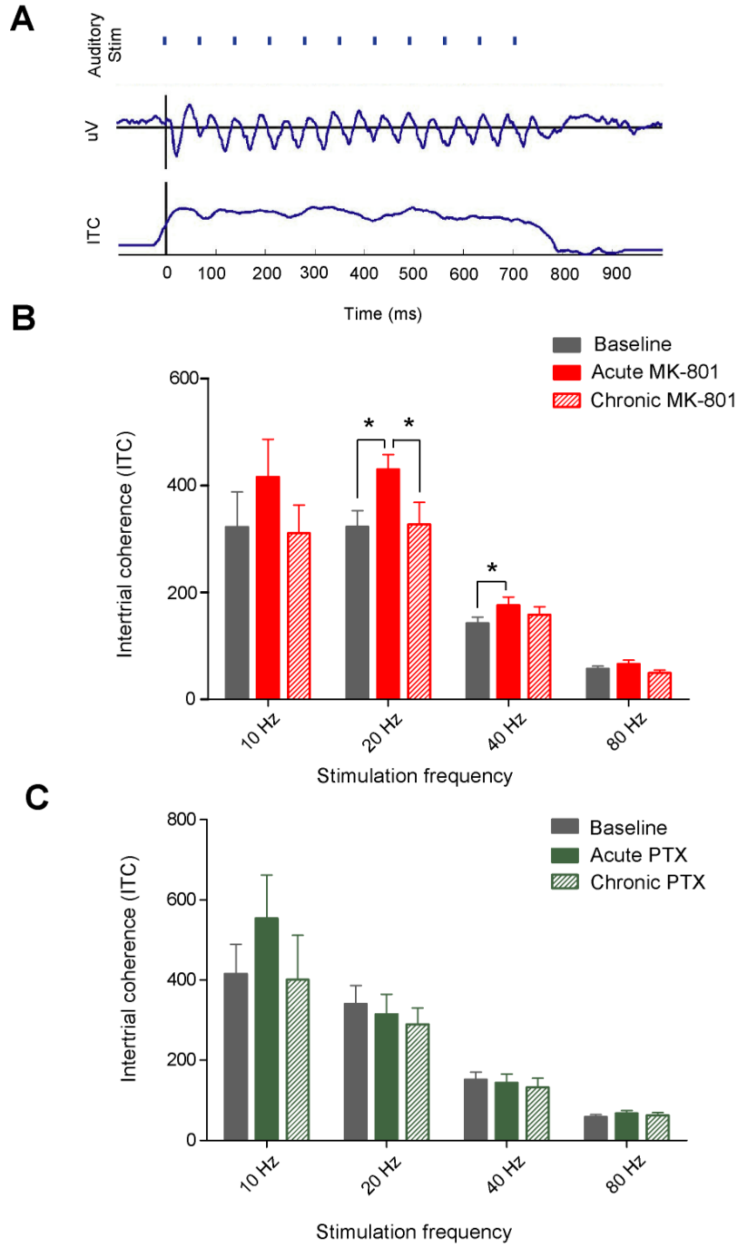

Figure 7. Effect of acute and chronic MK-801 and PTX on A1 cortex intertrial coherence during ASSR. (A) Representative example of a 20 Hz ASSR experiment. (*Top)* Tick marks represent auditory clicks presented at 20 Hz for 750 ms. *(Middle)* Average waveform recorded across 150 trials. *(Bottom)* Intertrial coherence (ITC) over the duration of the stimulus presentation. Quantification of ITC was done by computing the area under the curve for the duration of the auditory stimulation.

(B) Mean ITC values at 10 Hz, 20 Hz, 40 Hz and 80 Hz stimulation frequencies from 11 rats at baseline, after acute MK-801(0.1 mg/kg i.p.) and after 21-day (chronic) MK-801 treatment (0.1 mg/kg i.p. ITC at 20 and 40 Hz stimulation frequencies was elevated after acute, but not chronic, MK-801. There was no significant effect of MK-801 at 10 or 80 Hz stimulation frequencies.

(C) Mean ITC values at 10 Hz, 20 Hz, 40 Hz and 80 Hz stimulation frequencies from 11 rats at baseline, after acute PTX (0.5 mg/kg i.p.), and after 21-day chronic PTX (0.5 mg/kg i.p.). There was no significant effect of PTX at any stimulation frequency tested.

Baseline data shown are average values of the three baseline sessions for each animal, while acute and chronic data are from single sessions. Quantification of ITC was done by computing the area under the curve for the duration of the auditory stimulation. All data are plotted as mean ± SEM. (*p<0.05).

Oscillatory power during Auditory Steady State Response in A1

To test whether the significant effect of acute MK-801 on ITC at 20 and 40 Hz was related to changes in oscillatory power, we examined A1 LFP power during auditory stimulation. Acute MK-801 did not significantly change power at 20 Hz ($t_{(10)}$=0.2923, p=0.776) and 40 Hz ($t_{(10)}$=1.772, p=0.107) compared to pre-drug values. Acute PTX also did not affect power at 20 Hz ($t_{(10)}$=0.619, p=0.550) and 40 Hz ($t_{(10)}$=1.727, p=0.115) compared to pre-drug power. Thus, acute MK-801 augments inter-trial synchronization in the absence of significant alterations in oscillatory power.

Intertrial Coherence during Auditory Steady State Response across Recording Sites

In order to assess the location specificity of ASSR and examine the relationship between local A1 responses and skull EEG signals, we analyzed the ITC from HP and skull EEG in response to acute MK-801. We found that the magnitude of HP and EEG ITC was much lower than that of A1 cortex at baseline and after acute MK-801 (Figure 8). Using a repeated measures ANOVA, we observed a main effect of location at 20 Hz ($F_{(2,20)}$=114.24, p<0.001) and 40 Hz ($F_{(2,20)}$=43.73, p<0.001), with post-hoc tests showing that A1 ITC was significantly higher in A1 than in HP and EEG (all p <0.001). In spite of the low coherence magnitude, the effects of acute MK-801 in the HP and EEG were similar to what observed in the A1 cortex. In the HP, acute MK-801 produced a significant increase in ITC at 40 Hz stimulation ($t_{(10)}$=3.980, p=0.003), but not at 20 Hz (p=0.139). In the skull EEG, there was an insignificant decrease in ITC at 40 Hz ($t_{(10)}$=2.108, p=0.061), and a nominally significant increase in ITC at 20 Hz stimulation ($t_{(10)}$=2.237, p=0.049). Overall, the low coherence values in the HP and EEG combined with the somewhat inconsistent effects of acute MK-801 in these electrodes suggest that the A1 cortex is predominantly responsible for generating the auditory steady state response. Furthermore, the fact that the skull EEG response is not very robust suggests that using recording A1 cortex field potentials may be the better method for studying ASSR mechanisms in rodents.

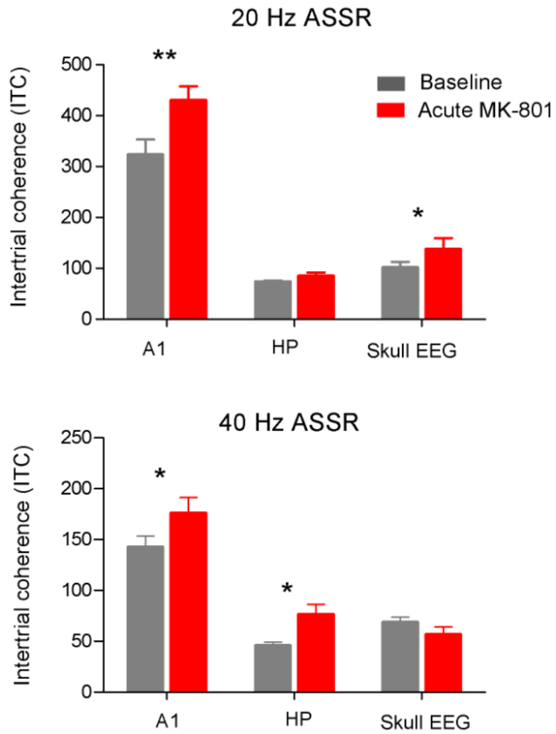

Figure 8. Comparison of intertrial coherence recorded from primary auditory (A1) cortex, hippocampus (HP) and skull EEG. Mean ITC values at 20 Hz *(top)* and 40 Hz *(bottom)* stimulation frequencies recorded from A1 cortex, hippocampus and vertex skull EEG. There was a main effect of recording location at both 20 Hz ($p<0.001$) and 40 Hz ($p<0.001$), indicating that ITC magnitude recorded from the A1 cortex was significantly larger than the HP and vertex EEG. Acute MK-801 enhanced ITC at 40 Hz stimulation but not 20 Hz in the HP, while the vertex EEG showed increased ITC at 20 Hz but not 40 Hz. All data are plotted as mean ± SEM. (*$p<0.05$, **$p<0.01$).

Discussion

In this study we showed that in awake behaving rodents, acute MK-801 enhances ASSR in beta and gamma frequencies, showing significant elevations in ITC at both 20 and 40 Hz ASSR, but not 10 and 80 Hz ASSR. Acute PTX, at the chosen dose, did not affect ASSR at any frequency, suggesting that ASSR may be more sensitive to NMDAR than GABAergic disruption. We also showed that the MK-801-induced increase in ITC was not associated with significant changes in oscillatory power at the frequencies explored, indicating that synchrony was affected somewhat independently of power. Furthermore, we demonstrated that MK-801 increases ITC with the largest effect in the

A1 cortex with weaker effects in the HP and skull EEG, suggesting that this signal was likely generated in the A1 cortex.

ASSR measures the ability of neuronal oscillations to entrain to auditory stimuli delivered at specific frequencies. This measure has been shown to be disrupted in chronic schizophrenia (Kwon et al., 1999; Light et al., 2006; Krishnan et al., 2009) as well as first episode patients (Spencer et al., 2008), suggesting that it may be a useful biomarker of the disorder. A large body of work has implicated reduced activity in cortical glutamatergic (Coyle, 2012) and GABAergic (Akbarian et al., 1995; Hashimoto et al., 2003) systems in the pathophysiology of schizophrenia. Previous studies have measured the effect of acute NMDAR-antagonism on ASSR in anesthetized animals (Sivarao et al., 2013), or acute GABAergic manipulations in freely moving rodents (Vohs et al., 2010, 2012). Building on these studies, we compared NMDAR vs. GABA-A channel blockers, and their acute vs. chronic effects, on ASSR in awake-behaving rats. We obtained ASSR at 10, 20, 40 and 80 Hz stimulation frequencies in unrestrained, awake rats. However, only 20 and 40 Hz ASSR were affected by acute MK-801. This frequency-specific effect of MK-801 is consistent with previous studies showing that NMDAR-antagonists primarily affect oscillations in the 30-80 Hz gamma band (Pinault, 2008; Hakami et al., 2009; Hong et al., 2010). Interestingly, a recent study in anesthetized rats also tested ASSR under acute MK-801 at 10, 20, 40 and 80 Hz, and similarly found that only 20 and 40 Hz phase locking was disrupted. However, in contrast to our study where we found an increase in phase locking, Sivarao et al., found a reduction in phase locking with MK-801 at 20 and 40 Hz (Sivarao et al., 2013). The discrepancy between the two findings is likely due to the fact that our current study was conducted in awake rodents, while the previous study used anesthetized rodents. Indeed, ASSR has been extensively shown to be affected by consciousness and is even used as a metric for consciousness during surgery. In humans, ASSR at 40 Hz was shown to be drastically reduced to 15% of pre-anesthesia levels by isoflurane (Plourde and Picton, 1990). Additionally, ASSR has been shown to be diminished during sleep (Linden et al., 1985; Cohen et al., 1991), indicating that a reduction in ASSR may not be primarily due to the pharmacological action of anesthetics, but may be more generally reflective of the level of consciousness. Interestingly, using ketamine, an NMDAR antagonist, for purposes of anesthesia in humans did not produce a reduction of ASSR even though unconsciousness was obtained. In fact, the 40 Hz ASSR response in human EEG recordings was *increased* during ketamine anesthesia (Plourde et al., 1997). This increase in 40 Hz ASSR with ketamine is consistent with our finding of increased 40 Hz ASSR with MK-801 in rodents. Our studies differ, however, in that the humans were given a large enough dose of NMDAR antagonist induce unconsciousness, whereas the rodents in our study were given a low dose and did not show any observable signs of altered consciousness. Given the sensitivity of the ASSR to level of alertness, we assert that in order for recordings in rodents to be a useful cross-species translational tool for schizophrenia research, recordings must be done in the same state in both humans and rodents.

A strength of our approach in rodents is that we had the ability to record LFP and EEG signals simultaneously from multiple locations during the ASSR in unrestrained rats. This enabled us to examine the location of ASSR generation within the rodent brain.

The most robust response we recorded was from within the A1 cortex, where we observed the highest magnitude of response and coherence, which is consistent with other animal studies suggesting that A1 cortex is a main generator of ASSR (Franowicz and Barth, 1995; Kuwada et al., 2002). We also analyzed the ASSR response from the skull EEG electrode, which was placed on the vertex, and LFP responses from the HP. Although coherence values in both sites were much lower than in the A1 cortex, we did observe a similar albeit weaker effect of MK-801 on 20 Hz ITC from skull EEG and 40 Hz ITC from HP field recordings. Given that LFPs and EEGs are known to be a summation of activity from a large area, we would expect the strong A1 cortex signals to spread via volume conduction and thus be evident in other nearby brain regions. Thus, the low EEG coherence we found is likely due to signal spread and contamination from signals being generated by other brain regions. To fully understand the whole brain dynamic and contributions to vertex EEG ITC, denser, well-distributed depth electrode recording is needed.

Much evidence suggests that GABAergic inhibition is responsible for oscillations and maintenance of synchronous firing (Lewis et al., 2005; Gonzalez-Burgos and Lewis, 2008; Sohal et al., 2009), which led us to also examine ASSR under acute GABA-A antagonism. Surprisingly, we did not observe any effect of PTX on ASSR generation at any of the frequencies tested. A previous study assessed ASSR in rats with muscimol (GABA-A agonist) and found an increase in phase locking during 40 ASSR (Vohs et al., 2010). We therefore hypothesized that blocking GABA-A channels would alter ITC at 40 Hz, but we did not observe this effect. While it is possible that the dose was a factor, when we tested higher doses of PTX (1.0 mg/kg), seizures were observed in 3 out of 4 rats tested. Therefore, the 0.5 mg/kg PTX dose was likely close to a maximal dose without epileptogenic activity. Using this same dose in another study, our group did find a significant reduction in beta-band oscillations from skull-EEG, suggesting that this dose is sufficient to alter neural oscillations. Overall, this study suggests that A1 coherence may be more sensitive to NMDAR-antagonism, which is thought to preferentially inhibit fast-spiking interneurons, than by direct GABA-A blockade which would inhibit all GABA neurons. Further studies will be needed to fully parse out the role of GABA-A receptors in ASSR.

We have shown that acute MK-801 enhances ITC at 20 and 40 Hz, which is not consistent with the majority of ASSR EEG findings in schizophrenia patients that have shown decreased 40 Hz ITC (Kwon et al., 1999; Light et al., 2006). However, this effect is highly consistent with a large body of animal literature demonstrating that NMDAR antagonists increased gamma frequency activities (Pinault, 2008; Hakami et al., 2009). There is also evidence suggesting that elevated 40 Hz activity in the A1 cortex is correlated with positive symptoms, most specifically hallucinations (Spencer et al., 2009). Our data suggest that the increased ASSR at 40 Hz may be a useful translational biomarker to study mechanisms behind positive symptoms in schizophrenia

Chapter 4: Subchronic NMDAR-antagonist exposure in adolescence produces impaired medial prefrontal - hippocampal synchrony in adult rats[3]

Introduction

Schizophrenia is a devastating psychiatric disorder that generally emerges during the transition from adolescence to adulthood (Häfner et al., 1993). While typical age of onset of schizophrenia is at 16 to 30 years of age, many patients include a period of prodromal, sub-clinical symptom presentation before full psychosis onset (Cornblatt et al., 2001). Many have proposed that altered brain maturation during late adolescence or early adulthood is crucially involved in the pathophysiology of the disorder and its prodromal stage (Feinberg, 1982; O'Donnell, 2011; Uhlhaas, 2011). Indeed, adolescence is a period of significant cortical reorganization and maturation, exemplified by rewiring of white matter fiber connections (Ashtari et al., 2007a; Kochunov and Hong, 2014), decreases in gray matter (Gogtay et al., 2004), reduction of theta and delta band oscillations (Campbell and Feinberg, 2009) and increase in cortical gamma-band oscillations (Uhlhaas et al., 2009). Physiologically, dopamine-NMDAR interactions in the PFC mature during adolescence (Tseng and O'Donnell, 2007b), along with refinement of GABAergic neurotransmission (Hashimoto et al., 2009). This anatomical and functional maturation during adolescence yields a circuit with more precise temporal synchrony and the capability to support more complex cognitive processes (Catts et al., 2013). However, this period of reorganization may also be a window of increased vulnerability for disruption.

[3] Sullivan EM, Du X, Timi P, Hong LE, O'Donnell P
In preparation for submission

While several animal models recapitulate a developmental trajectory of deficit onset occurring during adolescence (O'Donnell, 2011), an important piece of missing information is how NMDA signaling can relate to the adolescent vulnerability proposed to underlie schizophrenia onset. NMDAR hypofunction has received considerable attention over the past decades, stemming from the discovery that non-competitive antagonists like ketamine or PCP induce a transient psychotic state reminiscent of schizophrenia when given to healthy controls (Luby et al., 1959; Krystal et al., 1994; Malhotra et al., 1996), and exacerbate psychotic symptoms in SZ patients (Lahti et al., 1995, 2001). The mechanisms underlying these effects are thought to occur due to preferential blockade of NMDARs on GABAergic interneurons (Homayoun and Moghaddam, 2007), resulting in increased extracellular glutamate and an overall disinhibited cortex (Moghaddam et al., 1997). Acute NMDAR-antagonism has also been shown to reliably alter oscillatory activity in both humans and rodents (Pinault, 2008; Hong et al., 2010), recapitulating the impaired neural coordination seen in patients with SZ (Uhlhaas and Singer, 2010). Given that adolescence is a critical time for time for the re-arrangement of neural oscillatory synchrony, particularly in the beta and gamma band ranges (Uhlhaas et al., 2009), we postulate that impairing NMDAR transmission during adolescence will have long-term effects on neural synchrony, leading to circuit dysfunction in adulthood.

We administered the NMDAR-antagonist MK-801 during adolescence (postnatal day (P) 45-50), then implanted chronic electrodes in the medial prefrontal cortex (mPFC) and hippocampus (HP) along with skull-surface EEG leads. Upon reaching adulthood, we measured oscillatory activity from the HP and mPFC as well as the phase-synchrony between these regions at baseline, and after re-exposing the animals to an acute MK-801 challenge. In order to test if effects were specifically due to the drug exposure during adolescence, we also conducted identical experiments using rats exposed to 5 days of MK-801 in adulthood.

Methods and Materials

Animals & drug treatment

All procedures were conducted according to the USPHS *Guide for the Care and Use of Laboratory Animals*, and were approved by the University of Maryland School of Medicine Institutional Animal Care and Use Committee. Juvenile (n=21) and adult (n=13) male Sprague-Dawley rats were purchased from Charles River Laboratories (Wilmington, MA) and group-housed (3 per cage) upon arrival in a room maintained at 23º C with a 12 hr light/dark cycle (lights on at 7 PM) with *ad libitum* access to food and water. Rats were allowed 10 days of acclimation to the animal facility before any drug treatment. On P41-45 for the adolescent group or P64-68 for the adult group, (+)-MK-801 hydrogen maleate (0.1 mg/kg, i.p.; Sigma, St. Louis, MO) or saline was administered once a day for 5 consecutive days.

Electrode implanting surgery

Electrode arrays (Innovative Neurophysiology, Durham, NC) consisting of skull EEG electrodes and microwires for deep recordings (35 µm in diameter; Figure 1) were implanted in rats on P50 for the adolescent group and P75 for the adult group under isoflurane anesthesia (5% in oxygen for induction and 2-3% for maintenance). Skull EEG electrodes consisted of 2 mm diameter Ag/AgCl disks that were cemented onto the skull surface at bregma, equivalent to the human vertex EEG site. Deep electrodes were implanted in mPFC (3.2 mm rostral from bregma, 0.8 mm lateral to midline, 4.2 mm from dura), A1 (5.2 mm caudal from bregma, 6.5 mm lateral to midline, 2.2 mm ventral to dura) and the CA1 region of the HP (5.2 mm caudal from bregma, 5.5 mm lateral, 3.8 mm from dura) and secured with dental cement. Carprofen (5 mg/kg i.p.) was given once daily for 72 hours post-surgery. Rats were allowed 3 weeks recovery before the recordings. At the end of the study, rats were anesthetized with chloral hydrate and transcardially perfused with 0.9% saline followed by 4% paraformaldehyde. Brains were removed and sectioned at 50 µm on a freezing microtome. Electrode tracts were identified as small lesions in the tissue using a rat brain atlas (Paxinos and Watson, 1998). Only animals with appropriate electrode placement in PFC, A1 and HP were used for analyses.

Recordings in behaving rats

Recording sessions were conducted in clear 12” x 12” plexiglass boxes (Med Associates, St. Albans VT) housed within a sound-attenuated chamber with rats on P75-82 for the adolescent-treated group and P95-100 for the adult-treated group. All rats were given 5 sessions of 30 minutes each to habituate to the recording box and to being plugged in and tethered to the commutator (Plexon, Dallas, TX). Electrophysiological signals were sampled at 1 kHz using a 32-channel Omniplex system (Plexon). Tones were driven by an RZ6 system (Tucker Davis Technologies, Alachua, FL) and delivered via speakers mounted in the recording chambers. After 5 days of habituation, each rat underwent 3 baseline recording sessions on consecutive days, followed by a single acute MK-801 re-exposure session on the 4th day where each rat received MK-801 (0.1 mg/kg i.p) injection 15 minutes before the beginning of the recording session (Figure 8). Each of the 4 recording session started with 10 minutes of habituation, then rats were presented with 200 pairs of single white-noise sounds (1 ms, 75 dB clicks) with 500 ms intervals with a jittered time interval between click pairs (2 ± 0.5 sec). Sound parameters were the same as those used in humans (Hong *et al*, 2010; Hong *et al*, 2008b). We assessed oscillations and phase-locking during presentation of the first click.

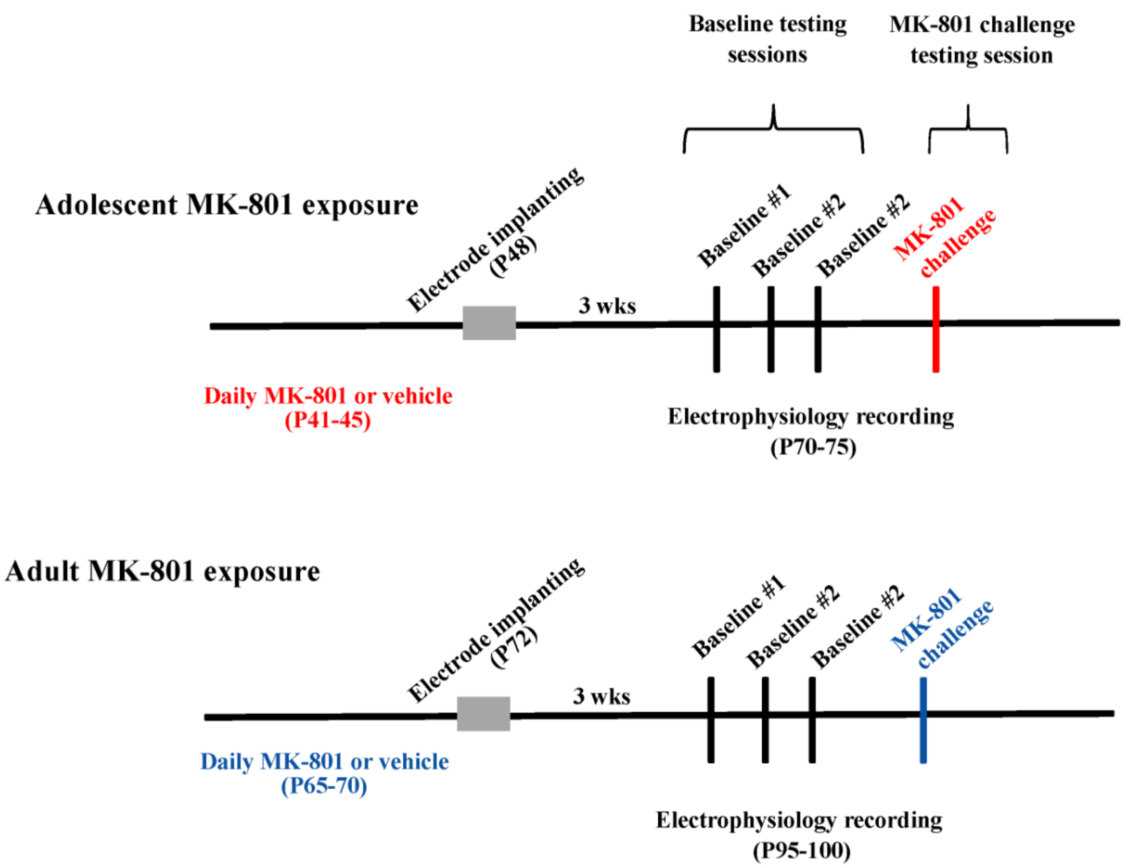

Figure 9. Schematic of experiment. Illustration of the ages of subchronic MK-801 or saline exposure, implanting of electrode arrays, and electrophysiological recording sessions for the adolescent-treated group (*top*) and the adult-treated group (*bottom*). All rats underwent three testing sessions with no acute injections, termed here as “baseline testing sessions”, and then a single acute MK-801 challenge session, termed here as “MK-801 challenge testing session”.

Signal processing and analysis

We used Neuroscan v5.4 (Compumedics, El Paso, TX) to analyze sound-evoked oscillations. EEG signals from the S1 response obtained during the paired-sound task were filtered at 1-180 Hz, and sorted into 300 ms post-stimulus epochs. An automated artifact rejection using an amplitude filter at ±300 µV was used for all data to reject contaminated trials. This was followed by visual inspection of EMG and EEG data for movement-contaminated trials. The average number of trials used for each animal was 150.3 ± 27.6. We employed data analysis methods identical to those used in human studies (Hong *et al*, 2010; Hong *et al*, 2008b) to maximize comparability between species. To evaluate oscillatory power at different frequency bands of each single trial, we used an 8-level discrete biorthogonal wavelet (Matlab bio5.5, Wavelet Toolbox, MathWorks, Inc.) to separate evoked responses into 8 details representing 8 frequency bands. By simulation, we estimated the frequency bands of each detail: D1-D3 correspond to very high gamma frequencies >85 Hz, D4: 40-85 Hz (gamma), D5: 20-40 Hz (low gamma), D6: 12-20 Hz (beta), D7: 5-12 Hz (theta-alpha), D8: 1-5 Hz (delta). This method measured oscillations in single trials that include both stationary and non-stationary oscillatory responses associated with the stimulus, rather than only the stationary, time-locked component as in averaged evoked potentials. Energy within each frequency band was measured by power spectrum density (PSD) using a Welch method. The PSD in each frequency range from the accepted trials were then averaged. We converted the PSD data from each subject into relative power by normalizing the power in each frequency band to the total power in the 1-180 Hz range.

In order to assess phase coherence between mPFC and HP, we used the same 300ms post-stimulus epochs from the oscillatory analysis and using custom Matlab scripts computed the phase-locking value (PLV) between recording electrodes in the mPFC and HP across a frequency range of 1-50 Hz. The continuous complex Morlet wavelet transform (CWT) was applied to each trial to decompose the oscillatory activities without manual scoring. For a given center frequency f_0 and time t, the PLV for EEG data from two electrodes m and n is defined as

$$PLV_{mn}(t, f_0) = \frac{1}{K}\left|\sum_{k=1}^{K} e^{i(\varphi_k^m(t,f_0)-\varphi_k^n(t,f_0))}\right|$$

Where K denotes the number of trials, and $\varphi_k^m(t, f_0)$ and $\varphi_k^n(t, f_0)$ denote the instantaneous phases of the EEG data from two electrodes that were computed during the k-th trial with center frequency f_0. Thus, the PLV ranged from 0 to 1. The larger phase-synchrony between those two electrodes, the higher is the PLV.

Statistical methods

SPSS and Graphpad programs were used for statistical analyses. For phase synchrony analysis we used a repeated measures ANOVA with 4 frequency bands (1-4 Hz, 5-12 Hz, 13-30 Hz, 31-50 Hz) and 2 sessions (baseline, MK-801 re-exposure) as within-subjects factors, and adolescent or adult treatment (saline or MK-801) as a between subjects factor. Similarly, for oscillatory analysis, we used a repeated measures ANOVA with 6 frequency bands (1-5 Hz, 5-12 Hz, 12-20 Hz, 20-40 Hz, 40-85 Hz, >85 Hz) and 2 sessions (baseline, MK-801 re-exposure) as within-subjects factors, and adolescent or adult treatment (saline or MK-801) as a within-subjects factor. All data passed the Shapiro-Wilks test of normality and violations of sphericity were subjected to greenhouse-Geisser correction when necessary. A Bonferroni post hoc analysis was used for multiple comparisons following significant ANOVA for the phase coherence analysis, and a Bonferroni corrected p-value was used for post-hoc tests in the oscillatory power analysis where $p<0.05/6$ frequency bands= $p<0.008$.

Results

mPFC-HP phase synchrony in response to auditory stimuli in adolescent-treated group:

We analyzed how NMDAR-antagonist treatment affected the phase synchrony between mPFC and HP sites. To obtain a measure of oscillatory synchrony, we measured mPFC-HP phase locking across 4 frequency bands (1-4 Hz, 5-12 Hz, 13-30 Hz, 31-50 Hz) in rats treated with MK-801 or vehicle for 5 days during adolescence at baseline in adulthood and also after an acute MK-801 challenge session (Figure 8). Repeated measures ANOVA analysis included frequency bands and testing sessions in adulthood (baseline and MK-801 challenge) as within-subjects factors, and adolescent drug exposure (saline or MK-801) as a between subjects factor. We found a main effect of testing session ($F_{(1,21)}=4.449$, $p=0.047$), a testing session by adolescence drug exposure interaction ($F_{(1,21)}=4.821$, $p=0.039$) , and a 3-way frequency by testing session by adolescence exposure interaction ($F_{(3,63)}=2.754$, $p=0.049$), suggesting that adolescent subchronic MK-801 affects phase-locking in adulthood in a frequency-dependent manner. Subsequent analysis of this 3 way interaction revealed significant main effects of testing session at delta (1-4 Hz; $F_{(1,21)}=4.630$, $p=0.043$) and theta (5-12 Hz; $F_{(1,21)}=28.412$, $p<0.001$), indicating that regardless of which treatment the rats received in adolescence, there was an increase in phase-locking at these low frequency bands after MK-801 re-exposure compared with baseline. In comparison, we found a significant adulthood testing session by adolescence exposure interaction in the gamma band (31-50 Hz; $F_{(1,21)}$=7.497, p=0.012), showing a decrease in phase-locking after the MK-801 challenge only in the rats previously treated with MK-801 in adolescence ($t_{(21)}$=2.472, p=0.022). Overall, this data shows a gamma-band specific mPFC-HP phase synchrony reduction in the group previously treated with MK-801 in adolescence when they were re-exposed to MK-801 during adulthood. In comparison, MK-801 exposure in adulthood also increases lower frequency delta-theta band mPFC-HP synchrony regardless of adolescent exposure to MK-801.

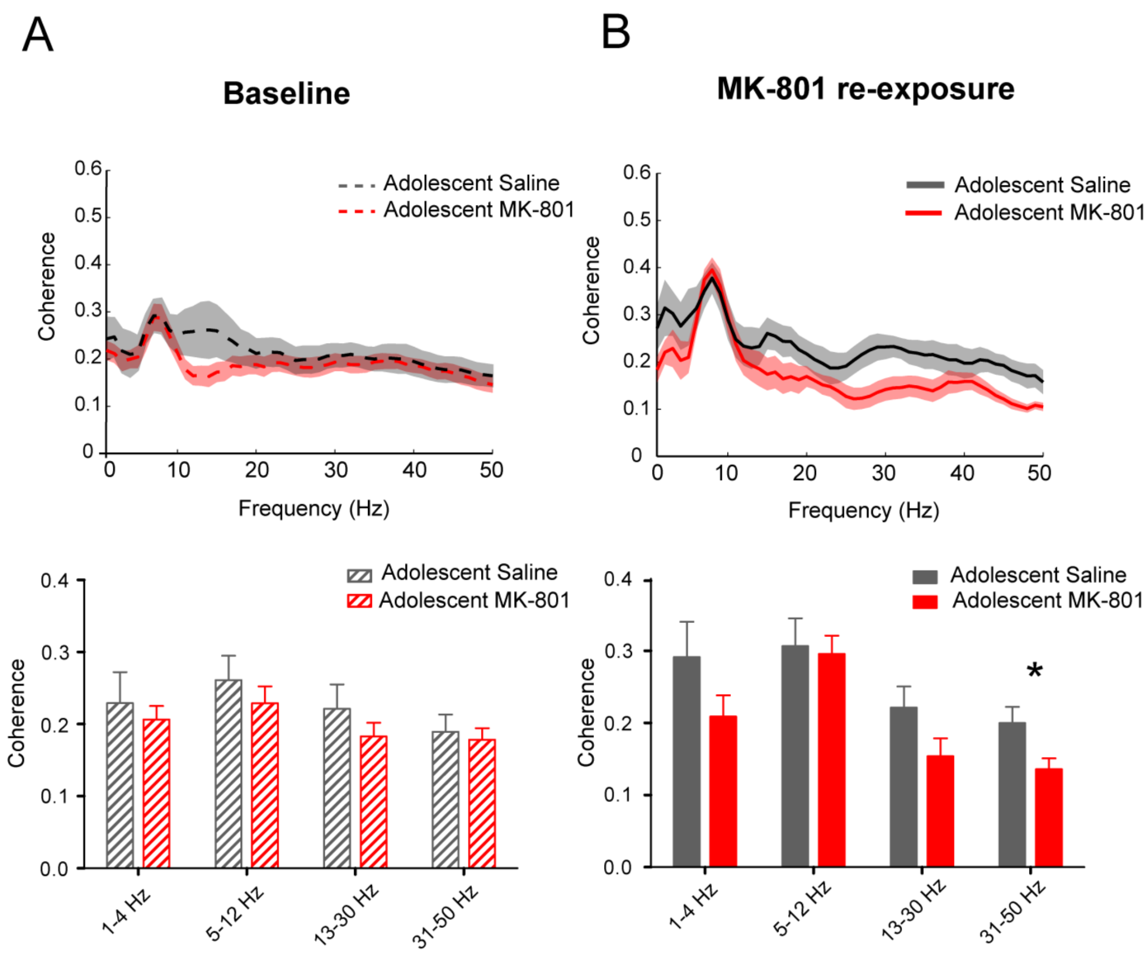

Figure 10. Phase coherence between medial prefrontal cortex (mPFC) and hippocampus (HP) in adult rats treated during adolescence with either MK-801 or vehicle. mPFC-HP coherence during adulthood at baseline (A) or after acute MK-801 rexposure (B). Coherence is measured during 300ms epochs during the presentation of 1ms white-noise clicks. This data shows a gamma-band specific mPFC-HP phase synchrony reduction in the group treated with MK-801 in adolescence when they were re-exposed to MK-801 during adulthood (p=0.02) . In comparison, MK-801 exposure in adulthood also increases lower frequency delta-theta band mPFC-HP synchrony regardless of adolescent exposure to MK-801. Baseline data shown are average values of the three baseline sessions for each animal. MK-801 rexposure data is from a single session after acute MK-801 injection in both groups. Data is presented as mean ± SEM. (*p<0.05).

mPFC-HP phase synchrony in response to auditory stimuli in adult-treated group:

To determine if this effect on mPFC-HP phase synchrony was specific to the adolescent time point of MK-801 administration, we repeated the experiment by administering subchronic MK-801 during adulthood instead of adolescence. We found a main effect of testing session ($F_{(1,12)}$=12.507, p<0.001), but no testing session by adult subchronic drug exposure ($F_{(1,12)}$=0.000, p=0.996) or 3-way ($F_{(3,36)}$=1.105, p=0.360) interactions. This suggests that in contrast to MK-801 treatment in adolescence, subchronic exposure in adulthood does not significantly alter mPFC-HP phase synchrony.

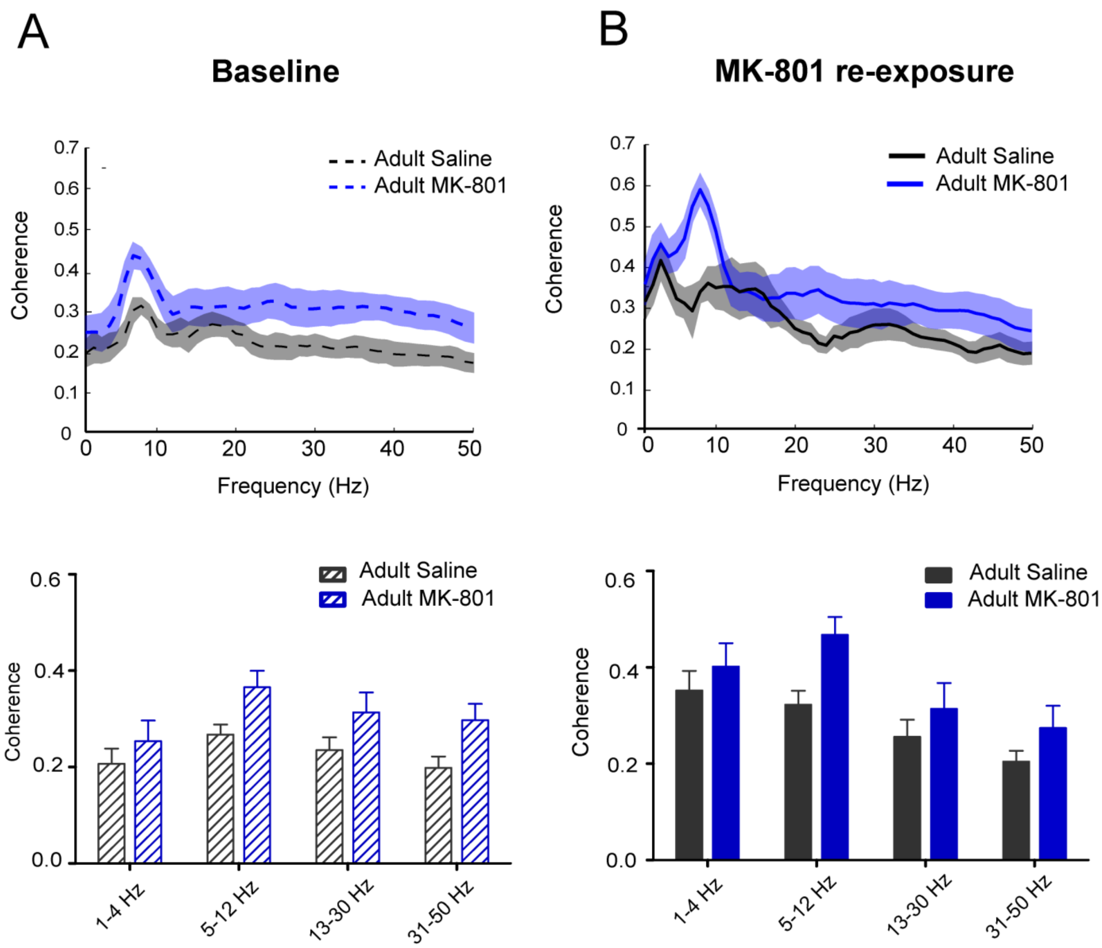

Figure 11. Phase coherence between medial prefrontal cortex (mPFC) and hippocampus (HP) in adult rats treated during adulthood with either MK-801 or vehicle. mPFC-HP coherence during adulthood at baseline (A) or after acute MK-801 rexposure (B). Coherence is measured during 300ms epochs during the presentation of 1ms white-noise clicks. In contrast to what we found with adolescent exposure, we found no effect of subchronic MK-801 exposure in adulthood on mPFC-HP phase coherence. Baseline data shown are average values of the three baseline sessions for each animal. MK-801 rexposure data is from a single session after acute MK-801 injection in both groups. Data is presented as mean ± SEM.

Oscillatory responses to auditory stimuli in adolescent-treated group:

Besides mPFC-HP coherence, we explored if local oscillatory activity measured using a discrete wavelet transform in either of these regions or the skull-surface EEG was also affected. We did not find a significant main effect of adolescence exposure in mPFC ($F_{(1,21)}$=0.094, p=0.762), HP ($F_{(1,21)}$=1.548, p=0.227) or EEG ($F_{(1,20)}$=2.687, p=0.117), no adolescence exposure by frequency interaction in mPFC ($F_{(5,105)}$=0.630, p=0.677), HP ($F_{(5,105)}$=1.522, p=0.189) or EEG ($F_{(5,100)}$=0.350, p=0.881) and no 3 way adolescence exposure by frequency by testing session interaction (PFC; $F_{(5,105)}$=0.665, p=0.651, HP; $F_{(5,105)}$=1.040, p=0.398, EEG; $F_{(5,100)}$=1.324, p=0.260). This indicates that subchronic MK-801 administration in adolescence has no effect on mPFC, HP or vertex EEG oscillatory power in adulthood compared to saline-treated controls; rather, the findings were specific to the cross-regional synchrony.

However, consistent with our earlier findings in chapter 1, we found a frequency by adulthood testing session interaction in all three regions (HP; ($F_{(5,105)}$=6.626, p<0.001, PFC; ($F_{(5,105)}$=12.507, p<0.001, EEG; $F_{(5,100)}$=8.686, p<0.001) regardless of pre-treatment drug exposure, suggesting that acute MK-801 re-exposure does have an effect on oscillations in a frequency-dependent manner. Post-hoc tests on both groups showed that acute MK-801 re-exposure significantly increased power in the high-gamma band (>85 Hz, PFC: $t_{(22)}$=5.253, p<0.001; HP: $t_{(22)}$=5.985, p<0.001; EEG: $t_{(21)}$=6.543, p<0.001) and mid-gamma band (40-85 Hz, PFC: $t_{(22)}$=5.813, p<0.001; HP: $t_{(22)}$=6.324, p<0.001; EEG: $t_{(21)}$=3.340, p=0.003), and a decrease in power in the PFC at the low-gamma (20-40 Hz,

$t_{(22)}=5.828$, $p<0.001$) and beta bands (12-20 Hz: $t_{(22)}=4.810$, $p<0.001$) compared to baseline. This pattern largely replicated our previous findings using acute NMDA antagonism in animals (Chapter 1) and humans (Hong et al 2010).

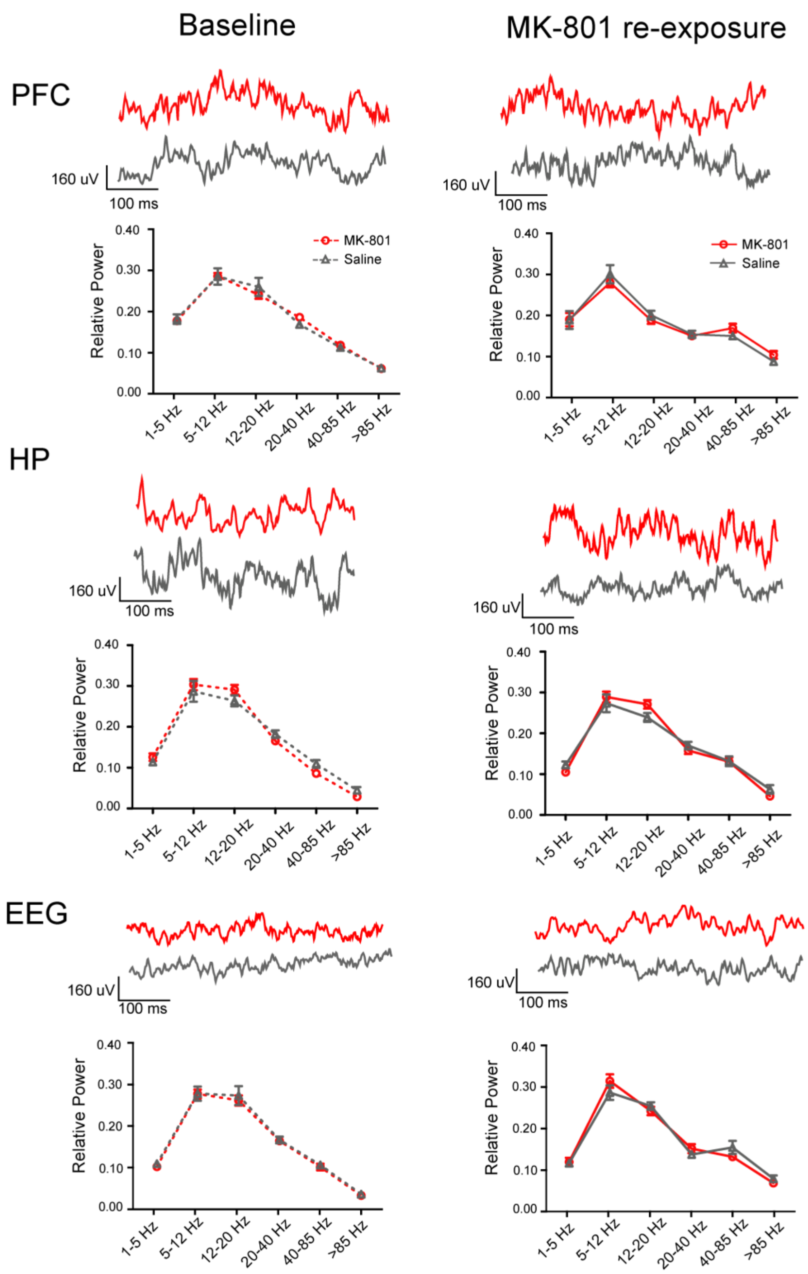

Figure 12. Oscillatory activity in adult rats treated with MK-801 or vehicle during adolescence at baseline *(left)* and after MK-801 challenge *(right)*. Power spectrum density (PSD) plot of medial prefrontal cortex (mPFC) *(top)*, hippocampus (HP) *(middle)* and vertex EEG *(bottom)* from 21 rats during a 300 ms post-stimulation epoch across 5 frequency bands at baseline and after MK-801 (0.1 mg/kg i.p.). Baseline data shown are average values of the three baseline sessions for each animal. Acute MK-801 data is from a single session after acute MK-801 injection. We normalized the evoked power in each of the 5 frequency bands to the total power for each subject, represented here as relative power. Adolescent subchronic MK-801 did not alter oscillatory activity compared to saline treated animals at baseline or after the acute MK-801 challenge. All data are plotted as mean ± SEM.

Oscillatory responses to auditory stimuli in adult-treated group:

In line with our oscillation results in the adolescent treated group, we also did not find any effect of adult subchronic exposure to MK-801 on subsequent adulthood testing at baseline or after an acute MK-801 challenge. There was no main effect of drug pretreatment (PFC: $F_{(1,12)}=0.468$, $p=0.507$; HP: $F_{(1,12)}=0.032$, $p=0.860$; EEG: $F_{(1,11)}=1.088$, $p=0.319$), no frequency by drug pretreatment interaction (PFC: $F_{(5,60)}=0.215$, $p=0.955$; HP: $F_{(5,60)}=2.335$, $p=0.053$; EEG: $F_{(5,55)}=0.168$, $p=0.973$) and no 3 way interaction (PFC: $F_{(5,60)}=2.951$, $p=0.056$; HP: $F_{(5,60)}=0.905$, $p=0.484$; EEG: $F_{(5,55)}=0.963$, $p=0.448$). However, there was a frequency by session interaction regardless of whether the rats had received subchronic MK-801 or saline (PFC: $F_{(5,60)}=5.108$, $p=0.008$; HP: $F_{(5,60)}=5.621$, $p=0.017$; EEG: $F_{(5,55)}=106.27$, $p<0.001$), suggesting that like we found previously, acute MK-801 in adulthood alters oscillatory power in a frequency-specific manner. Post-hoc tests revealed that acute MK-801 administration following a subchronic exposure to saline or MK-801 elevated relative power in the high-gamma band (>85 Hz, PFC: $t_{(13)}=4.051$, $p=0.001$; HP: $t_{(13)}=6.602$, $p<0.001$; EEG: $t_{(12)}=4.767$, $p<0.001$), mid-gamma band (40-85 Hz, PFC: $t_{(13)}=3.467$, $p=0.004$; HP: $t_{(13)}=5.807$, $p<0.001$), and reduced power in the beta-band range (12-20 Hz, PFC: $t_{(13)}=3.603$, $p=0.003$; EEG: $t_{(12)}=6.314$, $p<0.001$), similar to the acute effects of MK-801 observed in the adolescent group.

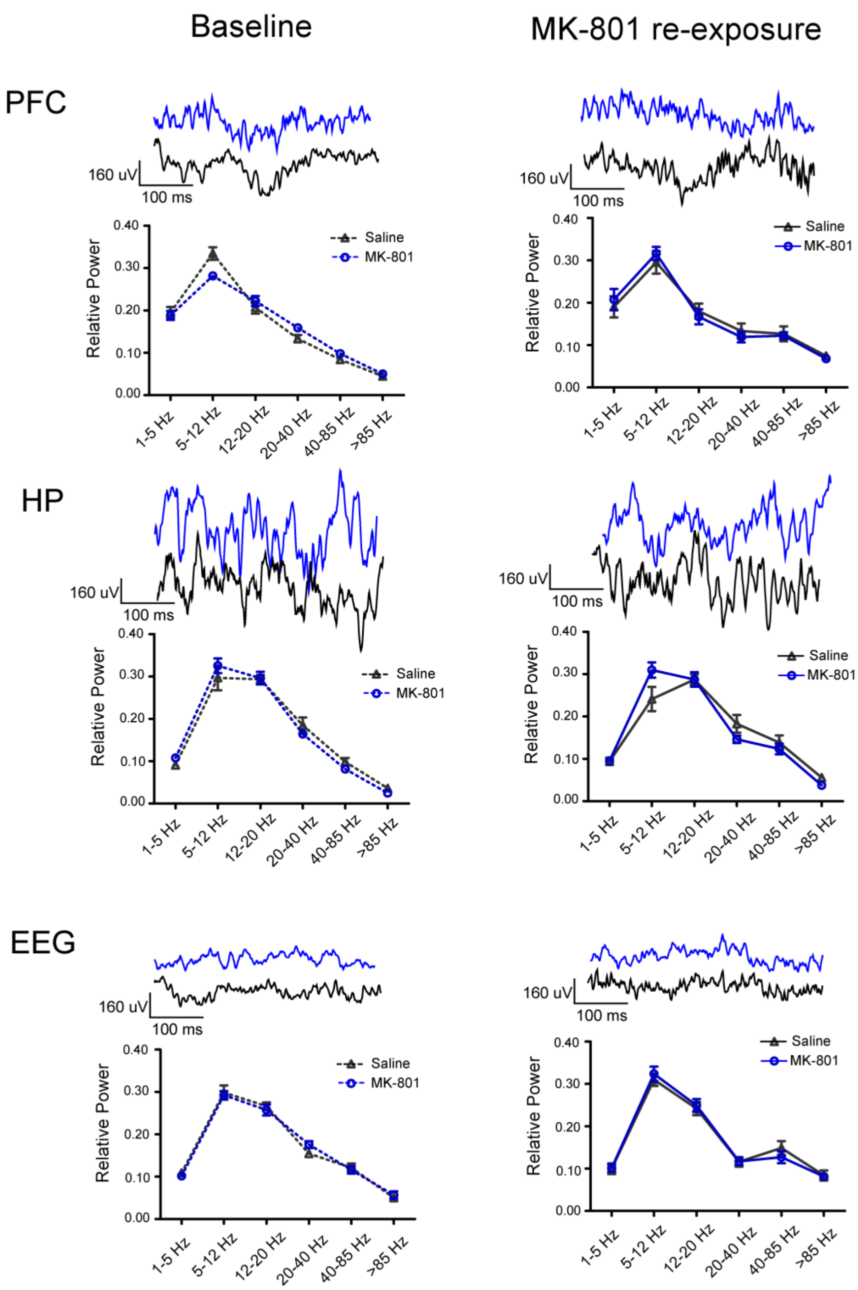

Figure 13. Oscillatory activity in adult rats treated with MK-801 or vehicle in adulthood at baseline *(left)* and after MK-801 challenge *(right)*. Power spectrum density (PSD) plot of medial prefrontal cortex (mPFC) *(top)*, hippocampus (HP) *(middle)* and vertex EEG *(bottom)* from 13 rats during a 300 ms post-stimulation epoch across 5 frequency bands at baseline and after MK-801 (0.1 mg/kg i.p.). Baseline data shown are average values of the three baseline sessions for each animal. Acute MK-801 data is from a single session after acute MK-801 injection. We normalized the evoked power in each of the 5 frequency bands to the total power for each subject, represented here as relative power. Adult subchronic MK-801 did not alter oscillatory activity compared to saline treated animals at baseline or after the acute MK-801 challenge. All data are plotted as mean ± SEM.

Discussion

We found that an acute MK-801 challenge increased mPFC-HP coherence regardless of previous subchronic drug exposure, and that this was found in both the adult and adolescent treated groups. In the adult-treated group, this increase in coherence after acute MK-801 occurred across all frequency bands, whereas in the adolescent group, MK-801 failed to increase coherence in the gamma band in the animals that received subchronic MK-801 in adolescence. This suggests that disruption of NMDAR signaling in adolescence produces a specific blunting of higher-frequency coherence. Interestingly, this effect was observed without disruptions in local oscillatory activity in the HP and mPFC, suggesting that long-range coherence may be more sensitive to adolescent NMDAR-antagonism than local oscillatory activity. These results show that disruption of normal excitatory signaling during adolescence causes long-lasting disruptions in neural communication, specifically in the gamma band, which may have relevance to SZ pathology.

Much evidence has implicated altered NMDAR function in the pathophysiology of SZ (Gilmour et al., 2011; Coyle, 2012; Gonzalez-Burgos and Lewis, 2012), however very little is known about the consequences of disrupting NMDAR activity during adolescence. NMDARs are known to play important roles in neural development via involvement in synaptic pruning (Aamodt and Constantine-Paton, 1999; Woo and Crowell, 2005) and axon myelination (Salter and Fern, 2005). Thus, a disruption in NMDAR activity during a developmental critical period is likely to have a long lasting impact on neural circuit function. Furthermore, cortical maturation is known to occur along a caudal to rostral gradient, with the more frontal cortical areas being the last to mature (Gogtay et al., 2004), which may render the PFC more vulnerable to disruption during adolescence than more caudal regions. Consistent with our results showing disrupted mPFC-HP coherence after adolescent MK-801 exposure, a study by Thomases et al., found that subchronic NMDAR-antagonism during adolescence resulted in impairments in PFC processing of HP inputs, specifically in beta and gamma frequency range, in anesthetized rodents (Thomases et al., 2013). Interestingly, this impairment could be rescued by a GABA-A positive allosteric modulator, suggesting that NMDARs have a critical role in regulating adolescent maturation of GABAergic networks in the PFC. Indeed, NMDAR-antagonists are thought to preferentially affect GABAergic interneuron activity (Homayoun and Moghaddam, 2007). Several studies have shown that subchronic NMDAR-antagonism induces long-lasting reductions in the expression of the activity-dependent calcium-binding protein parvalbumin (PV) in cortical fast-spiking GABAergic neurons (Abdul-Monim et al., 2007; Amitai et al., 2012). Importantly, PV-IN's are also known to undergo extensive maturation during adolescence (Wang and Gao, 2009; Caballero et al., 2013), rendering them potentially more vulnerable to insults during this developmental time. Furthermore, there is substantial evidence suggesting that GABA interneurons, particularly PV-IN's, are critical for precise temporal coordination of cell firing (Cardin et al., 2009; Sohal et al., 2009; Carlén et al., 2011) and for establishing experience-dependent plasticity (Markram et al., 1997; Wespatat et al., 2004). Thus, taking NMDARs offline during adolescence may disrupt the development of precise neuronal coordination and synchrony during adolescence, which in turn can produce the phase-locking deficit seen after re-exposure to MK-801 in adulthood.

Current theories of SZ have posited that pathophysiology may be due to impaired coordination of distributed neural activity (Friston, 1998; Phillips and Silverstein, 2003; Uhlhaas and Singer, 2010). Consistent with these theories is evidence in SZ patients of disruptions in communication between and within brain regions (Ardekani et al., 2003; Burns et al., 2003; Kubicki et al., 2003; Spencer et al., 2008), along with reduced white matter volume (Lim et al., 1999; Ashtari et al., 2007b; Rotarska-Jagiela et al., 2008; Kubicki et al., 2009). A study by Uhlhaas et al., found a reduction in fronto-temporal phase synchrony specifically in the beta-band during Gestalt perception in SZ patients (Uhlhaas et al., 2006). Interestingly, this study did not find alterations in local oscillatory activity in the beta or gamma bands, suggesting that long-range neural coordination may be preferentially disrupted in SZ. This finding of impaired long-range coherence, but intact local oscillations, is in line with our findings in the current study, supporting the idea that abnormal neural synchrony in SZ may be due to the failure of cortical circuits to mature normally during adolescence.

Although we found no effect of adolescent or adult MK-801 subchronic exposure on local mPFC or PFC oscillatory activity, we did observe a robust effect of acute MK-801 challenge in both groups. Consistent with our previous findings in Chapter 1, we found an increase in gamma-band power and a decrease in beta-band power after acute MK-801 in the mPFC, HP and skull surface EEG. Given the substantial evidence showing the involvement of PV-INs in gamma-band oscillatory activity (Cardin et al., 2009; Sohal et al., 2009), we hypothesize that this local oscillatory effect of MK-801 may be related to alteration of GABAergic interneuron activity, perhaps via the interaction of PV and SOM interneurons as discussed in Chapter 1. However this effect was only observed acutely, and we found no long-lasting consequences of adolescent MK-801 exposure on local oscillatory activity. Interestingly, a study using a maternal immune activation model of SZ in mice also found impaired long-range mPFC-HP coherence with intact local oscillatory (Dickerson et al., 2010), suggesting that the maturation of long-range connectivity may be more sensitive to developmental disruption than local network activity.

The fact that we only saw a disruption in long-range synchronization in the adolescent MK-801 treated group after acute MK-801 re-exposure, but not at baseline, brings up the possibility that adolescent NMDAR-antagonism is inducing a priming effect, that on its own does not elicit a disruption in phase-locking, but that renders the circuit more vulnerable to subsequent insults. This concept of a “double-hit” hypothesis has received a lot of attention in relation to SZ (Giovanoli et al., 2013; Pacheco-López et al., 2013), with many positing that an early environmental or genetic insult renders an individual susceptible, but a second environmental hit is then required to transition to full-blown psychosis. For instance, many studies have shown that marijuana use in adolescence is a risk factor for development of psychosis (Arseneault et al., 2004; Moore et al., 2007), and this may be a second hit to already susceptible individuals (Caspi et al., 2005). A similar phenomenon has been demonstrated in rodents where prenatal immune activation paired with stress during adolescence induces cognitive and behavioral impairments in adulthood (Giovanoli et al., 2013). These studies suggest that developmental insults could function as a primer for psychiatric disorders, imparting increased vulnerability for subsequent insults. We hypothesize that this type of phenomenon may be at play in our current model, where developmental NMDAR-hypofunction during a critical period of cortical maturation and reorganization renders the circuit more vulnerable to effects of MK-801 re-exposure later in life. Importantly, we did not see the same effects in the animals exposed to subchronic MK-801 during adulthood, suggesting that NMDAR disruption during a critical period of development such as adolescence elicits a more robust effect that the same disruption experienced by a more mature circuit. Indeed, Raver et al., recently demonstrated persistent oscillatory deficits after adolescent, but not adult, exposure to THC in mice (Raver et al., 2013). Taken together with previous studies, our data support the hypothesis that adolescence is a critical period for cortical development and that disruption to normal maturation may cause long-lasting consequences.

Overall, we can conclude that our model of long-range synchrony disruptions following adolescent exposure to NMDAR-antagonists maps well onto what is known about the developmental trajectory of SZ, and provides an intriguing model to study electrophysiological deficits seen in SZ patients. Furthermore, previous studies in SZ patients and in animal models of SZ have shown a strong relationship between long-range synchrony measures and cognitive function (Uhlhaas et al., 2006; Sigurdsson et al., 2010), suggesting that disruptions in fronto-temporal connectivity may be causal in the cognitive deficits in the disorder. Given that mPFC-HP phase-locking in the theta band has been shown to increase with learning (Jones and Wilson, 2005), we may expect that our finding of increased theta coherence after acute MK-801 re-exposure would be beneficial to cognitive function. However, it is also possible that this increase in coherence in the absence of learning may actually be disruptive and may contribute to working memory deficits and thought disorder. Future studies will be needed to determine the cognitive effects of our adolescent MK-801 paradigm and if cognitive performance correlates with mPFC-HP synchrony.

Chapter 5: General Discussion

Overall Summary

Throughout my thesis work I have demonstrated the feasibility of recording skull-surface EEG signals in freely moving rodents, and have evaluated their potential as a cross-species translational approach for studying neurophysiological alterations in schizophrenia. Using acute NMDAR-antagonism to compare EEG signals between human subjects and rodents, I found a shift in power from low to high frequency after acute MK-801 administration in rodents which is very similar to the oscillatory effects after acute ketamine infusion in humans, providing support for the use of this EEG technique moving forward. In order to explore underlying mechanisms of altered oscillatory activity, I tested how a NMDAR-antagonists and a GABA-A channel blocker affected local oscillatory activity in the HP, A1 cortex and skull surface EEG, and found that GABA-A blockade reduced EEG beta power similarly to acute MK-801, but did not affect gamma band power. These effects suggest that the increase in gamma power induced by NMDAR antagonism may be due to actions on a specific subtype of GABAergic interneurons and not on an overall reduction in interneuron activity. I also tested whether chronic NMDAR antagonism had differing effects from acute exposure, and although I did not see a robust frequency-specific shift in response to chronic MK-801 exposure, I did observe a general blunting of total oscillatory power across all frequencies. Finally, given the late-adolescent onset of symptoms in schizophrenia, I explored whether developmental disruption of NMDAR signaling has enduring neurophysiological consequences in adulthood. I found that rats exposed to 5 days of NMDAR-antagonism during adolescence showed decreased gamma synchrony between the mPFC and HP that was evident after re-exposure to MK-801 during adulthood. The same treatment given to adult rats did not produce this disruption, suggesting that adolescent disruption of NMDA signaling may have more robust long-term effects than a similar adult disruption. Overall, the experiments presented in this Dissertation provide support for the use of EEG as a cross-species translational tool to study schizophrenia across multiple animal models.

Cross-species translation of EEG

The first goal of this dissertation work was to establish a novel approach for acquiring electroencephalogram (EEG) from freely moving rodents in a manner similar to the way EEG are acquired in human subjects. EEG abnormalities in schizophrenia patients have been well-characterized over the past several decades (Cho et al., 2006; Rutter et al., 2009; Uhlhaas and Singer, 2010; Hong et al., 2012), and provide a non-invasive approach to understanding the underlying pathophysiology of schizophrenia. However, most rodent EEG studies in the past have been conducted using implanted electrodes that are in direct contact with brain tissue or sub-dural space, referred to as local field potentials (LFP), which is methodologically quite different from the scalp-electrode approach used in human EEG studies. LFP electrodes in direct contact with brain tissue can capture strong regional signals that may differ from the activity recorded from the skull. Additionally, human EEG signals are greatly attenuated and “smoothed” by non-conductive tissue (i.e., the skull and skin) which would not occur when recording from electrodes within the brain. Therefore, although LFPs are useful for measuring spatially specific neural activity, questions remain on how well signals recorded via direct contact with brain tissue approximate scalp EEG signals.

Some studies exploring EEG in rodents have done so using anesthetized animals, which can significantly alter the neural signals obtained. Different stages of sleep and consciousness are known to manifest themselves with different EEG signatures, from slow-wave sleep which is characterized by high-amplitude low frequency activity, to REM sleep that is characterized by lower amplitude activity in the theta-beta ranges (Inostroza and Born, 2013). Furthermore, the auditory steady state response (ASSR) has been shown to be reliably altered by state of consciousness and is even utilized as a metric for appropriate levels of anesthesia during surgery (Plourde and Picton, 1990; Plourde and Boylan, 1991; Plourde, 1996). Taken together, this indicates that EEG signals are robustly altered by level of consciousness making recordings in anesthetized rodents less desirable for translational studies. Thus, it was important for our method of EEG recording to be amenable for use in freely-moving rodents. Furthermore, the EEG and ERP paradigms we chose to examine involve pre-attentive information processing, meaning that the subject does not actively have to attend to or respond to the auditory stimuli in order for a robust neural response to be detected. This enabled us to readily implement the same EEG measures used in human studies in our rodent models without having the added complexity of training the animals on a behavioral paradigm.

Using our novel EEG method, in which disc electrodes were chronically affixed to the intact skull of the rat, we assessed how well rodent EEG signals reflect human EEG signals across several different EEG and ERP measures known to be altered in schizophrenia patients (Chapters 1 & 2). Furthermore, we were able to assess if different experimental manipulations such as acute or chronic NMDAR-antagonism (Chapter 1), neonatal ventral hippocampal lesion (NVHL) (Appendix I), or adolescent NMDAR-antagonism (Chapter 3) recapitulated EEG deficits seen in schizophrenia patients. Importantly, all experimental parameters and signal processing approaches in these studies were adapted from those used in human EEG studies in order to increase the translatability of the findings across species.

A. Skull-EEG Oscillatory responses

Neural oscillations can be assessed and analyzed using several different methods depending on the particular design of each study. Oscillations that are tightly time and phase-locked to a given stimulus are referred to as evoked oscillations, while activity that is modulated by a stimulus but not strictly phase-locked to event onset are called induced oscillations (Gandal et al., 2011). Furthermore, there is also background oscillatory activity that is not time or phase locked to a stimulus but that contributes to the total EEG signal. Some analysis procedures utilize a baseline subtraction to normalize the post-stimulus signal to a pre-stimulus baseline. However, this can be problematic when groups differ in background oscillatory activity, which has been noted in schizophrenia (Winterer et al., 2004). We mirrored our approach for this study on that used by Hong et al., 2010 which measured total power in response to a short white-noise click using a discrete wavelet transform. This method measures oscillations that include both stationary and non-stationary oscillatory responses associated with the stimulus in a single-trial manner.

Figure 14. Comparison of Auditory evoked oscillations in rodents (left) and humans (right) under acute NMDAR-antagonism. Figure reproduced with permission from L.E Hong.

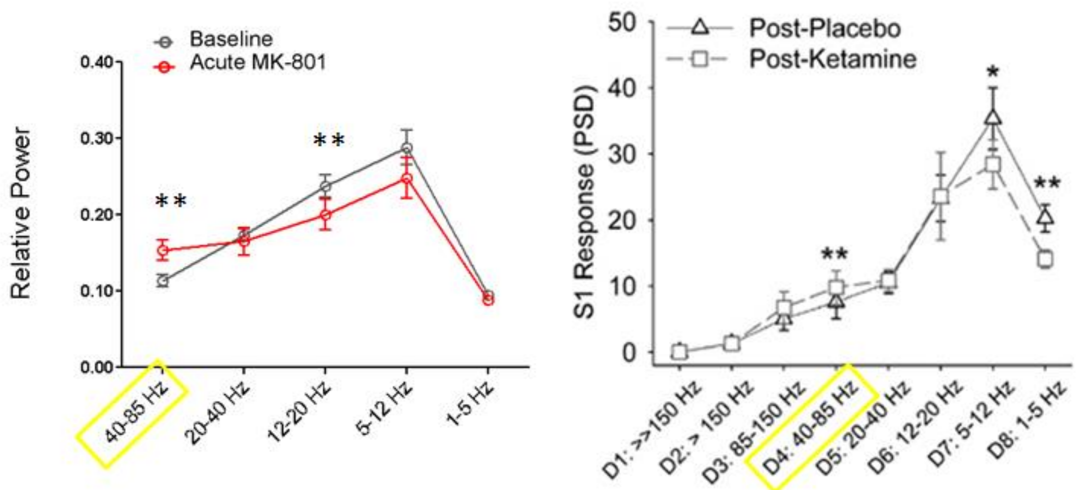

We found that oscillatory responses to auditory stimuli in rodents under acute NMDAR-antagonism showed remarkable similarities to what is seen in humans under similar conditions (Chapter 1). A study by Hong et al., measured EEG in healthy control human subjects after infusion of subanesthetic ketamine in a double-blind, placebo controlled, cross-over study and found that ketamine significantly increased high-frequency gamma band oscillations, reduced low-frequency oscillations, and increased disordered thought and dissociative symptoms (Hong et al., 2010). This finding in humans directly parallels our finding of a shift from low-frequency to high-frequency power in rodents under NMDAR-antagonism (Figure 13), supporting the hypothesis that EEG oscillations are highly translatable across species when recorded in a similar manner. Importantly, in Chapter 3 we replicated this same oscillatory shift in power from low to high frequency with acute MK-801 in the HP, mPFC and EEG. These results are also consistent with previous studies in rodents using NMDAR-antagonism (Pinault, 2008; Ehrlichman et al., 2009a; Hakami et al., 2009), suggesting that the NMDAR antagonist-induced elevation in gamma power is conserved across species and is very reproducible. Given that we have established that high and low frequency oscillatory activity can be measured with this EEG approach, this opens up the possibility of exploring oscillations in other animal models.

The synchronous firing of groups of neurons is thought to facilitate precise temporal communication over short and long distances within the brain (Buzsáki, 2006). Thus, it is hypothesized that altering the dynamics of these neural oscillations would result in impaired cognitive activities such as information processing and working memory in which the brain is required to integrate different types of information and form a coherent entity. Indeed, studies in schizophrenia patients have demonstrated aberrant oscillations particularly in the beta and gamma bands during working memory tasks (Basar-Eroglu et al., 2007; Haenschel et al., 2009; Barr et al., 2010), suggesting that abnormal oscillatory activity may be contributing to cognitive deficits in the disorder. Given that we can obtain consistent high-frequency oscillatory activity using the approach developed in this project, exploring if cognitive deficits in rodent models of schizophrenia are related to aberrant oscillatory activity is an intriguing future direction.

B. Gating of Auditory evoked potentials.

Clinical observations have suggested that schizophrenia patients are unable to correctly filter out irrelevant sensory stimuli (Brockhaus-Dumke et al., 2008), which has been attributed to a deficient inhibitory neural signaling (Adler et al., 1982). This phenomenon can be measured experimentally in humans and rodents using a paired-click paradigm, where two identical auditory clicks are presented with a 500ms inter-stimulus interval (ISI) and the amplitudes of the averaged evoked potentials are measured. The first large positive-going peak of the AEP occurs approximately 50 ms after the stimulus and is referred to as the P50 or P1 wave. P50 waves are generated in response to each click, and in control subjects the magnitude of the response to second click of the pair is reduced or gated compared to the first. The magnitude of the suppression of the second click compared to the first is an index of sensory gating (Turetsky et al., 2007). Schizophrenia patients generally show a reduction in P50 gating compared to controls, which has been interpreted to be indicative of deficient inhibitory mechanisms, resulting in the inability to ignore irrelevant stimuli (Adler 1982, Boutros 1991, Freedman 1983, Nagamoto 1989). However, when healthy controls are given ketamine, this P50 deficit is not seen (Oranje 2002, Hong 2010), suggesting that this gating deficit is not reproduced by acute ketamine administration. Thus, it is important when embarking on translational studies in rodents to appreciate that not all domains may mirror deficits seen in schizophrenic patients.

We found intact P50 auditory sensory gating in rats after acute NMDAR-antagonism which is in line with human EEG studies (Chapter 1). However, this lack of effect on paired-click gating is not as consistent in the literature, as some rodent studies have shown disruption of gating after acute NMDAR-antagonism using LFP recordings (Dissanayake et al., 2009; Ma et al., 2009). These differing results throughout the literature may be a result of different drugs, doses, or possibly due to recording method (i.e. LFP vs. EEG). However, compared to the high reproducibility of gamma-band oscillations using NMDAR-antagonists, paired-click gating has proven to be quite variable across studies, rendering it less useful as a cross-species translational biomarker.

Furthermore, there is not a consensus in the literature on what the rodent equivalent of the P50 component in humans is, as some groups use the P20 wave (Bickel et al., 2008; Vohs et al., 2009; Broberg et al., 2010) and others use the N40 wave (Stevens et al., 1995; Swerdlow et al., 2006). It will important for furture studies to investigate further what the rodent equivalanet of the human P50 wave, and what methods for recording are the most consistent.

C. Mismatch Negativity

Schizophrenia patients also show a consistent deficit in mismatch negativity (MMN), which is an ERP component elicited when a sequence of repetitive standard sounds is interrupted infrequently by deviant “oddball” stimuli. MMN is an index of auditory sensory or echoic memory and of context-dependent information processing at the level of the primary and secondary auditory cortices (Näätänen & Kähkönen 2009). Typically, the deviant tone will elicit an evoked response with a larger N1 amplitude compared to the standard tones, and the difference between the standard and deviant response is used to quantify the extent of MMN. Schizophrenia patients have decreased MMN amplitude compared to healthy controls, which is indicative of impaired pre-attentive deviance detection (Javitt et al. 1993; Hong et al. 2012). A meta-analysis in 2005 of 32 studies that measured MMN in schizophrenia patients found the average effect size of the MMN deficit to be 0.99, which is quite a robust effect by common standards (Umbricht and Krljes, 2005). Furthermore, this effect is seen across varying auditory stimulation parameters, in which the deviant tone differs in pitch, duration or intensity. Compared to some other EEG measures which show considerable variability across studies, reduced MMN in schizophrenic patients appears to be one of the most consistent and robust effects, which makes it an attractive candidate for use in translational studies.

Given that normal MMN expression depends strongly on auditory sensory memory, impairments in schizophrenia patients supports the idea that cognitive deficits in schizophrenia may be not only be evident during complex working memory tasks, but also during early steps of information processing. Indeed, MMN deficits are particularly pronounced in patients with severe cognitive deficits (Baldeweg et al., 2004). The fact that information processing impairments are evident even during basic sensory processing tasks increases the ease of implementing this measurement in animal models. One study in a genetic mouse model of schizophrenia found attenuated MMN in the transgenics along with deficits in contextual fear conditioning and social interactions (Ehrlichman et al., 2009b), suggesting that MMN has translational potential in rodents. However, despite strong interest in translating MMN into rodent models of schizophrenia, there have been few other reports in the literature of use in rodents.

In Chapter 1, we demonstrated that we could acquire MMN-like activity from the skull EEG in freely moving rodents; however, we did not find any effect of NMDAR-antagonism. This was surprising to us given that MMN has been shown to be attenuated by NMDAR-antagonists in both human subjects and non-human primates (Javitt et al., 1995; Umbricht et al., 2000). One possibility for our lack of effect with acute NMDAR-antagonism is that we had a high amount of variability of responses from session to session; suggesting that this response may not be very stable and that much larger groups would be needed to detect consistent effects. Alternatively, there is an ongoing debate about whether deviance-related activity in rodents is homologous to humans. One study in mice found MMN-like activity only using a tone-duration oddball paradigm but not a frequency-oddball paradigm as was used in our current study (Umbricht et al., 2005). Thus, it is possible that a more consistent effect could be detected using different auditory parameters.

Interestingly, however, we did find a reduction in MMN in NVHL rats compared to sham animals (Appendix 1). Furthermore, we found that NVHL rats treated as juveniles with the antioxidant, N-acetyl-cysteine (NAC), showed significantly elevated MMN compared NVHL without NAC treatment. This suggests that increased oxidative stress early in life may contribute to MMN deficits in adulthood, and that preventing oxidative stress may prevent neurophysiological deficits resulting from the NVHL. This finding is in line with studies in humans showing that adjunct treatment with NAC improved negative symptoms and corrected mismatch negativity deficits in schizophrenia patients (Berk et al., 2008; Lavoie et al., 2008). The fact that we were able to detect a significant MMN deficit using the NVHL model and not the NMDAR-antagonist model suggests that certain rodent models may be better suited for studying MMN than others. Moving forward, it will be important to examine further if the deviance-related signal we see in rodents is actually homologous to human MMN, and if this signal is disrupted in other rodent models of schizophrenia.

GABAergic interneuron dysfunction in schizophrenia

After establishing the feasibility and reliability of EEG and ERPs in rodents, we aimed to investigate the role of inhibitory and excitatory signaling in these measures. Impaired inhibitory circuitry has been heavily implicated in the pathophysiology of schizophrenia (Nakazawa et al., 2011). There are many different subtypes of GABAergic cells in the cortex that can be classified by their firing properties and the expression of certain peptides or calcium-binding proteins. Additionally, interneuron subtypes differ in their morphology and the targets of their projections with some subtypes making perisomatic contact with pyramidal cells and others targeting distal dendrites (Gonzalez-Burgos and Lewis, 2008). Furthermore, many GABAergic subtypes synapse onto other interneurons in addition to pyramidal cells. This complex network of inhibition results in flexible yet fine-tuned control over neural circuit function.

Postmortem studies in schizophrenia patients have found decreases in the enzyme responsible for synthesizing GABA in two subtypes of interneurons: parvalbumin (PV)-containing fast-spiking neurons and somatostatin (SOM)-containing regular-spiking interneurons (Akbarian et al., 1995; Hashimoto et al., 2003; Morris et al., 2008). These studies are suggestive of reduced inhibitory control of pyramidal cells, however, it is not known if these alterations are a primary consequence of the disorder or due to compensatory mechanisms (Gonzalez-Burgos and Lewis, 2008). Physiologically, PV-IN's have been shown to be especially important in generation of neural oscillations *in vivo*, due to their perisomatic innervation and fast-spiking phenotype (Cardin et al., 2009; Sohal et al., 2009). Thus, an alteration in the ability of interneurons to control cortical circuitry is hypothesized to contribute to altered oscillations in schizophrenia.

A. GABAergic interneurons and gamma oscillations: Insights from NMDAR-antagonism

NMDAR antagonists such as ketamine have acute psychotomimetic effects in healthy subjects including hallucinations, thought disorder and impairments in working memory that are reminiscent of symptoms of schizophrenia patients (Krystal et al., 1994; Malhotra et al., 1996; Rowland et al., 2005a). Neurophysiologically, NMDAR-antagonists alter neural oscillations in the gamma band (Hong et al., 2010), which is also commonly seen in patients with schizophrenia, suggesting that acute NMDAR-antagonism may be a useful model to study neurophysiological alterations in schizophrenia. However, the exact mechanisms mediating the effects of NMDAR-antagonism are not fully understood.

Studies in rodents have demonstrated that non-competing NMDARs like ketamine, MK-801 and PCP may act preferentially on GABAergic interneurons more than pyramidal cells (Homayoun and Moghaddam, 2007), thereby producing a state of disinhibition in the cortex (Moghaddam et al., 1997) that could lead to increases in high-frequency oscillatory activity. If this is true, and NMDAR antagonists produce increased gamma-band activity by inhibiting interneuron activity, then directly blocking fast inhibitory transmission in pyramidal cells should mimic this gamma power elevation. Therefore, in Chapter 1 we examined whether blockade of fast GABAergic neurotransmission produced the same EEG effects as NMDAR antagonists by recording oscillatory activity from skull surface EEG and LFP activity in the HP and A1. We found that although both MK-801 and PTX produced a similar decrease in beta-band power, only MK-801 caused an increase in gamma-band activity. Similarly, in Chapter 2 we examined the effects of MK-801 and PTX on the ability of the A1 cortex to generate and sustain synchronous activity driven by auditory click-trains, and found a frequency specific increase in intertrial coherence (ITC) at 20 and 40 Hz stimulations after acute MK-801, but no effect of PTX. Taken together, this suggests that a global decrease in fast-inhibitory transmission via PTX is not sufficient to mimic the gamma band increase observed with NMDAR-antagonists because if MK-801 was acting to inhibit NMDAR transmission on all GABAergic-INs, we would expect to see identical effects of PTX and MK-801. This supports the idea that MK-801 may be acting at a specific subtype of GABAergic cells, such as PV-INs, in order to produce the high-frequency power increase seen in our data.

Indeed, optogenetic studies suggest that driving PV-INs can increase gamma oscillations, and that inhibiting these cells can suppress this activity (Cardin et al., 2009; Sohal et al., 2009). However, if the mechanism of action of MK-801 is to block NMDARs preferentially on PV-INs, thus reducing the activity of these neurons, we would expect a gamma-power decrease instead of the increase that we see. One potential mechanism that we propose to explain the increase in gamma-power is that MK-801 may be preferentially acting on a different subtype of interneurons that project to PV-INs in order to alter their activity (Figure 14). A recent study in mouse visual cortex showed that SOM-INs strongly inhibit other interneuron subtypes, including PV cells, but do not inhibit each other, whereas PV cells send very few projections to other subtypes of interneurons, but strongly inhibit each other (Pfeffer et al., 2013). Thus, it is possible that NMDAR-antagonists preferentially inhibit SOM-INs, which in turn alter PV-IN and pyramidal cell activity to produce circuit disinhibition (Lewis, 2014). Furthermore, postmortem studies in schizophrenia patients also show altered somatostatin mRNA levels (Morris et al., 2008; Fung et al., 2010), suggesting that this subtype of cells may also contribute to oscillatory impairments in schizophrenia.

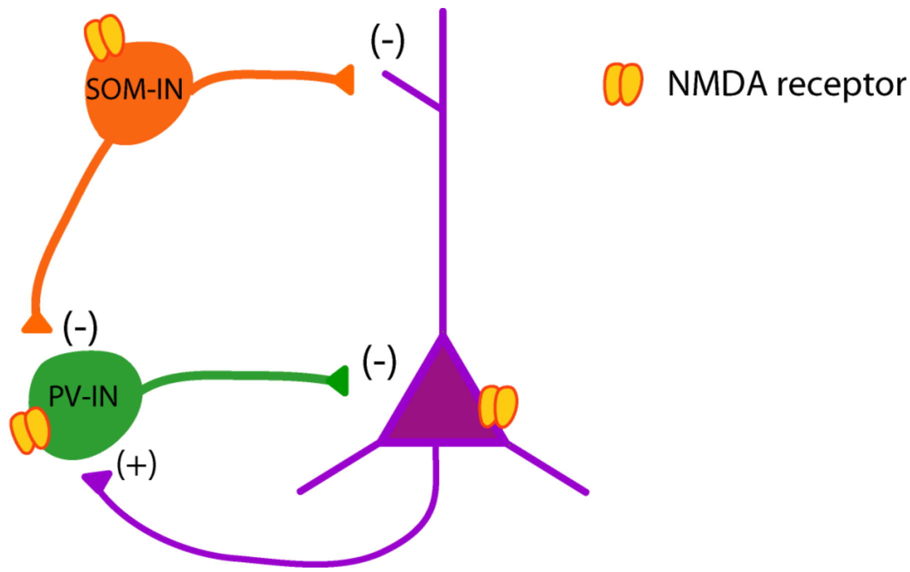

Figure 15. Complexity of local excitatory-inhibitory circuitry. While research into the effects of NMDAR-antagonists has focused on parvalbumin (PV) interneuron and pyramidal cell dynamics, other subtypes of GABAergic interneurons, such as somatostatin-expressing (SOM) interneurons also express NMDA receptors and provide an important source of inhibition within the cortex.

Another factor to take into account in interpreting pharmacological vs. optogenetic studies is that the nature of the inhibition or stimulation may be very different depending on the approach used. For instance, optogenetic inhibition of PV-INs using halorhodopsin would function to prevent the cell from firing regardless of the nature of the inputs to the cell, whereas MK-801 would only reduce excitatory transmission through NMDARs, leaving AMPARs intact. Thus, even if MK-801 is acting in a cell-type specific manner, pharmacological blockade of NMDAR transmission may be less robust or have different consequences than optogenetic inhibition. Overall, the work presented in this thesis supports the hypothesis that MK-801 acts in a cell-type specific manner to alter neural oscillations, but future studies will be needed to fully flesh out the exact mechanisms at play.

Acute vs. chronic NMDAR-antagonist administration: Relevance to schizophrenia

In addition to exploring acute models of NMDAR-antagonism, there is considerable support for utilizing chronic NMDAR-antagonist exposure to study schizophrenia. Long-term ketamine or PCP use is associated with cognitive deficits, reduced frontal lobe blood flow and decreased glucose utilization (Hertzmann et al., 1990; Wu et al., 1991; Morgan and Curran, 2006), which is consistent with the hypothesis that cognitive deficits in schizophrenia may be due to a state of "hypofrontality" (Weinberger and Berman, 1988). In a longitudinal study, Morgan et al., found that frequent ketamine users (more than 4x a week) had impaired episodic and working memory as well as impaired executive function. However, infrequent users or users that had been abstinent for at least 1 month (ex-ketamine users) showed no significant cognitive impairments (Morgan et al., 2009, 2010). This indicates that there may be cognitive deficits from chronic ketamine use, even in the drug-free state. However, these impairments may resolve after prolonged abstinence from the drug and may not be permanent.

Chronic NMDAR antagonism cannot be studied in a controlled way in human subjects due to ethical reasons, thus in order to fully study consequences of chronic NMDAR antagonism research must move into animal studies. Behavioral effects of chronic NMDAR-antagonists have been studied (see General Introduction), however very little is known about long-lasting neurophysiologic effects. In this study we aimed to address whether causing a state of enduring NMDAR hypofunction via chronic NMDAR-antagonist administration in adulthood would disrupt oscillatory activity when tested in the drug-free state (Chapter 1). Surprisingly, we found no effect of chronic MK-801 on tone-evoked oscillations tested 24 h after the last drug administration. However, we did find a significant decrease in total broadband power, suggesting that repeated NMDAR-antagonism may blunt oscillatory activity in a non-frequency specific manner. This effect could possibly be due to habituation to the effects of the drug over time. Indeed, repeated NMDAR-antagonism has been shown to attenuate PCP-induced glutamate release (Amitai et al., 2012) and also to induce a behavioral tolerance to repeated injections of MK-801 (Manallack et al., 1989). Furthermore, other studies measuring neural oscillations several weeks after chronic NMDAR antagonism found reduced theta and gamma power (Featherstone et al., 2012; Kittelberger et al., 2012) which suggests that perhaps withdrawal from chronic NMDAR-antagonist exposure induces a long-lasting reduction of oscillatory activity. Although we did not see robust frequency-specific oscillatory impairments in our data, the fact that we did see a dampening of overall activity along with previous studies showing reduced gamma-band activity after chronic NMDAR-antagonism suggests that chronic administration paradigms should be studied further. It is possible that withdrawal after chronic NMDAR-antagonist exposure may more accurately reflect oscillatory impairments, such as reduction in gamma-band activity, commonly seen in patients with schizophrenia.

Developmental timing of NMDAR-antagonism

An important aspect of schizophrenia is the characteristic onset of symptoms during the transition between adolescence and adulthood (Häfner et al., 1993). However, it is currently unknown how NMDAR-antagonist models may relate to this adolescent vulnerability. Early developmental exposure to NMDAR-antagonists in the first two weeks of life has been studied as a potential model for schizophrenia in animals, with studies showing that early postnatal ketamine administration can cause decreased PV expression (Wang and Johnson, 2005; Behrens et al., 2007), disrupted sensorimotor gating (Wang et al., 2001), and impaired working memory (Andersen and Pouzet, 2004). However, this early exposure does not address what may trigger symptom onset during late adolescence. Recently, it was shown that adolescent exposure to an antimitotic agent, methylazoxymethanol (MAM), caused persistent sensorimotor gating deficits in adulthood (Guo et al., 2013), suggesting that later developmental time points, such as those during adolescence, may be crucial for normal development of circuits supporting sensorimotor gating. Similarly, Raver et al., found that subchronic exposure to THC during adolescence caused persistent neural oscillatory deficits in adulthood, however, exposure during adulthood did not cause these effects (Raver et al., 2013), highlighting the importance of adolescent development in shaping oscillatory activity.

Adolescence is a time of significant cortical maturation, marked by the emergence of high-frequency oscillations and cross-region coherence (Rojas et al., 2006; Uhlhaas et al., 2009, 2010). In light of our previous study demonstrating a robust, but transient, alteration of local oscillatory activity in the HP and skull surface EEG (Chapter 1), we tested if blocking NMDARs during adolescence would produce a more long-lasting alteration of neural function (Chapter 3). We found that although adolescent NMDAR-antagonism did not alter local oscillatory activity, we did find a disruption in mPFC-HP phase synchrony, suggesting that NMDAR signaling during adolescence is important for establishing precise long-range communication. Indeed, NMDAR-mediated currents have been shown to play a role in activity-dependent myelineation in the CNS (Lundgaard et al., 2013). Given that that myelination increases throughout adolescence (Ashtari et al., 2007a), it is possible that disrupting NMDAR signaling during this time may affect the white matter integrity on long-axonal tracts, and that this may be responsible for the neural synchrony abnormalities seen in our study. Additionally, NMDAR-signaling is also crucial for experience-dependent plasticity, in which synchronized activity of afferent inputs can trigger LTP and synapse stabilization, and asynchronous activity may promote synapse elimination (Bear, 2003). This experience-dependent plasticity may be especially crucial during adolescence given the robust cortical reorganization and synapse elimination occurring during this time (Huttenlocher, 1979; Hoffman and Dobscha, 1989). Thus, it is possible that disruption of NMDA signaling during adolescence would lead to an altered pattern of synaptic stabilization and decreased axonal myelineation, resulting in the impaired transmission of information in the brain.

Abnormal neural synchrony and cognitive impairments in schizophrenia

Synchronous firing of distributed populations of cells is thought to mediate information processing in the brain. This synchrony allows certain cell assemblies that represent the same object or are involved in a common tasks to be activated simultaneously with millisecond precision (König et al., 1996). Precise neural synchronization in the beta to gamma-band range occurs in sensory, motor and association structures, and has been demonstrated across a wide range of species, suggesting that this is a highly conserved mechanism for binding distributed information (Engel and Singer, 2001). Studies in monkeys and cats have demonstrated that inter-region synchrony is enhanced during tasks where selective attention is necessary (Steinmetz et al., 2000; von Stein et al., 2000). In a study in which cats were trained to perform a visuomotor coordination task, Roelfsma et al., found evidence of increased synchrony between the visual and motor cortices specifically during epochs of the task where the animal had to attend to visual cues in order to initiate a motor response (Roelfsema et al., 1997). In humans, EEG studies also have demonstrated enhanced inter-region synchrony, particularly in the gamma-band range, during tasks requiring associative learning (Miltner et al., 1999), facial recognition (Rodriguez et al., 1999), and emotional evaluation (Müller et al., 1999). Taken together, these studies suggest that increased long-range synchrony may constitute a mechanism to enhance communication between brain regions involved in cognitive and behavioral tasks that is conserved across species.

Given that high-frequency activity is elicited during cognitive tasks, it is hypothesized that conditions with cognitive impairments may show disrupted activity in this range. Indeed, while healthy controls show elevated phase synchrony in the beta-frequency range during Gestalt perception, schizophrenia patients show blunted synchrony in the this range (Uhlhaas et al., 2006). Importantly, this study found that poor performance on the perceptual task was correlated with reduced phase synchrony, suggesting that impaired long-range synchrony may be causally related to cognitive or perceptual deficits in schizophrenia patients; however the cause of this impairment is unclear. It has been hypothesized that developmental disturbances may lead to altered connectivity in adulthood, but this has not been fully explored. In Chapter 3, we found that disrupting NMDAR signaling during a critical period of adolescent development causes reduced mPFC-HP coherence in the gamma band after MK-801 re-exposure in adulthood. Although our task was a simple pre-attentive auditory sensory processing task, our results are quite similar to those observed in schizophrenia patients, suggesting that signaling through the NMDAR during adolescence is critical for establishing proper long-range synchrony. Furthermore, we have demonstrated that adolescent NMDAR-antagonism may be a useful model for further studies into the mechanisms of cross-regional synchrony deficits in schizophrenia. An important next step would be to investigate this mPFC-HP synchrony in animals during a behavioral task requiring attention and information processing in order to determine if similar synchrony deficits are seen.

In contrast to observations showing decreased inter-region coherence during a visual processing task in schizophrenia patients, several studies have found elevated frontal gamma-power compared to healthy controls during N-back working memory tasks. Basar-Eroglu et al., showed that while healthy controls had increased gamma-band activity with increasing task difficulty, schizophrenia patients did not show gamma modulation in relation to task difficulty and actually showed elevated gamma activity compared to controls at all cognitive loads (Basar-Eroglu et al., 2007). Similar evidence of excessive gamma activity during working memory tasks was observed by Barr et al., accompanied by a reduction in beta-band activity in schizophrenia patients, indicating a shift from lower to higher frequency activity during the task in schizophrenia patients

(Barr et al., 2010). These studies suggest that in order to achieve similar cognitive performance, schizophrenia patients had to evoke more gamma activity than healthy controls. Alternatively, this excessive gamma-band activity may be aberrant and in fact be detrimental to performance. For example, auditory hallucinations in schizophrenia patients are associated with increased power or synchrony of beta and gamma activity (Spencer et al., 2009; Mulert et al., 2011), suggesting that too much high-frequency activity may reflect impaired information processing.

Given the substantial evidence of altered gamma-band activity in schizophrenia patients, therapeutic approaches that normalize cortical excitability may be promising targets for addressing symptoms in schizophrenia. Indeed, preclinical studies of an mGluR2/3 agonist LY354740, which reduced ketamine-induced glutamate levels without affecting baseline glutamate levels in rodents (Moghaddam and Adams, 1998), showed promise for testing this idea. In preliminary clinical trials, LY354740 showed comparable efficacy at treating positive and negative symptoms and had notably fewer metabolic and motor side effects compared to a current atypical antipsychotic (Patil et al., 2007). However, follow-up trials no longer showed efficacy at reducing symptoms compared to placebo (Kinon et al., 2011). It is important to note that the atypical antipsychotic that the mGluR2/3 agonist was tested against in this follow-up trial also failed to show greater efficacy than placebo, making the results difficult to interpret. Although clinical trials into this compound have stalled, the promising initial effects have prompted the investigation into other similar approaches, such as mGluR5 positive allosteric modulators, that may be a promising solution to treat schizophrenia with fewer side effects. Given the substantial evidence for disrupted neural synchrony in schizophrenia and the connection to cognitive impairments, it may also prove useful moving forward to explore pharmacological manipulations that can normalize or correct aberrant synchronous neural activity. In that vein, if future studies can establish correlations between altered neural oscillations symptom clusters in animal models, the EEG technique established in the course of this thesis work may prove extremely useful as a screen for novel therapeutic approaches.

Overall conclusions

NMDAR-antagonist models have provided great utility to the field of schizophrenia research due to the fact that acute administration reproduces many symptoms of schizophrenia and that this pharmacological manipulation can be used in both human subjects and in animal studies. However, our data and others have shown that acute NMDAR-antagonists do not reproduce many of the neurophysiological findings seen in schizophrenia. For example, while schizophrenia patients consistently show reduced gamma-band power and coherence during simple sensory processing tasks, acute NMDAR-antagonism in rodents and in healthy control subjects causes increased gamma activity. Although NMDAR-antagonism does not produce gamma alterations in the same direction as in schizophrenia patients, these studies have helped elucidate the role of glutamate-GABA interactions in generation of oscillations at different frequencies. Thus, although acute NMDAR-antagonist models may not reproduce all aspects of schizophrenia, they have proved very useful for exploring mechanisms of disrupted network dynamics that have relevance to abnormal synchrony in the disorder. Going forward, it will be important to build on what we have learned from acute NMDAR disruption models and incorporate this into a developmental framework with the goal of recapitulating the late adolescent onset of symptoms. The work in this thesis has pointed to subchronic NMDAR-antagonism during adolescence as a potential approach for modeling long-range synchrony deficits. It would also be interesting to investigate if this adolescent disruption paired with a genetic predisposition or other early developmental insult would trigger a more robust effect in the adult brain. Overall, the work in this Dissertation has paved the way for the use of EEG paired with deep-electrode recordings in order to investigate the underpinnings of abnormal neural synchrony in schizophrenia, and suggested a new approach for modeling long-range synchrony deficits in the disorder.

Appendix I: Juvenile antioxidant treatment prevents adult deficits in a developmental model of schizophrenia[4]

Jan Harry Cabungcal[1]*, Danielle S. Counotte[3]*, Eastman Lewis[2,3]*, Hugo A. Tejeda[2,3], Patrick Piantadosi[3], Cameron Pollock[3], Gwendolyn G. Calhoon[2,3], Elyse Sullivan[2,3], Echo Presgraves[3], Jonathan Kil[4], L. Elliot Hong[2,5,6], Michel Cuenod[1], Kim Q Do[1]¶, Patricio O'Donnell[2,3,5]¶

[1] Centre for Psychiatric Neuroscience, Department of Psychiatry, Lausanne University Hospital, Lausanne, Switzerland.

[2] Program in Neuroscience, University of Maryland School of Medicine, Baltimore, MD, USA.

[3] Department of Anatomy & Neurobiology, University of Maryland School of Medicine, Baltimore, MD, USA.

[4] Sound Pharmaceuticals, Inc, Research and Development, Seattle, WA, USA

[5] Department of Psychiatry, University of Maryland School of Medicine, Baltimore, MD, USA.

[6] Maryland Psychiatric Research Center, Baltimore, MD, USA

[4] Cabungcal J-H, Counotte DS, Lewis EM, Tejeda HA, Piantidosi P, Pollock C, Calhoon GG, Sullivan EM, Presgraves E, Kil J, Hong LE, Cuenod M, Do KQ, O'Donnell P. As published in Neuron (2014).

Introduction

Developmental insults can yield adolescent or adult brains with heightened vulnerability to deleterious environmental factors, an interaction likely to play a role in neuropsychiatric disorders of adolescent onset (O'Donnell, 2011). Despite intense research efforts, we still do not understand the mechanisms that could link genetic risk and early developmental disturbances with adult deficits. Among the hypotheses being advanced, oxidative stress stands out as a strong possible mechanism (Cabungcal et al., 2013b; Do et al., 2009; O'Donnell, 2012b). This idea is supported by the observation of various polymorphisms in genes encoding glutathione (GSH) synthesis conferring risk for schizophrenia (Gysin et al., 2007; Tosic et al., 2006). GSH, the most abundant endogenous antioxidant, is responsible for maintaining cellular oxidative balance (Do et al., 2009). Decreased GSH levels have been observed in peripheral tissues, cerebrospinal fluid, and postmortem brains of schizophrenia patients (Do et al., 2000; Gawryluk et al., 2011; Yao and Keshavan, 2011), and the GSH precursor *N*-acetyl cysteine (NAC) increases peripheral GSH levels and improves neurophysiological deficits in patients (Berk et al., 2008; Carmeli et al., 2012; Lavoie et al., 2008). Furthermore, brain GSH levels assessed with magnetic resonance spectroscopy are decreased in the prefrontal cortex (PFC) of patients with schizophrenia (Do et al., 2000). However, while mounting evidence does suggest a role of oxidative stress in schizophrenia, the time course and neural substrates of oxidative stress induced by developmental disturbances are not well understood, and whether oxidative stress is causal to behavioral deficits remains to be determined.

Several rodent models have been designed to test possible developmental pathophysiological scenarios in major psychiatric disorders. Mice with GSH deficit or mitochondrial dysfunction, for example, show schizophrenia-related electrophysiological, morphological, and behavioral anomalies (Steullet et al., 2010). As these deficits are reversed with NAC (Cabungcal et al., 2013a; Otte et al., 2011), GSH is likely critical for proper postnatal brain maturation. Another example is the latent neuropathological alteration induced by maternal immune activation, which becomes evident when combined with juvenile social isolation (Giovanoli et al., 2013). A widely used tool to assess developmental trajectories of adult-onset prefrontal cortical deficit is the neonatal ventral hippocampal lesion (NVHL). This procedure yields adult animals with PFC-dependent electrophysiological, neurochemical, and behavioral anomalies related to phenomena observed in schizophrenia, all of which emerge during adolescence (O'Donnell, 2011; Tseng et al., 2009). Of note, NVHL rats show altered prefrontal inhibitory interneuron maturation during adolescence (Tseng et al., 2008), highlighting this as a model of developmentally induced, late-onset alterations in prefrontal cortical excitation-inhibition balance. The NVHL is therefore a useful tool to test whether oxidative stress is responsible for adult deficits in a model that does not directly manipulate GSH or alter redox status, which is important to determine whether oxidative stress is a consequence of developmental cortical deficits. Here, we tested whether antioxidant treatment with NAC during juvenile and adolescent periods affects maturation of NVHL rats; the aim was to assess whether restoring redox balance prevented adult deficits in a developmentally compromised brain.

Results

One of the most replicated findings in schizophrenia research is a reduction of markers associated with cortical inhibitory interneurons (Lewis et al., 2012). Adult NVHL rats exhibit electrophysiological anomalies caused by altered cortical interneuron maturation, characterized by abnormal modulation by dopamine (Tseng et al., 2008). We tested whether parvalbumin (PV) positive interneurons in the PFC, including the dorsal prelimbic and anterior cingulate cortex (ACC), are altered in NVHL rats using unbiased stereological counting techniques. Between postnatal day (P) 21 and P61, the number of PV immunoreactive interneurons (PVI) increased in sham-operated rats, but not in NVHL rats (Figure 1A, B). In juvenile rats (P21), there was no significant difference in PVI counts between NVHL and sham rats, but adult (P61) NVHL rats showed significantly fewer PVI in the PFC compared to sham rats. The PVI reduction was prevented with NAC treatment starting at P5 (i.e., 2 days prior to the hippocampal lesion) and lasting into adolescence (P50; Figure 1A-C), suggesting juvenile oxidative stress induced by the neonatal lesion impairs PVI maturation. Caspase 3 labeling did not reveal apoptotic activation in the PFC of NVHL rats (data not shown), suggesting that reduced PVI immunoreactivity more likely reflects reduced interneuron activity than cell loss.

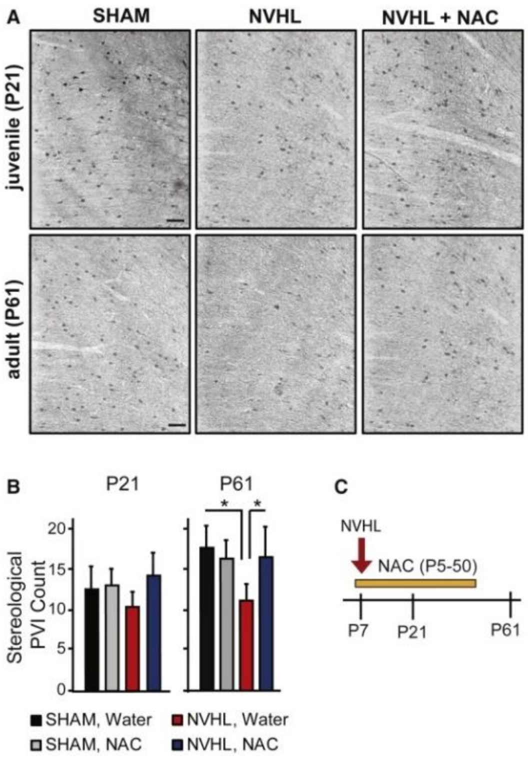

Figure 15. A NVHL blocks the adolescent increase in PV interneuron labeling in the PFC. (A) Representative micrographs of prefrontal PV staining in juvenile (P21) and adult (P61) SHAM, NVHL, and NAC-treated NVHL rats. Scale bar is 80 µm. See Suppl. Fig 1 for lesion extent. (B) Bar graphs illustrating PV cell counts using unbiased stereology at P21 (left) and P61 (right) in all four treatment groups. PV cell count increased between P21 and P61 in SHAM, but not in NVHL rats. Juvenile NAC treatment rescued the progression in PV cell numbers in NVHL rats. ANOVA $F_{(5,36)}=4.7$, $p=0.002$. Age: $F_{(1,36)}=10.2$, $p=0.003$, Lesion: $F_{(1,36)}=1.36$, $p=0.11$, Lesion x Age: $F_{(1,36)}=6.7$, $p=0.014$, Treatment: $F_{(1,36)}=3.9$, $p=0.057$, Treatment x Age: n.s. (C) Diagram illustrating the time course of NAC treatment and juvenile (P21) and adult (P61) assessments. In this and all other figures, data are expressed as mean ± SEM, *p<0.05.

To assess oxidative stress, we quantified DNA oxidation with 8-oxo-7, 8-dihydro-20-deoxyguanine (8-oxo-dG) labeling. At P21, NVHL rats exhibited a massive increase in 8-oxo-dG staining in the PFC compared to sham rats, in both pyramidal neurons and interneurons, which was completely prevented by NAC treatment (Figure 2A, B). When NVHL rats reached adulthood (P61), they still showed increased 8-oxo-dG, albeit less than

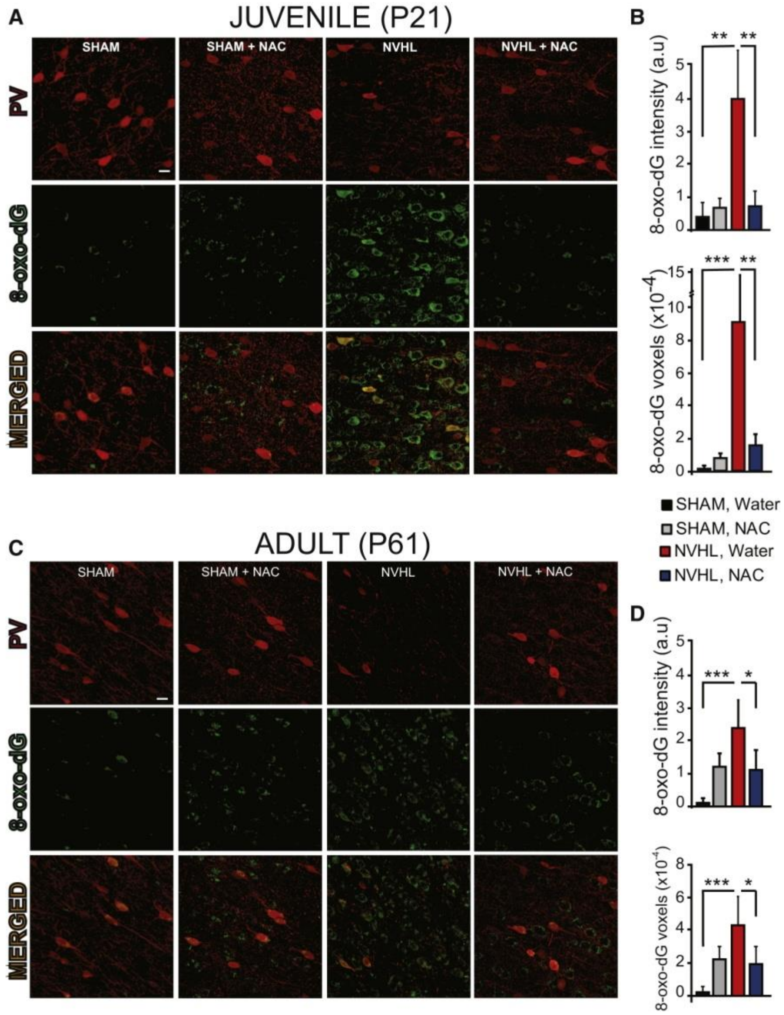

Figure 16. Oxidative stress shown with 8-oxo-dG in the PFC of NVHL rats. (A) Representative micrographs showing double labeling for PV (red) and 8-oxo-dG (green) in the PFC in the four groups at P21. Scale bar is 10 µm. (B) Summary of the data showing that an NVHL causes a massive increase in 8-oxo-dG labeling in the PFC at P21 that is prevented with juvenile NAC treatment. Top graph illustrates 8-oxo-dG fluorescence intensity and the bottom graph quantifies the number of labeled voxels in each group. ANOVA for 8-oxo-dG intensity: $F_{(3,14)}$=13.7, p=0.00002, Lesion $F_{(1,14)}$=18.4, p=0.008, Treatment $F_{(1,14)}$=9.6, p=0.008, Lesion x Treatment $F_{(1,14)}$=13.0, p=0.003. (C) Representative micrographs showing double labeling for PV (red) and 8-oxo-dG (green) in the PFC at P61. Scale bar is 10 µm. (D) Summary of the data showing that the NVHL increases 8-oxo-dG in the PFC at P61, which is prevented with juvenile NAC treatment. ANOVA for 8-oxo-dG intensity: $F_{(3,18)}$=7.8, p=0.001, Lesion $F_{(1,18)}$=12.5, p=0.002, Treatment $F_{(1,18)}$=0.13, p=n.s., Lesion x Treatment $F_{(1,18)}$=10.8, p=0.004.

at P21 (Figure 2C, D). We also observed an increase in 3-Nitrotyrosine (3-NT) levels in adult PFC of NVHL rats. 3-NT indicates nitration of proteins due to oxidative and nitrosative stress (Radi, 2004), and its increase in NVHL rats was prevented by NAC treatment during development (Figure 3). Thus, juvenile NAC treatment decreased multiple markers of oxidative stress in adult NVHL rats to levels comparable to control rats, without affecting the extent of the lesion (Figure S1). A possible explanation for the levels of oxidative stress detected in the adult PFC following an NVHL is the reduced glutamatergic input from ventral hippocampus during development, as blocking NMDA receptors induces oxidative stress in PVI (Behrens et al., 2007). Our data indicate that impairing hippocampal inputs to the PFC during a critical developmental period elicits PFC oxidative stress in juvenile rats that has deleterious effects on the adolescent maturation of PVI.

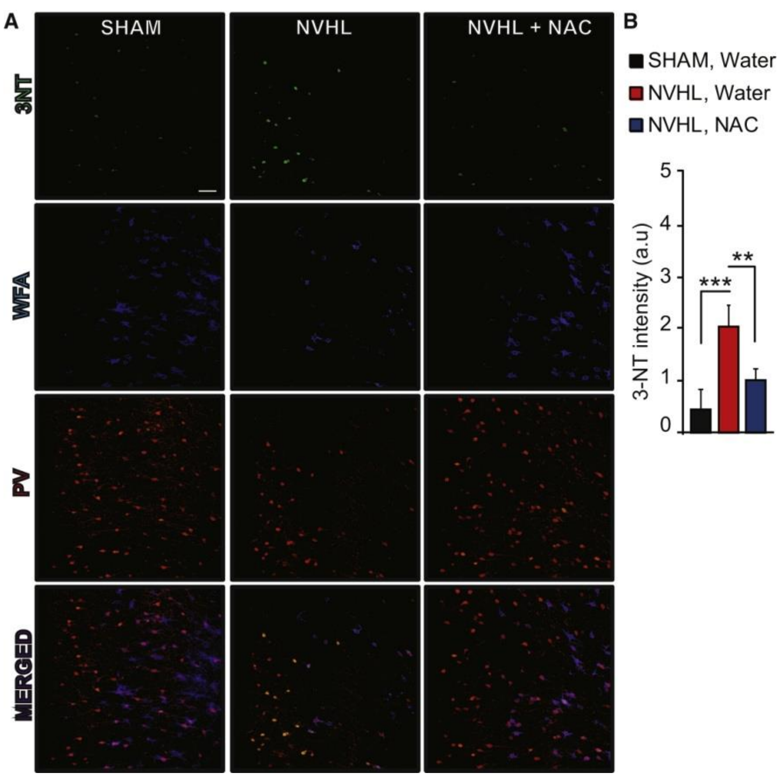

Figure 17. Oxidative stress in the PFC of adult NVHL rats shown with 3-NT. (A) Representative micrographs showing triple labeling for 3-NT (green), WFA (blue) and PV (red) in the three groups. Scale bar is 100 μm. b, (B) Summary of the data showing that an NVHL causes a significant increase in 3-NT labeling in the PFC at P61 that is prevented with juvenile NAC treatment. Top graph illustrates 3-NT fluorescence intensity in each group. One-way ANOVA for 3-NT intensity revealed a very significant effect of treatment ($F_{(2,53)}$=85.2, p<0.0001). Comparisons between each pairs using Tukey-Kramer also showed significant differences (P<0.0001) for SHAM versus NVHL and NVHL versus NAC.

To determine the types of interneurons expressing oxidative stress in NVHL rats, we co-labeled 8-oxo-dG with PV, calbindin (CB) and calretinin (CR). In addition to pyramidal neurons, increased 8-oxo-dG staining was observed in PVI, but not in CB or CR interneurons (Figure 4). About 50% of PVI were co-labeled with 8-oxo-dG, indicating oxidative stress is pervasive in this cell population. A marker of PVI maturation is *Wisteria Floribunda agglutinin* (WFA), a lectin that recognizes the perineuronal nets (PNN) enwrapping mature cortical PVI. The NVHL lesion reduced WFA staining (Figure 5), suggesting that PVI in adult PFC of NVHL rats show an immature phenotype. These extracellular matrix alterations were restored with juvenile NAC treatment (Figure 5). PVI may be highly exposed to increased oxidative stress because they make up the majority of fast-spiking interneurons and their high energy metabolism may generate more reactive oxygen species than non-fast spiking neurons. It is possible that juvenile PVI are functional while exhibiting oxidative stress, with the deleterious effects of oxidative stress becoming evident upon periadolescent PVI maturation.

If juvenile oxidative stress is the cause of physiological anomalies observed in adult NVHL rats, NAC treatment should rescue these alterations. We conducted whole-cell recordings from pyramidal neurons in adult brain slices containing the medial PFC of SHAM (n=12), NVHL (n=16), and NAC-treated NVHL rats (n=14). As previously shown

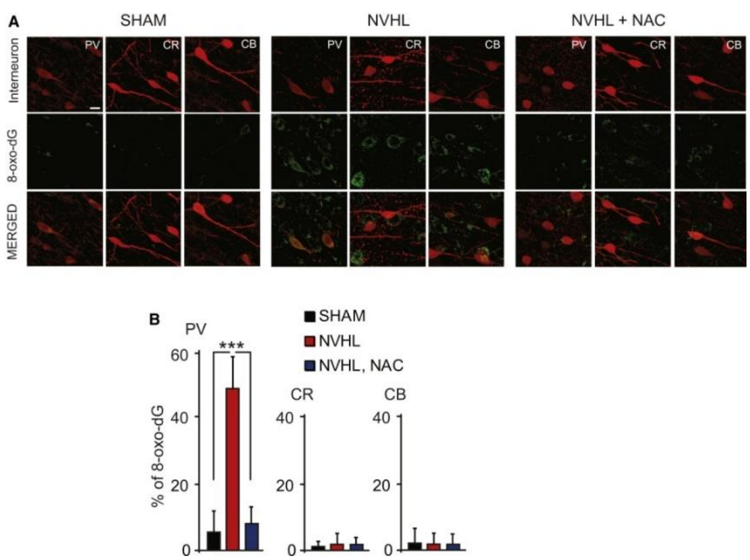

Figure 18. The NVHL causes increased oxidative stress in PV, but not CR and CB interneurons, which is prevented by developmental NAC treatment. (A) Micrographs showing 8-oxo-dG labeling (green) of parvalbumin (PV)-, calretinin (CR)- and calbindin (CB)-positive interneurons (red) in the PFC of SHAM, NVHL and NAC-treated NVHL rats. Scale bar is 10 µm. (B) Summary of the data. In PV interneurons, 8-oxo-dG labeling increased following an NVHL lesion, which was prevented with NAC treatment (Treatment: $F_{(2,65)}=212.97$, $p<0.0001$). ***$p<0.001$.

in adult NVHL rats and other rodent models of schizophrenia (Niwa et al., 2010; Tseng et al., 2008), the dopamine D2-dependent modulation of excitatory postsynaptic potentials (EPSPs) in layer V pyramidal cells was lost in NVHL rats (Figure 6A-C). This loss is likely due to abnormal maturation of PFC interneurons, as the normal adult D2 modulation includes a GABA-A receptor component (Tseng and O'Donnell, 2007), but oxidative stress in pyramidal neurons may also play a role. To determine whether altered PVI-dependent PFC synaptic responses are due to oxidative stress, rats were treated with NAC during development and then tested for D2 modulation of PFC physiology. NAC treatment rescued the D2 modulation of synaptic responses in NVHL rats (Figure 6A-C), indicating that juvenile and adolescent oxidative stress in NVHL rats alters function of local circuits in the adult PFC.

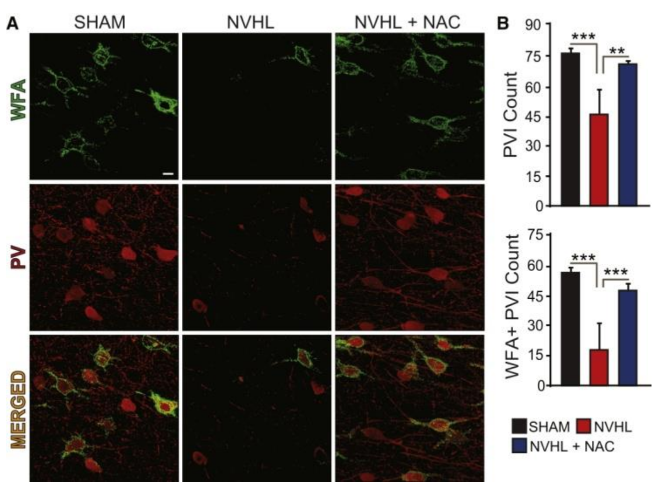

Figure 19. Perineuronal nets (PNN) are reduced in the PFC of adult NVHL rats, but rescued by juvenile NAC treatment. (A) Representative micrographs showing double labeling of PV (red) and *Wisteria floribunda agglutinin* (WFA; green), which labels PNN. Scale bar is 10 µm. (B) Plots illustrating PV interneuron (PVI) counts (top) and the number of cells co-labeled with PV and WFA (bottom). PVI count is reduced following an NVHL lesion, and this reduction is prevented with juvenile NAC treatment. (Overall effect: $F_{(8,16)}=3.8$, $p=0.01$, PVI count: $F_{(2,11)}=15.3$, $p<0.0007$). The number of WFA PVI decreases in NVHL rats compared to controls, and this reduction is prevented with juvenile NAC treatment (PNN count: $F_{(2,11)}=28.5$, $p<0.0001$). $^{**}p<0.01$, $^{***}p<0.001$.

The abnormal dopamine modulation of PFC function in NVHL rats is also observed *in vivo*. We performed *in vivo* intracellular recordings in 38 pyramidal neurons from adult rats (n=9 SHAM, n=5 NVHL, and n=7 NAC-treated NVHL). Baseline activity was consistent with what has been previously reported for PFC pyramidal neurons (Lewis and O'Donnell, 2000), and was not significantly affected by lesion status or NAC treatment. All recorded cells exhibited spontaneous transitions between the resting membrane potential (down state; -76.2 ± 1.1 mV) and the up state (-67.6 ± 0.7 mV). Up states occurred at a frequency of 0.6 ± 0.1 Hz with a duration of 523.6 ± 24.7 ms. The majority of cells (n=21) fired spontaneously at a rate of 2.1 ± 0.7 Hz. As previously reported (O'Donnell et al., 2002), *in vivo* intracellular recordings from anesthetized adult NVHL rats revealed an abnormal increase in pyramidal cell firing in response to burst stimulation of the Ventral Tegmental Area (VTA) (Figure 6D, E) compared to sham rats. This abnormal increase in firing was prevented by juvenile NAC treatment (Figure 6D, E). These data indicate that abnormal dopamine function in the PFC of NVHL rats depends on oxidative stress during juvenile and adolescent stages.

Abnormal cortical synaptic function in adult NVHL rats should yield altered information processing that would be prevented by NAC treatment if it depended on oxidative stress. We tested mismatch negativity (MMN) using auditory evoked potentials in an oddball paradigm in SHAM (n=6), NVHL (n=3), and NAC-treated NVHL rats (n=3). MMN has high translational relevance, as it is attenuated in schizophrenia patients (Javitt et al., 1993) and in animal models (Ehrlichman et al., 2009). We implanted EEG electrodes in NVHL, NAC-treated NVHL, and sham rats. MMN was significantly different among groups, with NAC treatment improving MMN in NVHL rats (Figures 7A, B). This observation is consistent with the effect of NAC on MMN in patients (Lavoie et al., 2008), and indicates the NVHL model reproduces an important disease marker that can be prevented by juvenile antioxidant treatment. As MMN depends on NMDA receptor function (Umbricht et al., 2000) and NMDA hypofunction in PVI is suspected in schizophrenia, it is possible that MMN improvement with NAC results from restored PVI activity.

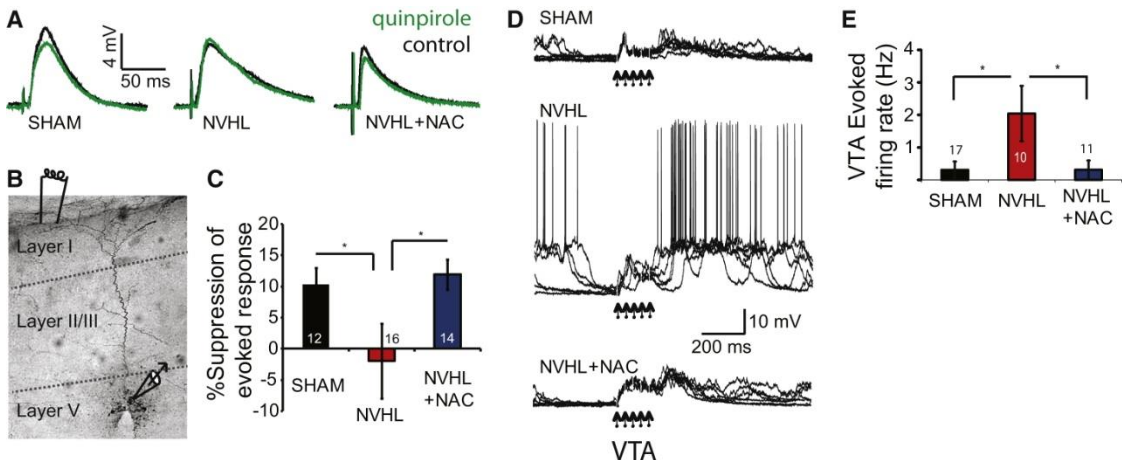

Figure 20. Electrophysiological deficits are rescued by NAC treatment in NVHL rats. (A) Representative traces of excitatory post-synaptic potentials (EPSP) evoked by superficial layer electrical stimulation in adult PFC before (black trace) and after (green trace) bath application of the D2-agonist quinpirole (5 µM). (B) Neurobiotin-filled layer V pyramidal cell in the PFC; the relative position of the bipolar stimulating electrode and the recording electrode are shown schematically. (C) Bar graphs illustrating the magnitude of EPSP attenuation by quinpirole in slices from SHAM, NVHL, and NAC-treated NVHL rats. In sham rats, quinpirole reduces the size of the synaptic response, whereas in NVHL rats this attenuation is absent. NAC treatment during development reverses this deficit in NVHL animals (ANOVA: $F_{(2,39)}=3.328$, $p=0.046$). (D) Traces from *in vivo* intracellular recordings in PFC pyramidal neurons showing responses to electrical stimulation of the ventral tegmental area (VTA) with trains of 5 pulses at 20 Hz in anesthetized SHAM (top), NVHL (middle), and NAC-treated NVHL (bottom) rats. Each panel is an overlay of 5 traces that illustrate the representative type of response observed in each group, with NVHL showing enhanced firing following VTA stimulation, while firing is sparse in SHAM and NAC-treated NVHL rats. (E) Bar graph illustrating group data for action potential firing in the 500 ms epoch following VTA stimulation in all three groups. ANOVA: $F_{(2,37)}=4.5$, $p<0.05$; NVHL firing was higher than in shams (post-hoc Tukey's q=3.9, $p<0.05$) and higher than in NAC-treated NVHL rats (post-hoc Tukey's q=3.6, $p<0.05$). In all electrophysiology experiments data from SHAM and NAC-treated SHAM rats were combined as they did not show differences.

To assess whether juvenile oxidative stress leads to behavioral deficits, we used a behavioral paradigm tested in both animal models and schizophrenia patients. Prepulse inhibition of the acoustic startle response (PPI) is a measure of sensorimotor gating that is reduced in patients (Geyer and Braff, 1987) and NVHL rats (Lipska et al., 1995). We tested PPI in adult sham (n=11), NAC-treated sham (n=12), NVHL (n=9), and NAC-treated NVHL rats (n=17). Juvenile NAC treatment prevented the reduced PPI observed in untreated NVHL rats (Figure 8A). In addition to loss of PVI maturation and electrophysiological anomalies, developmental oxidative stress in juvenile NVHL rats can cause schizophrenia-relevant adult behavioral deficits.

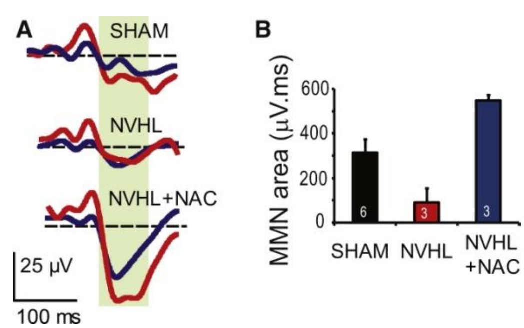

Figure 21. Mismatch negativity (MMN) deficits are rescued by NAC treatment. (A) Representative traces of auditory evoked potentials from standard (blue) and deviant (red) stimuli in a sham (n=6; top), NVHL (n=3; middle), and NAC-treated NVHL rat (n=3; bottom). The green box highlights the epoch in which the negativity was measured (35-100 ms following the stimulus). All traces are averages of at least 80 repetitions. (B) Group data comparing MMN measured as the area under the curve in the highlighted region reveal a significant difference among groups (ANOVA: $F_{(2,11)}$=9.742; p=0.006). The data illustrated are averages from 3 different sessions in each rat. A post-hoc comparison between NVHL and NVHL+NAC revealed a significant difference (Bonferroni test; p=0.005).

The beneficial effect of NAC treatment reported above includes a large postnatal treatment that starts prior to the lesion and stops once rats become young adults. For these results to have a full translational value, it is critical to determine whether NAC is efficacious when started at an age that corresponds to the time when prodromal stages can be identified in humans. In another set of rats, we administered NAC in the drinking water starting at P35, an age that in rats is equivalent to early adolescence. We tested for PPI deficits in adult sham (n=15), untreated NVHL (n=12), and NAC-treated NVHL rats (n=14). Although there was only a trend for a deficit in untreated NVHL rats compared to shams in this group, there was a significant difference between untreated and treated NVHL (Figure 8B). The data indicate that GSH precursors such as NAC can still be effective even if initiated after oxidative stress has begun.

One important caveat of NAC is that it also alters glutamate levels by virtue of its action on the cysteine-glutamate transporter (Moussawi et al., 2009). To test whether redox modulation and not glutamate level changes were responsible for NAC effects in NVHL rats, we assessed the effect of two other antioxidants that do not alter glutamate. Ebselen is a glutathione peroxidase (GPx) mimic (Muller et al., 1984) that induces GPx expression (Kil et al., 2007) and enhances GSH levels in neurons, replenishing GSH depleted by neurotoxic mechanisms (Pawlas and Malecki, 2007). We tested PPI in adult vehicle-treated SHAM (n=10), ebselen-treated SHAM (n=7), vehicle-treated NVHL (n=8), and ebselen-treated NVHL rats (n=9). Ebselen treatment during adolescence reversed PPI deficits in NVHL rats (Figure 8C). In another group of rats, we assessed the effects of the NADPH oxidase inhibitor and antioxidant apocynin, in this case delivered through juvenile and adolescent stages. We tested PPI in adult vehicle-treated SHAM (n=10), apocynin-treated SHAM (n=11), vehicle treated NHVL (n=7), and apocynin-treated NVHL (n=5). We again observed a reversal of PPI deficits (Figure 8D). The data indicate that elevation of GSH and not glutamate during adolescence rescues PPI deficits in NVHL rats.

Discussion

We observed increased level of oxidative stress immunolabeling in the PFC of juvenile NVHL rats, along with a decrease in PV cell counts, PPI deficit, altered dopamine modulation of local PFC circuits, and deficits in evoked-related potentials in the EEG of adult NVHL rats. All these deficits were prevented with NAC treatment from P5 to P50. PPI deficits were also prevented if NAC treatment was initiated during adolescence (P35) and by two other redox modulators. Our data suggest that oxidative stress in prefrontal cortex is a core feature mediating alterations induced by the NVHL, and antioxidant treatment prevents these alterations. Presymptomatic oxidative stress, highly present in PVI and also observed in pyramidal neurons, is therefore responsible for diverse schizophrenia-relevant phenomena in a neurodevelopmental model that does not entail a direct manipulation of redox pathways.

Oxidative stress can affect PFC function via several mechanisms. With high levels of oxidative stress, cell damage or death can occur via membrane lipid peroxidation, DNA mutagenesis, alterations in chromatin structure, inactivation of critical enzymes, or activation of kinase and caspase cascades (Bitanihirwe and Woo, 2011). Redox imbalance can also lead to brain development disturbances by affecting redox-sensitive cysteine residues at the DNA-binding sites of transcription factors (Haddad, 2002) and affecting mitochondrial DNA, highly susceptible to oxidation (Jones and Go, 2010). Furthermore, many synaptic proteins include regulatory redox sites; for example, NMDA receptors become hypofunctional following oxidation (Steullet et al., 2006). We detected oxidative stress and nitrosative stress in PFC pyramidal neurons and PVI in juvenile rats with a NVHL prior to the onset of electrophysiological and behavioral deficits. This indicates PVI may still be somewhat functional, and that upon their periadolescent maturation the deleterious effect of oxidative stress renders them into a diseased state as revealed by the reduction in PV and PNN labeling. Our data indicate that redox alterations in the NVHL model encompass both oxidative and nitrosative stress, and treatments that increase GSH (NAC and ebselen) or decrease reactive oxygen species (ROS) generation (ebselen and apocynin) prevent adult-onset behavioral deficits. The increases in 3NT levels point to dysregulation of nitric oxide (NO) and arginine signaling, as well as nitrosative stress, as reported in schizophrenia (Yao et al., 2004). Whether this dysregulation implicates the various isoforms of NO synthase (nNOS, eNOS, or iNOS) is still unknown. Thus, the NVHL model presents a widespread alteration in redox pathways that could be reversed by targeting different modulators, such as GSH, GPx, and NADPH oxidase.

Oxidative stress is also seen in another animal model of schizophrenia: the dominant negative DISC1 (DN-DISC1) mouse (Johnson et al., 2013). Similar to our findings, DN-DISC1 mice show increased 8-oxo-dG staining in the PFC that is associated with several behavioral deficits (Johnson et al., 2013). Our results add to this observation by showing a causal link between heightened oxidative stress in the PFC and the electrophysiological and behavioral deficits associated with schizophrenia, as the anti-oxidant NAC prevents both the increase in oxidative stress and electrophysiological and behavioral deficits in NVHL rats.

PFC physiology was dysfunctional in adult NVHL rats, and this deficit was prevented by NAC treatment. We used several endpoints to assess PFC function, including dopamine modulation of synaptic responses in pyramidal neurons in slices, *in vivo* intracellular recordings of responses to VTA stimulation, and auditory evoked potentials. Recordings from pyramidal neurons showed loss of D2-mediated attenuation of cortico-cortical EPSPs in slices and exaggerated firing evoked by VTA stimulation *in vivo* in adult NVHL rats, as we had reported previously (O'Donnell et al., 2002; Tseng et al., 2008). Both the slice D2 attenuation of pyramidal cell synaptic responses and the *in vivo* silencing of pyramidal neurons by VTA stimulation are dependent on activation of FSI by dopamine in naïve rats (Tseng and O'Donnell, 2007). The absence of alterations in these responses in NAC-treated NVHL rats indicates that oxidative stress during postnatal development has a deleterious effect on dopamine-modulated FSI-pyramidal cell interactions. Currently, there is a debate as to whether interneurons or pyramidal neurons are the primary site of dysfunction in schizophrenia. Our data are agnostic to which cell type is primarily affected and highlights oxidative stress as a cause of altered interactions between pyramidal neurons and inhibitory interneurons.

Oxidative stress could be brought up in the NVHL model by a number of mechanisms. First, this could be the result of the administration of an excitotoxic agent, such as ibotenic acid. Our previous work showing that neonatal ventral hippocampal injection of the bacterial endotoxin LPS yielded anomalies similar to the NVHL (Feleder et al., 2010) suggests this could be the case. However, a variation of this model in which the hippocampus was just reversibly inactivated produces similar behavioral alterations as the lesion (Lipska et al., 2002), suggesting the excitotoxic damage in the NVHL may not be what causes the deficits. It is more likely that the loss of hippocampal-prefrontal synaptic activity and/or the loss of trophic factors in the PFC induced by the loss of hippocampal inputs during a critical developmental stage may affect the developing prefrontal cortical neurons. This possibility is supported by work by Margarita Behrens showing that NMDA receptor antagonists can induce oxidative stress in PV interneurons (Behrens et al., 2007; Behrens et al., 2008). Thus, oxidative stress in NVHL rats may be a consequence of network developmental alterations.

Mismatch negativity is a measure of high translational relevance. MMN tests the attribution of saliency to deviant auditory stimuli, and it is disrupted in schizophrenia patients (Javitt et al., 1993). Here, we report MMN deficits in NVHL rats, which are prevented by NAC treatment. As MMN is dependent on NMDA receptor activity (Ehrlichman et al., 2009), it is likely that oxidative stress impairs NMDA-dependent synaptic cortical mechanisms involved in processing of salient vs. common signals. The functional assessment of the impact of antioxidant treatment was complemented by testing of sensorimotor integration with PPI. Both juvenile and adolescent-only NAC treatment prevented adult PPI deficits in NVHL rats. The observation that adolescent treatment with NAC or ebselen is sufficient to prevent PPI deficits has important implications for redox mechanisms as potential targets for schizophrenia treatment. We showed that it is possible to prevent or reverse a deficit even if antioxidant treatment is initiated after the development of oxidative stress. As ultra-high risk subjects for schizophrenia cannot be identified until adolescence, our finding keeps open the possibility that redox modulation can be beneficial even if initiated once high risk has been identified.

Our data reveal that presymptomatic oxidative stress can cause aberrant adult PFC function in NVHL rats. This developmental manipulation is a well-established model of altered cortical excitation-inhibition balance. As is the case with any schizophrenia-related models, the NVHL should not be seen as reproducing the disease (there is no such thing as a schizophrenic rat). In addition, the model entails a lesion, which is not observed in schizophrenia. However, the NVHL and other developmental models have been useful to test specific hypotheses about developmental trajectories of electrophysiological and behavioral phenomena of relevance to the disease (O'Donnell, 2013). Major strengths of the NVHL model include the adolescent onset of deficits and the ability to reproduce phenomena observed in schizophrenia when translatable measures are evaluated (O'Donnell, 2012a). Remarkably, the NVHL model converges with several other manipulations used as animal models for schizophrenia research in producing loss of PVI immunolabeling and altered excitation-inhibition balance (O'Donnell, 2011). Despite their limitations, the behavioral and physiological endpoints we used here are widely used to assess integrity of cortical inhibitory networks and their impact on pyramidal cell activity. Inhibitory networks, developing at the time of the lesion and beyond, play a crucial role in experience-dependent refinement of neural networks (Hensch, 2005) that extends into adolescence. This role may be reflected in cognitive training during adolescence preventing cognitive impairments in adult NVHL rats (Lee et al., 2012) and adolescent stress unmasking latent neuropathology in mice with maternal immune activation (Giovanoli et al., 2013). Adolescence is therefore a critical developmental stage in which pathophysiological conditions involving oxidative stress can affect a still developing PFC, but it yet provides a window of opportunity for therapeutic intervention. This suggests that antioxidants or redox regulators without serious side effects may prove effective to reduce conversion in subjects at risk for psychiatric disorders by preventing pathophysiological changes associated with loss of cortical pyramidal cell and PVI function.

Experimental Procedures

Animals

Timed-pregnant Sprague-Dawley rats were obtained at gestational days 13-15 from Charles River (Wilmington, MA) and were individually housed with free access to food and water in a temperature- and humidity-controlled environment with a 12:12h light/dark cycle (lights on at 7:00 AM). When pups reached P5, half of the dams received NAC in their drinking water. Pups were left undisturbed until P7-9 when healthy offspring were randomly separated and received either NVHL or sham surgery. At P21, male and female pups were either transcardially perfused with 4% paraformaldehyde for immunocytochemistry or weaned and housed in groups of two to three, counterbalanced across lesion status. NAC treatment lasted throughout adolescence until P50. After reaching adulthood (>P60), animals were either perfused with 4% paraformaldehyde for immunocytochemistry, perfused with artificial cerebrospinal fluid (aCSF) for slice electrophysiology, utilized for *in vivo* intracellular recordings, or tested for PPI or MMN. All experiments were approved by the University of Maryland School of Medicine Institutional Animal Care and Use Committee.

Neonatal ventral hippocampal lesion surgery

Between P7 and P9, pups (15-20 g) received either an excitotoxic lesion of the ventral hippocampus (NVHL) or sham procedure, as previously described (Chambers and Lipska, 2011). Pups were anesthetized with hypothermia and secured to a Styrofoam platform attached to a stereotaxic frame (David Kopf Instruments, Tujunga, CA). NVHL rats received a bilateral infusion of ibotenic acid (10 µg/µl in aCSF, 0.3 µl/side; Tocris, Minneapolis, MN) into the ventral hippocampus (3 mm rostral to Bregma, 3.5 mm lateral to midline, and 5 mm from surface) at a rate of 0.15 µl/min. Sham surgeries were done in exactly the same fashion, but the guide cannula was lowered only 3 mm and without any liquid infusion to control for the surgical procedure while avoiding hippocampal damage. After the surgery, wounds were clipped and when pups activity level had returned to normal, they were returned to their dams and remained undisturbed until the wound clips were removed and rats weaned at P21.

In all rats, lesions were verified by sectioning (40 µm) the dorsal and ventral hippocampus using a freezing microtome. Sections were mounted on glass slides and Nissl stained. The hippocampus was examined microscopically for evidence of bilateral damage, which typically included cell loss, thinning, gliosis, cellular disorganization and enlarged ventricles (Chambers and Lipska, 2011).

Antioxidant pretreatment regimen

NAC (BioAdvantexPharma, Mississauga, Ontario, Canada) was administered in the drinking water at 900 mg/l. NAC treatment started at P5 or at P35, and previous work in mice has shown that NAC consumed by the dam is transmitted to the pups through her milk (das Neves Duarte et al., 2012). NAC treatment ended at P50. Fresh solutions were prepared every 2-3 days. Ebselen (Sound Pharmaceuticals Inc., Seattle, WA) was administered i.p. 5 days a week starting at P35 until the day of PPI testing (P60). Stock ebselen solution (20 mg/ml DMSO, frozen aliquots) was diluted 1:5 in sterile water and administered at a dose of 10 mg/kg. Control animals received an equivalent concentration of DMSO diluted 1:5 in water. Apocynin (Sigma-Aldrich, St. Louis, MO) was administered in the drinking water at a target dose of 100 mg/kg (Nwokocha et al., 2013). Prior to weaning at P21, drinking water contained a dose of 2 g apocynin per 0.5 l of water, to ensure delivery through the dam's milk. Apocynin concentration was lowered after weaning to 750 mg/l to best approximate the target dose. Treatment lasted from P5 to P50 with fresh solutions prepared every other day.

Immunohistochemistry

Immunohistochemistry and stereological quantification.

A total of 18 (P21) and 25 (P61) male rats were anesthetized, perfused and their brains fixed as previously described (Cabungcal et al., 2006). Coronal sections (40 µm) were used to investigate the inhibitory circuitry of anterior cingulate cortex (ACC). Brain sections were immunolabeled for parvalbumin (PV) as described previously (Steullet et al., 2010). PV-immunoreactive cell (cell bodies) count was quantified in ACC using the StereoInvestigator 7.5 software (MBF Bioscience Inc, Williston, VT, USA). Briefly, stereological counting started with low magnification (x2.5 objective) to identify and delineate the boundaries of the region of interest (ROI) on 2-4 consecutive sections from each animal. The ACC (at Bregma approximately 0.70-1.70 mm) was delineated from the secondary motor (M2) cortical regions following the anatomical cytoarchitectonic areas given by Paxinos and Watson (Paxinos and Watson, 1998). The selected region of interest (ROI) included the majority of the cingulate cortex area 1 (cg1) and part of cingulate cortex area 2 (cg2). A small intermediate allowance was set between ACC and M2 regions to ensure that the ROI in ACC did not overlap with the secondary motor cortex. A counting box (optical dissector) within the section thickness and sampling frames adapted to ACC were used to analyze and count neurons (Schmitz and Hof, 2005). The counting boxes (40 x 40 µm with 15 µm in depth) were placed by the software in each sampling frame starting from a random position inside the ROI of the ACC. Counting was carried out using higher magnification (x40 objective). PV cells were counted when they were in focus at the surface of the box until out of focus at 15-µm depth of the counting box. A 5-µm guard zone was used to distance from artifacts that can be influenced by tissue shrinkage due to the immunopreparation processing. We used 25 counting frames in the ROI volume of the ACC for P21 and P61 rats.

Immunofluorescence staining, confocal microscopy and image analysis

Oxidative stress was visualized using an antibody against 8-oxo-7, 8-dihydro-20-deoxyguanine (8-Oxo-dG), a DNA adduct formed by the reaction of OH radicals with the DNA guanine base (Kasai, 1997). Because of the proximity of the electron transport chain, mitochondrial DNA is prone to oxidative damage: levels of oxidized bases in DNA and levels of 8-oxo-dG are higher in mitochondria than in the nucleus. To assess 8-oxo-dG and 3-Nitrotyrosine (3NT) labeling in various types of interneurons, coronal sections between Bregma 0.70-1.70 mm were incubated for about 36 hours with rabbit polyclonal anti-PV, anti-calbindin-28k (anti-CB), or anti-calretinin (anti-CR) (1:2500; Swant, Bellinzona, Switzerland) primary antibodies together with the mouse monoclonal anti-8-oxo-dG (1:350; AMS Biotechnology, Bioggio-Lugano, Switzerland) primary antibody or mouse monoclonal anti-nitrotyrosine (1:1000; Chemicon International, Temecula, USA) primary antibody. To enable visualization of the PNN that surrounds PV cells, sections were incubated in a solution containing the biotin-conjugated lectin *Wisteria floribunda agglutinin* (WFA) (Hartig et al., 1994). Sections were first incubated with PBS + Triton

0.3% + sodium azide (1 g/l) containing 2% normal horse serum, followed by 36-hour incubation with rabbit polyclonal anti-PV (1:2500) and biotin conjugated-WFA (1:2000; Sigma). Sections were washed, incubated with appropriate fluorescent secondary antibodies (goat anti-mouse immunoglobulin G (1:300; Alexa Fluor 488; Molecular Probes, Eugene, Oregon), anti-rabbit immunoglobulin G (1:300; CY3; Chemicon International, Temecula, California), CY2-Streptavidin conjugate (1:300; Chemicon), and counterstained with 100 ng/ml DAPI (4'-6-diamidino-2-phenylindole; Vector Laboratories, California, USA). Sections were visualized with a Zeiss Confocal Microscope equipped with x10, x20, x40 and x63 Plan-NEOFLUAR objectives. All peripherals were controlled with LSM 510 software (Carl Zeiss AG, Switzerland). Z stacks of 9 images (with a 2.13 µm interval) were scanned (1024 x 1024 pixels) for analysis in IMARIS 7.3 software (Bitplane AG, Switzerland). All images of Z stacks were filtered with a Gaussian filter tool to remove unwanted background noise and sharpen cell body contours. An ROI as defined in the stereological procedure was created in ACC. The ROI was masked throughout the Z stacks to isolate regional subvolumes of the ACC in which PV-, CB-, and CR-expressing interneurons were analyzed. To quantify 8-oxo-dG, the staining intensity and number of labelled voxels within the ROI were measured. To quantify 8-oxo-dG in PV-, CB- and CR-cells, we used the *Coloc* module of the IMARIS software to calculate the proportion of all PV-immunolabeled voxels (respectively, CB- and CR-immunolabeled voxels), which were also 8-oxo-dG-immnolabeled. *Coloc* gives the count of colocalized voxels between the immunolabeled profiles of interest. To quantify the number of PV immunoreactive neurons surrounded by PNN, we used the spots module to assign spot markings on profile-labelled voxels that fall within a given size. The channels for PV and WFA immunolabeling were chosen, and profile size criterion (>9 and 4 µm, respectively) was defined to quantify labelled profiles above these sizes. Spots generated for PV that contacted and/or overlapped with spots generated for WFA were considered as those PVI surrounded by PNN (WFA-positive PVI).

Slice electrophysiology

Starting at P60, male rats were anesthetized with chloral hydrate (400 mg/kg, i.p.) 15 min before being decapitated. Brains were quickly removed from the skull into ice-cold artificial CSF (aSCF) oxygenated with 95% O_2-5% CO_2 and containing the following (in mM): 125 NaCl, 25 $NaHCO_3$, 10 glucose, 3.5 KCl, 1.25 NaH_2PO_4, 0.1 $CaCl_2$ and 3 $MgCl_2$, pH 7.45 (295-300 mOsm). Coronal slices (300 µm thick) containing the medial PFC were obtained with a vibratome in ice-cold aCSF and incubated in warm (~35°C) aCSF solution constantly oxygenated with 95% O_2-5% CO_2 for at least 45 min before recording. The recording aCSF (with 2 $CaCl_2$ and 1 $MgCl_2$) was delivered to the recording chamber with a pump at the rate of 2 ml/min.

Patch electrodes (7-10 MΩ) were obtained from 1.5 mm borosilicate glass capillaries (World Precision Instruments) with a Flaming-Brown horizontal puller (P97; Sutter Instruments) and filled with a solution containing 0.125% Neurobiotin and the following (in mM): 115 K-gluconate, 10 HEPES, 2 $MgCl_2$, 20 KCl, 2 MgATP, 2 Na_2-ATP, and 0.3 GTP, pH 7.25-7.30 (280-285 mOsm). Quinpirole (5 µM, Tocris) was freshly mixed into oxygenated recording aCSF every day before an experiment. Both control and drug-containing aCSF were oxygenated continuously throughout the experiments.

All experiments were conducted at 33-35°C and prelimbic or ACC PFC pyramidal cells from layer V were identified under visual guidance using infrared (IR) differential interference contrast video microscopy with a 40X water-immersion objective (Olympus BX-51WI). The image was detected with an IR-sensitive CCD camera and displayed on a monitor. Whole-cell current-clamp recordings were performed with a computer-controlled amplifier (Multiclamp 700A; Molecular Devices), digitized (Digidata 1322; Molecular Devices), and acquired with Axoscope 9 (Molecular Devices) at a sampling rate of 10 kHz. Electrode potentials were adjusted to zero before recording without correcting the liquid junction potential. Baseline activity in each neuron was monitored for 10 minutes during which membrane potential and input resistance (measured with the slope of a current-voltage (I/V) plot obtained with 500-ms-duration depolarizing and hyperpolarizing pulses) were measured.

Synaptic responses were tested in pyramidal neurons with electrical stimulation of superficial layers with a bipolar electrode made from a pair of twisted Teflon-coated Tungsten wires (tips separated by ~200 μm) and placed ~500 μm lateral to the vertical axis of the apical dendrite of the recorded neuron. Stimulation pulses (20-400 µA; 0.5 ms) were delivered every 15 s. The intensity was adjusted to evoke EPSPs with about half of the maximal amplitude. Throughout the experiment, changes in input resistance were monitored with repeated hyperpolarizing steps, and the cell was discarded when input resistance changed more than 20% during the course of the experiment. The amplitude of evoked EPSPs was measured with Clampfit 9.0 and averaged over 10 sweeps before and after 7 minutes of application of quinpirole. This period was chosen for consistency, with differences revealed by previous investigations of D2 modulation of PFC activity in rodent models of schizophrenia (Niwa et al., 2010; Tseng et al., 2008). At the end of each experiment, slices were placed in 4% paraformaldehyde and processed for DAB staining using standard histochemical techniques to verify morphology and location of the neurons.

In Vivo intracellular recordings

Female rats were anesthetized with choral hydrate (400 mg/kg, i.p) and placed on a stereotaxic apparatus (Kopf Instruments). Anesthesia was maintained through recording procedures with continuous choral hydrate (24-30 mg/kg/h) via an intraperitoneal catheter. Body temperature was maintained at approximately 37°C using a thermal probe-controlled heat pad (Fine Science Tools). Concentric bipolar stimulating electrodes (0.5 mm diameter, 0.5 mm pole separation; Rhodes Medical Instruments Inc.) were lowered into the VTA (5.8 mm caudal to bregma; 0.5-0.8 mm lateral to midline; 7-8 mm from surface) for stimulation. Recording sharp micro-electrodes were pulled from borosilicate glass (1 mm O.D.; World Precision Instruments) on a horizontal Flaming-Brown puller (Sutter Instruments). Sharp electrodes (50-110 MΩ) were filled with 2% Neurobiotin (Vector Laboratories) in 2M potassium acetate. Microelectrodes were lowered into the medial PFC using a hydraulic manipulator (Trent Wells, Coulterville, CA). Recordings were made in current clamp, and signals were acquired using a Neurodata Amplifier (Cygnus), digitized at 10 kHz using a Digidata A/D converter (Molecular Devices) and Axoscope 9 software (Molecular Devices) for offline analyses.

Microelectrodes were advanced through the medial PFC until a neuron was impaled. Neurons included in this study had a resting membrane potential more negative than –60 mV and action potentials with amplitudes $\geq$ 40 mV from threshold. To determine responses to endogenous dopamine, the VTA was stimulated with trains of 5 pulses at 20 Hz, delivered every 10 seconds. Eight to ten sweeps were used to determine cell firing in response to VTA stimulation. Firing was measured in the 500 ms epoch following the last VTA pulse in all sweeps, and compared among experimental groups. At the end of the experiment, animals were killed with anesthesia overdose, and their brains removed for histological verification of lesion status and electrode placement.

Mismatch Negativity

NVHL, NAC-treated NVHL, and sham female rats were implanted with chronic EEG electrodes under isoflurane anesthesia. Electrodes were constructed with 2 mm diameter silver disks coated with silver chloride, and glued on top of bregma, a location equivalent to human vertex, and the contacts led to an *Omnetics* connector on top of the head. Upon a 4-week recovery, rats were first habituated to the recording chamber, a 30 x 50 cm plexiglass box enclosed within a stainless steel box. NNM sessions consisted of exposing the rat to approximately 2,000 tones at two different frequencies (7 or 9 kHz; 30 ms duration) separated by 400 ms, with 95% of the repetitions at one frequency (standard) and 5% at the other frequency (deviant). Tones were delivered with a speaker mounted inside the enclosure using a TDT RZ6 system (Tucker Davis), and were counterbalanced so half of the time the deviant was either frequency. EEG signals were acquired using a 32 channel Omniplex system (Plexon Instruments) at 1 kHz sampling rate. For analysis, 300 ms epochs around the tone were selected, filtered at 1-30 Hz, baseline-corrected to the 100 ms prior to the stimulus, and averaged separately for standard and deviant tones. A difference wave was constructed by subtracting the standard wave from the deviant wave, and MMN was quantified by measuring the area under the curve in the period between 35 and 100 ms after the stimulus. All rats were exposed to three sessions in three different days, and values were averaged across sessions for every animal.

Prepulse inhibition

Starting at P60, both male and female rats were tested for PPI, as described previously (Feleder et al., 2010). As PPI deficits in NVHL rats are most evident when rats are challenged with apomorphine (Lipska et al., 1995), we injected apomorphine (0.1 mg/kg, i.p.) immediately prior to the PPI test session. Rats were placed in a sound-attenuated startle chamber (San Diego Instruments, San Diego, CA) with a 70 dB background white noise. After a 5 min adaptation period, the PPI test was initiated with pseudorandom trials every 15 to 25 sec. Either pulse (120 dB), prepulse (75 dB, 80 dB, or 85 dB), no pulse or prepulse + pulse were delivered. Trials lasted 23 min and 8 to 10 repetitions of pulse or prepulse + pulse trials were acquired, while null or prepulse only trials were repeated five times for each prepulse amplitude. Startle magnitude was measured using an acceleration-sensitive transducer, and PPI was calculated as the ratio in startle between prepulse + pulse and pulse alone and is expressed as percent reduction. The initial trials (all pulse alone) were used for habituation and not included in the analysis. Trials were excluded from analysis when the animal was moving in the chamber, and sessions were excluded from analysis when startle amplitude was low or more than 50% of trials were excluded for any prepulse + pulse combination. If a PPI session was discarded, rats were tested again a week later.

Statistics

The mean numbers of PV-immunoreactive cells per tissue volume in the ACC were compared among treatment groups using one-way ANOVA followed by post-doc Dunnett multiple comparisons. The mean number of PV-cells, PV-cell intensity, WFA-positive PV and WFA-positive intensity, the overall 8-oxo-dG, and WFA labelling were compared among groups using multivariate ANOVA (Wilk's Lambda) followed by post-hoc Dunnett test for multiple comparisons. Electrophysiology data were compared using a 1-way ANOVA with group as between-subject variable. PPI data were compared using a repeated-measures 2-way ANOVA with lesion status and treatment as between-subject variables, and prepulse intensity as within-subject variable.

References

Aamodt SM, Constantine-Paton M (1999) The role of neural activity in synaptic development and its implications for adult brain function. Adv Neurol 79:133–144

Abdul-Monim Z, Neill JC, Reynolds GP (2007) Sub-chronic psychotomimetic phencyclidine induces deficits in reversal learning and alterations in parvalbumin-immunoreactive expression in the rat. J Psychopharmacol 21:198–205

Adler LE, Pachtman E, Franks RD, Pecevich M, Waldo MC, Freedman R (1982) Neurophysiological evidence for a defect in neuronal mechanisms involved in sensory gating in schizophrenia. Biol Psychiatry 17:639–654

Agartz I, Andersson JL, Skare S (2001) Abnormal brain white matter in schizophrenia: a diffusion tensor imaging study. Neuroreport 12:2251–2254

Akbarian S, Kim JJ, Potkin SG, Hagman JO, Tafazzoli A, Bunney WE, Jones EG (1995) Gene expression for glutamic acid decarboxylase is reduced without loss of neurons in prefrontal cortex of schizophrenics. Arch Gen Psychiatry 52:258–266

Amitai N, Kuczenski R, Behrens MM, Markou A (2012) Repeated phencyclidine administration alters glutamate release and decreases GABA markers in the prefrontal cortex of rats. Neuropharmacology 62:1422–1431

Amitai N, Semenova S, Markou A (2007) Cognitive-disruptive effects of the psychotomimetic phencyclidine and attenuation by atypical antipsychotic medications in rats. Psychopharmacology (Berl) 193:521–537

Andersen JD, Pouzet B (2004) Spatial memory deficits induced by perinatal treatment of rats with PCP and reversal effect of D-serine. Neuropsychopharmacology 29:1080–1090

Ardekani BA, Nierenberg J, Hoptman MJ, Javitt DC, Lim KO (2003) MRI study of white matter diffusion anisotropy in schizophrenia. Neuroreport 14:2025–2029

Arseneault L, Cannon M, Witton J, Murray RM (2004) Causal association between cannabis and psychosis: examination of the evidence. Br J Psychiatry 184:110–117

Ashtari M, Cervellione KL, Hasan KM, Wu J, McIlree C, Kester H, Ardekani BA, Roofeh D, Szeszko PR, Kumra S (2007a) White matter development during late adolescence in healthy males: a cross-sectional diffusion tensor imaging study. Neuroimage 35:501–510

Ashtari M, Cottone J, Ardekani BA, Cervellione K, Szeszko PR, Wu J, Chen S, Kumra S (2007b) Disruption of white matter integrity in the inferior longitudinal fasciculus in adolescents with schizophrenia as revealed by fiber tractography. Arch Gen Psychiatry 64:1270–1280

Baldeweg T, Klugman A, Gruzelier J, Hirsch SR (2004) Mismatch negativity potentials and cognitive impairment in schizophrenia. Schizophr Res 69:203–217

Barr MS, Farzan F, Tran LC, Chen R, Fitzgerald PB, Daskalakis ZJ (2010) Evidence for excessive frontal evoked gamma oscillatory activity in schizophrenia during working memory. Schizophr Res 121:146–152

Basar-Eroglu C, Brand A, Hildebrandt H, Karolina Kedzior K, Mathes B, Schmiedt C (2007) Working memory related gamma oscillations in schizophrenia patients. Int J Psychophysiol 64:39–45

Bava S, Thayer R, Jacobus J, Ward M, Jernigan TL, Tapert SF (2010) Longitudinal characterization of white matter maturation during adolescence. Brain Res 1327:38–46

Bear MF (2003) Bidirectional synaptic plasticity: from theory to reality. Philos Trans R Soc Lond B Biol Sci 358:649–655

Behrens MM, Ali SS, Dao DN, Lucero J, Shekhtman G, Quick KL, Dugan LL (2007) Ketamine-induced loss of phenotype of fast-spiking interneurons is mediated by NADPH-oxidase. Science 318:1645–1647

Behrens MM, Ali SS, Dao DN, Lucero J, Shekhtman G, Quick KL, Dugan LL (2007) Ketamine-induced loss of phenotype of fast-spiking interneurons is mediated by NADPH-oxidase. Science (80-) 318:1645–1647 Available at: http://www.ncbi.nlm.nih.gov/pubmed/18063801 [Accessed March 11, 2013].

Behrens MM, Ali SS, Dugan LL (2008) Interleukin-6 mediates the increase in NADPH-oxidase in the ketamine model of schizophrenia. J Neurosci 28:13957–13966

Berk M, Copolov D, Dean O, Lu K, Jeavons S, Schapkaitz I, Anderson-Hunt M, Judd F, Katz F, Katz P, Ording-Jespersen S, Little J, Conus P, Cuenod M, Do KQ, Bush AI (2008) N-acetyl cysteine as a glutathione precursor for schizophrenia--a double-blind, randomized, placebo-controlled trial. Biol Psychiatry 64:361–368

Berk M, Copolov D, Dean O, Lu K, Jeavons S, Schapkaitz I, Anderson-Hunt M, Judd F, Katz F, Katz P, Ording-Jespersen S, Little J, Conus P, Cuenod M, Do KQ, Bush

AI (2008) N-acetyl cysteine as a glutathione precursor for schizophrenia--a double-blind, randomized, placebo-controlled trial. Biol Psychiatry 64:361–368

Berman RM, Cappiello A, Anand A, Oren DA, Heninger GR, Charney DS, Krystal JH (2000) Antidepressant effects of ketamine in depressed patients. Biol Psychiatry 47:351–354

Bickel S, Lipp H-P, Umbricht D (2008) Early auditory sensory processing deficits in mouse mutants with reduced NMDA receptor function. Neuropsychopharmacology 33:1680–1689

Bitanihirwe BKY, Woo T-UW (2011) Oxidative stress in schizophrenia: an integrated approach. Neurosci Biobehav Rev 35:878–893

Braun I, Genius J, Grunze H, Bender A, Möller H-J, Rujescu D (2007) Alterations of hippocampal and prefrontal GABAergic interneurons in an animal model of psychosis induced by NMDA receptor antagonism. Schizophr Res 97:254–263

Breier A, Malhotra AK, Pinals DA, Weisenfeld NI, Pickar D (1997) Association of ketamine-induced psychosis with focal activation of the prefrontal cortex in healthy volunteers. Am J Psychiatry 154:805–811

Brenner C a, Krishnan GP, Vohs JL, Ahn W-Y, Hetrick WP, Morzorati SL, O’Donnell BF (2009) Steady state responses: electrophysiological assessment of sensory function in schizophrenia. Schizophr Bull 35:1065–1077

Brenner CA, Sporns O, Lysaker PH, O’Donnell BF (2003) EEG synchronization to modulated auditory tones in schizophrenia, schizoaffective disorder, and schizotypal personality disorder. Am J Psychiatry 160:2238–2240

Broberg BV, Glenthøj BY, Dias R, Larsen DB, Olsen CK (2009) Reversal of cognitive deficits by an ampakine (CX516) and sertindole in two animal models of schizophrenia--sub-chronic and early postnatal PCP treatment in attentional set-shifting. Psychopharmacology (Berl) 206:631–640

Broberg BV, Oranje B, Glenthøj BY, Fejgin K, Plath N, Bastlund JF (2010) Assessment of auditory sensory processing in a neurodevelopmental animal model of schizophrenia-Gating of auditory-evoked potentials and prepulse inhibition. Behav Brain Res 213:142–147

Brockhaus-Dumke A, Mueller R, Faigle U, Klosterkoetter J (2008) Sensory gating revisited: relation between brain oscillations and auditory evoked potentials in schizophrenia. Schizophr Res 99:238–249

Buchsbaum MS, Tang CY, Peled S, Gudbjartsson H, Lu D, Hazlett EA, Downhill J, Haznedar M, Fallon JH, Atlas SW (1998) MRI white matter diffusion anisotropy and PET metabolic rate in schizophrenia. Neuroreport 9:425–430

Burns J, Job D, Bastin ME, Whalley H, Macgillivray T, Johnstone EC, Lawrie SM (2003) Structural disconnectivity in schizophrenia: a diffusion tensor magnetic resonance imaging study. Br J Psychiatry 182:439–443

Buzsáki G (2006) Rhythms of the brain. Oxford University Press.

Caballero A, Diah KC, Tseng KY (2013) Region-specific upregulation of parvalbumin-, but not calretinin-positive cells in the ventral hippocampus during adolescence. Hippocampus 23:1331–1336

Cabungcal JH, Nicolas D, Kraftsik R, Cuénod M, Do KQ, Hornung J-P (2006) Glutathione deficit during development induces anomalies in the rat anterior cingulate GABAergic neurons: Relevance to schizophrenia. Neurobiol Dis 22:624–637

Cabungcal JH, Steullet P, Kraftsik R, Cuenod M, Do KQ (2013a) Early-life insults impair parvalbumin interneurons via oxidative stress: reversal by N-acetylcysteine. Biol Psychiatry 73:574–582

Cabungcal JH, Steullet P, Morishita H, Kraftsik R, Cuenod M, Hensch TK, Do KQ (2013b) Perineuronal nets protect fast-spiking interneurons against oxidative stress. Proc Natl Acad Sci 110:9130–9135

Campbell IG, Feinberg I (2009) Longitudinal trajectories of non-rapid eye movement delta and theta EEG as indicators of adolescent brain maturation. Proc Natl Acad Sci U S A 106:5177–5180

Canolty RT, Edwards E, Dalal SS, Soltani M, Nagarajan SS, Kirsch HE, Berger MS, Barbaro NM, Knight RT (2006) High gamma power is phase-locked to theta oscillations in human neocortex. Science 313:1626–1628

Cardin JA, Carlén M, Meletis K, Knoblich U, Zhang F, Deisseroth K, Tsai L-H, Moore CI (2009) Driving fast-spiking cells induces gamma rhythm and controls sensory responses. Nature 459:663–667

Carlén M, Meletis K, Siegle JH, Cardin J a, Futai K, Vierling-Claassen D, Rühlmann C, Jones SR, Deisseroth K, Sheng M, Moore CI, Tsai L-H (2011) A critical role for NMDA receptors in parvalbumin interneurons for gamma rhythm induction and behavior. Mol Psychiatry:1–12

Carmeli C, Knyazeva MG, Cuénod M, Do KQ (2012) Glutathione precursor N-acetyl-cysteine modulates EEG synchronization in schizophrenia patients: a double-blind, randomized, placebo-controlled trial. PLoS One 7:e29341

Caspi A, Moffitt TE, Cannon M, McClay J, Murray R, Harrington H, Taylor A, Arseneault L, Williams B, Braithwaite A, Poulton R, Craig IW (2005) Moderation of the effect of adolescent-onset cannabis use on adult psychosis by a functional polymorphism in the catechol-O-methyltransferase gene: longitudinal evidence of a gene X environment interaction. Biol Psychiatry 57:1117–1127

Catts VS, Fung SJ, Long LE, Joshi D, Vercammen A, Allen KM, Fillman SG, Rothmond DA, Sinclair D, Tiwari Y, Tsai S-Y, Weickert TW, Shannon Weickert C (2013) Rethinking schizophrenia in the context of normal neurodevelopment. Front Cell Neurosci 7:60

Cho RY, Konecky RO, Carter CS (2006) Impairments in frontal cortical gamma synchrony and cognitive control in schizophrenia. Proc Natl Acad Sci USA 103:19878–19883

Clementz BA, Sponheim SR, Beiser M (1994) Resting EEG in first-episode schizophrenia patients, bipolar psychosis patients, and their first-degree relatives. Psychophysiology 31:486–494

Cohen LT, Rickards FW, Clark GM (1991) A comparison of steady-state evoked potentials to modulated tones in awake and sleeping humans. J Acoust Soc Am 90:2467–2479

Condé F, Lund JS, Jacobowitz DM, Baimbridge KG, Lewis DA (1994) Local circuit neurons immunoreactive for calretinin, calbindin D-28k or parvalbumin in monkey prefrontal cortex: distribution and morphology. J Comp Neurol 341:95–116

Cornblatt BA, Lencz T, Kane JM (2001) Treatment of the schizophrenia prodrome: is it presently ethical? Schizophr Res 51:31–38

Costa L, Bauer L (1997) Quantitative electroencephalographic differences associated with alcohol, cocaine, heroin and dual-substance dependence. Drug Alcohol Depend 46:87–93

Coyle JT (2012) NMDA receptor and schizophrenia: a brief history. Schizophr Bull 38:920–926

Das Neves Duarte JM, Kulak A, Gholam-Razaee MM, Cuenod M, Gruetter R, Do KQ (2012) N-acetylcysteine normalizes neurochemical changes in the glutathione-deficient schizophrenia mouse model during development. Biol Psychiatry 71:1006–1014

De Lima MNM, Laranja DC, Bromberg E, Roesler R, Schröder N (2005) Pre- or post-training administration of the NMDA receptor blocker MK-801 impairs object recognition memory in rats. Behav Brain Res 156:139–143

Dickerson DD, Wolff AR, Bilkey DK (2010) Abnormal long-range neural synchrony in a maternal immune activation animal model of schizophrenia. J Neurosci 30:12424–12431

Didriksen M, Skarsfeldt T, Arnt J (2007) Reversal of PCP-induced learning and memory deficits in the Morris' water maze by sertindole and other antipsychotics. Psychopharmacology (Berl) 193:225–233

Dissanayake DWN, Zachariou M, Marsden CA, Mason R (2009) Effects of phencyclidine on auditory gating in the rat hippocampus and the medial prefrontal cortex. Brain Res 1298:153–160

Do KQ, Cabungcal JH, Frank A, Steullet P, Cuenod M (2009) Redox dysregulation, neurodevelopment, and schizophrenia. Curr Opin Neurobiol 19:220–230

Do KQ, Trabesinger AH, Kirsten-Krüger M, Lauer CJ, Dydak U, Hell D, Holsboer F, Boesiger P, Cuénod M (2000) Schizophrenia: glutathione deficit in cerebrospinal fluid and prefrontal cortex in vivo. Eur J Neurosci 12:3721–3728

Driesen NR, McCarthy G, Bhagwagar Z, Bloch M, Calhoun V, D'Souza DC, Gueorguieva R, He G, Ramachandran R, Suckow RF, Anticevic A, Morgan PT, Krystal JH (2013a) Relationship of resting brain hyperconnectivity and schizophrenia-like symptoms produced by the NMDA receptor antagonist ketamine in humans. Mol Psychiatry

Driesen NR, McCarthy G, Bhagwagar Z, Bloch MH, Calhoun VD, D'Souza DC, Gueorguieva R, He G, Leung H-C, Ramani R, Anticevic A, Suckow RF, Morgan PT, Krystal JH (2013b) The Impact of NMDA Receptor Blockade on Human Working Memory-Related Prefrontal Function and Connectivity. Neuropsychopharmacology

Egerton A, Reid L, McGregor S, Cochran SM, Morris BJ, Pratt JA (2008) Subchronic and chronic PCP treatment produces temporally distinct deficits in attentional set shifting and prepulse inhibition in rats. Psychopharmacology (Berl) 198:37–49

Ehrlichman RS, Gandal MJ, Maxwell CR, Lazarewicz MT, Finkel LH, Contreras D, Turetsky BI, Siegel SJ (2009a) N-methyl-d-aspartic acid receptor antagonist-induced frequency oscillations in mice recreate pattern of electrophysiological deficits in schizophrenia. Neuroscience 158:705–712

Ehrlichman RS, Luminais SN, White SL, Rudnick ND, Ma N, Dow HC, Kreibich AS, Abel T, Brodkin ES, Hahn C-G, Siegel SJ (2009b) Neuregulin 1 transgenic mice display reduced mismatch negativity, contextual fear conditioning and social interactions. Brain Res 1294:116–127

Engel AK, Singer W (2001) Temporal binding and the neural correlates of sensory awareness. Trends Cogn Sci 5:16–25

Featherstone RE, Liang Y, Saunders JA, Tatard-Leitman VM, Ehrlichman RS, Siegel SJ (2012) Subchronic ketamine treatment leads to permanent changes in EEG, cognition and the astrocytic glutamate transporter EAAT2 in mice. Neurobiol Dis 47:338–346

Feinberg I (1982) Schizophrenia: caused by a fault in programmed synaptic elimination during adolescence? J Psychiatr Res 17:319–334

Feleder C, Tseng KY, Calhoon GG, O'Donnell P (2010) Neonatal intrahippocampal immune challenge alters dopamine modulation of prefrontal cortical interneurons in adult rats. Biol Psychiatry 67:386–392

Franowicz MN, Barth DS (1995) Comparison of evoked potentials and high-frequency (gamma-band) oscillating potentials in rat auditory cortex. J Neurophysiol 74:96–112

Freedman R, Adler LE, Waldo MC, Pachtman E, Franks RD (1983) Neurophysiological evidence for a defect in inhibitory pathways in schizophrenia: comparison of medicated and drug-free patients. Biol Psychiatry 18:537–551

Friston KJ (1998) The disconnection hypothesis. Schizophr Res 30:115–125

Fung SJ, Webster MJ, Sivagnanasundaram S, Duncan C, Elashoff M, Weickert CS (2010) Expression of interneuron markers in the dorsolateral prefrontal cortex of the developing human and in schizophrenia. Am J Psychiatry 167:1479–1488

Gandal MJ, Edgar JC, Klook K, Siegel SJ (2011) Gamma synchrony: Towards a translational biomarker for the treatment-resistant symptoms of schizophrenia. Neuropharmacology

Gawryluk JW, Wang J-F, Andreazza AC, Shao L, Young LT (2011) Decreased levels of glutathione, the major brain antioxidant, in post-mortem prefrontal cortex from patients with psychiatric disorders. Int J Neuropsychopharmacol 14:123–130

Geyer MA, Braff DL (1987) Startle habituation and sensorimotor gating in schizophrenia and related animal models. Schizophr Bull 13:643–668

Gilmour G, Dix S, Fellini L, Gastambide F, Plath N, Steckler T, Talpos J, Tricklebank M (2011) NMDA receptors, cognition and schizophrenia - Testing the validity of the NMDA receptor hypofunction hypothesis. Neuropharmacology 62:1401–1412

Giovanoli S, Engler H, Engler A, Richetto J, Voget M, Willi R, Winter C, Riva MA, Mortensen PB, Feldon J, Schedlowski M, Meyer U (2013) Stress in puberty unmasks latent neuropathological consequences of prenatal immune activation in mice. Science 339:1095–1099

Gogtay N, Giedd JN, Lusk L, Hayashi KM, Greenstein D, Vaituzis AC, Nugent TF, Herman DH, Clasen LS, Toga AW, Rapoport JL, Thompson PM (2004) Dynamic mapping of human cortical development during childhood through early adulthood. Proc Natl Acad Sci USA 101:8174–8179

Gonzalez-Burgos G, Lewis D a (2012) NMDA Receptor Hypofunction, Parvalbumin-Positive Neurons and Cortical Gamma Oscillations in Schizophrenia. Schizophr Bull

Gonzalez-Burgos G, Lewis DA (2008) GABA neurons and the mechanisms of network oscillations: implications for understanding cortical dysfunction in schizophrenia. Schizophr Bull 34:944–961

Green MF (1996) What are the functional consequences of neurocognitive deficits in schizophrenia? Am J Psychiatry 153:321–330

Green MF, Kern RS, Braff DL, Mintz J (2000) Neurocognitive deficits and functional outcome in schizophrenia: are we measuring the "right stuff"? Schizophr Bull 26:119–136

Guo N, Yoshizaki K, Kimura R, Suto F, Yanagawa Y, Osumi N (2013) A sensitive period for GABAergic interneurons in the dentate gyrus in modulating sensorimotor gating. J Neurosci 33:6691–6704

Gysin R, Kraftsik R, Sandell J, Bovet P, Chappuis C, Conus P, Deppen P, Preisig M, Ruiz V, Steullet P, Tosic M, Werge T, Cuénod M, Do KQ (2007) Impaired glutathione synthesis in schizophrenia: convergent genetic and functional evidence. Proc Natl Acad Sci 104:16621–16626

Haddad JJ (2002) Antioxidant and prooxidant mechanisms in the regulation of redox(y)-sensitive transcription factors. Cell Signal 14:879–897.

Haenschel C, Bittner R a, Waltz J, Haertling F, Wibral M, Singer W, Linden DEJ, Rodriguez E (2009) Cortical oscillatory activity is critical for working memory as revealed by deficits in early-onset schizophrenia. J Neurosci 29:9481–9489

Häfner H, Maurer K, Löffler W, Riecher-Rössler A (1993) The influence of age and sex on the onset and early course of schizophrenia. Br J Psychiatry 162:80–86

Hakami T, Jones NC, Tolmacheva E a, Gaudias J, Chaumont J, Salzberg M, O'Brien TJ, Pinault D (2009) NMDA receptor hypofunction leads to generalized and persistent aberrant gamma oscillations independent of hyperlocomotion and the state of consciousness. PLoS One 4:e6755

Hanania T, Hillman GR, Johnson KM (1999) Augmentation of locomotor activity by chronic phencyclidine is associated with an increase in striatal NMDA receptor function and an upregulation of the NR1 receptor subunit. Synapse 31:229–239

Härtig W, Brauer K, Bigl V, Brückner G (1994) Chondroitin sulfate proteoglycan-immunoreactivity of lectin-labeled perineuronal nets around parvalbumin-containing neurons. Brain Res 635:307–311

Hashimoto T, Nguyen QL, Rotaru D, Keenan T, Arion D, Beneyto M, Gonzalez-Burgos G, Lewis DA (2009) Protracted developmental trajectories of GABAA receptor alpha1 and alpha2 subunit expression in primate prefrontal cortex. Biol Psychiatry 65:1015–1023

Hashimoto T, Volk DW, Eggan SM, Mirnics K, Pierri JN, Sun Z, Sampson AR, Lewis DA (2003) Gene expression deficits in a subclass of GABA neurons in the prefrontal cortex of subjects with schizophrenia. J Neurosci 23:6315–6326

Heinrichs RW, Zakzanis KK (1998) Neurocognitive deficit in schizophrenia: a quantitative review of the evidence. Neuropsychology 12:426–445

Hensch TK (2005) Critical period plasticity in local cortical circuits. Nat Rev Neurosci 6:877–888

Hertzmann M, Reba RC, Kotlyarov E V (1990) Single photon emission computed tomography in phencyclidine and related drug abuse. Am J Psychiatry 147:255–256

Hoffman RE, Dobscha SK (1989) Cortical pruning and the development of schizophrenia: a computer model. Schizophr Bull 15:477–490

Homayoun H, Moghaddam B (2007) NMDA receptor hypofunction produces opposite effects on prefrontal cortex interneurons and pyramidal neurons. J Neurosci 27:11496–11500

Hong LE, Buchanan RW, Thaker GK, Shepard PD, Summerfelt A (2008a) Beta (~16 Hz) frequency neural oscillations mediate auditory sensory gating in humans. Psychophysiology 45:197–204

Hong LE, Moran L V, Du X, Donnell PO, Summerfelt A (2012) Clinical Neurophysiology Mismatch negativity and low frequency oscillations in schizophrenia families. Clin Neurophysiol

Hong LE, Summerfelt A, Buchanan RW, O'Donnell P, Thaker GK, Weiler MA, Lahti AC (2010) Gamma and delta neural oscillations and association with clinical symptoms under subanesthetic ketamine. Neuropsychopharmacology 35:632–640

Hong LE, Summerfelt A, McMahon R, Adami H, Francis G, Elliott A, Buchanan RW, Thaker GK (2004) Evoked gamma band synchronization and the liability for schizophrenia. Schizophr Res 70:293–302

Hong LE, Summerfelt A, Mitchell BD, McMahon RP, Wonodi I, Buchanan RW, Thaker GK (2008b) Sensory gating endophenotype based on its neural oscillatory pattern and heritability estimate. Arch Gen Psychiatry 65:1008–1016

Hong LE, Summerfelt A, Mitchell BD, O'Donnell P, Thaker GK (2011) A shared low-frequency oscillatory rhythm abnormality in resting and sensory gating in schizophrenia. Clin Neurophysiol

Huttenlocher PR (1979) Synaptic density in human frontal cortex - developmental changes and effects of aging. Brain Res 163:195–205

Inostroza M, Born J (2013) Sleep for preserving and transforming episodic memory. Annu Rev Neurosci 36:79–102

Javitt DC (2009) Sensory processing in schizophrenia: neither simple nor intact. Schizophr Bull 35:1059–1064

Javitt DC, Doneshka P, Grochowski S, Ritter W (1995) Impaired mismatch negativity generation reflects widespread dysfunction of working memory in schizophrenia. Arch Gen Psychiatry 52:550–558

Javitt DC, Doneshka P, Zylberman I, Ritter W, Vaughan HG (1993) Impairment of early cortical processing in schizophrenia: an event-related potential confirmation study. Biol Psychiatry 33:513–519

Javitt DC, Doneshka P, Zylberman I, Ritter W, Vaughan HG (1993) Impairment of early cortical processing in schizophrenia: an event-related potential confirmation study. Biol Psychiatry 33:513–519 Available at: http://www.ncbi.nlm.nih.gov/pubmed/8513035 [Accessed October 13, 2014].

Javitt DC, Steinschneider M, Schroeder CE, Arezzo JC (1996) Role of cortical N-methyl-D-aspartate receptors in auditory sensory memory and mismatch negativity generation: implications for schizophrenia. Proc Natl Acad Sci U S A 93:11962–11967

Johnson A, Jaaro-Peled H, Shahani N, Sedlak T, Zoubovsky S, Burruss D, Emiliani F, Sawa A, Gallagher M (2013) Cognitive and motivational deficits together with prefrontal oxidative stress in a mouse model for neuropsychiatric illness. Proc Natl Acad Sci 110:12462–12467

Jones DP, Go Y-M (2010) Redox compartmentalization and cellular stress. Diabetes Obes Metab 12 (Suppl :116–125

Jones MW, Wilson MA (2005) Theta rhythms coordinate hippocampal-prefrontal interactions in a spatial memory task. PLoS Biol 3:e402

Jones P, Cannon M (1998) The new epidemiology of schizophrenia. Psychiatr Clin North Am 21:1–25

Kasai H (1997) Analysis of a form of oxidative DNA damage, 8-hydroxy-2'-deoxyguanosine, as a marker of cellular oxidative stress during carcinogenesis. Mutat Res 387:147–163

Kawaguchi Y, Kubota Y (1997) GABAergic cell subtypes and their synaptic connections in rat frontal cortex. Cereb Cortex 7:476–486

Keilhoff G, Becker A, Grecksch G, Wolf G, Bernstein H-G (2004) Repeated application of ketamine to rats induces changes in the hippocampal expression of parvalbumin, neuronal nitric oxide synthase and cFOS similar to those found in human schizophrenia. Neuroscience 126:591–598

Kil J, Pierce C, Tran H, Gu R, Lynch ED (2007) Ebselen treatment reduces noise induced hearing loss via the mimicry and induction of glutathione peroxidase. Hear Res 226:44–51

Kinon BJ, Zhang L, Millen BA, Osuntokun OO, Williams JE, Kollack-Walker S, Jackson K, Kryzhanovskaya L, Jarkova N (2011) A multicenter, inpatient, phase 2, double-blind, placebo-controlled dose-ranging study of LY2140023 monohydrate in patients with DSM-IV schizophrenia. J Clin Psychopharmacol 31:349–355

Kittelberger K, Hur EE, Sazegar S, Keshavan V, Kocsis B (2012) Comparison of the effects of acute and chronic administration of ketamine on hippocampal oscillations: relevance for the NMDA receptor hypofunction model of schizophrenia. Brain Struct Funct 217:395–409

Kochunov P, Hong LE (2014) Neurodevelopmental and neurodegenerative models of schizophrenia: white matter at the center stage. Schizophr Bull 40:721–728

König P, Engel AK, Singer W (1996) Integrator or coincidence detector? The role of the cortical neuron revisited. Trends Neurosci 19:130–137

Krishnan GP, Hetrick WP, Brenner CA, Shekhar A, Steffen AN, O'Donnell BF (2009) Steady state and induced auditory gamma deficits in schizophrenia. Neuroimage 47:1711–1719

Krystal JH, Karper LP, Seibyl JP, Freeman GK, Delaney R, Bremner JD, Heninger GR, Bowers MB, Charney DS (1994) Subanesthetic effects of the noncompetitive NMDA antagonist, ketamine, in humans. Psychotomimetic, perceptual, cognitive, and neuroendocrine responses. Arch Gen Psychiatry 51:199–214

Kubicki M, McCarley R, Westin C-F, Park H-J, Maier S, Kikinis R, Jolesz FA, Shenton ME (2009) A review of diffusion tensor imaging studies in schizophrenia. J Psychiatr Res 41:15–30

Kubicki M, Westin C-F, Nestor PG, Wible CG, Frumin M, Maier SE, Kikinis R, Jolesz FA, McCarley RW, Shenton ME (2003) Cingulate fasciculus integrity disruption in schizophrenia: a magnetic resonance diffusion tensor imaging study. Biol Psychiatry 54:1171–1180

Kuwada S, Anderson JS, Batra R, Fitzpatrick DC, Teissier N, D'Angelo WR (2002) Sources of the scalp-recorded amplitude-modulation following response. J Am Acad Audiol 13:188–204

Kwon JS, O'Donnell BF, Wallenstein G V, Greene RW, Hirayasu Y, Nestor PG, Hasselmo ME, Potts GF, Shenton ME, McCarley RW (1999) Gamma frequency-range abnormalities to auditory stimulation in schizophrenia. Arch Gen Psychiatry 56:1001–1005

Lahti AC, Koffel B, LaPorte D, Tamminga CA (1995) Subanesthetic doses of ketamine stimulate psychosis in schizophrenia. Neuropsychopharmacology 13:9–19

Lahti AC, Weiler MA, Tamara Michaelidis BA, Parwani A, Tamminga CA (2001) Effects of ketamine in normal and schizophrenic volunteers. Neuropsychopharmacology 25:455–467

Lavoie S, Murray MM, Deppen P, Knyazeva MG, Berk M, Boulat O, Bovet P, Bush AI, Conus P, Copolov D, Fornari E, Meuli R, Solida A, Vianin P, Cuénod M, Buclin T, Do KQ (2008) Glutathione precursor, N-acetyl-cysteine, improves mismatch negativity in schizophrenia patients. Neuropsychopharmacology 33:2187–2199

Lazarewicz MT, Ehrlichman RS, Maxwell CR, Gandal MJ, Finkel LH, Siegel SJ (2010) Ketamine modulates theta and gamma oscillations. J Cogn Neurosci 22:1452–1464

Lee H, Dvorak D, Kao H-Y, Duffy ÁM, Scharfman HE, Fenton AA (2012) Early cognitive experience prevents adult deficits in a neurodevelopmental schizophrenia model. Neuron 75:714–724

Lee PR, Brady DL, Shapiro RA, Dorsa DM, Koenig JI (2005) Social interaction deficits caused by chronic phencyclidine administration are reversed by oxytocin. Neuropsychopharmacology 30:1883–1894

Lewis BL, O'Donnell P (2000) Ventral tegmental area afferents to the prefrontal cortex maintain membrane potential "up" states in pyramidal neurons via D(1) dopamine receptors. Cereb Cortex 10:1168–1175

Lewis DA (2014) Inhibitory neurons in human cortical circuits: substrate for cognitive dysfunction in schizophrenia. Curr Opin Neurobiol 26C:22–26

Lewis DA, Curley AA, Glausier JR, Volk DW (2012) Cortical parvalbumin interneurons and cognitive dysfunction in schizophrenia. Trends Neurosci 35:57–67

Lewis DA, Hashimoto T, Volk DW (2005) Cortical inhibitory neurons and schizophrenia. Nat Rev Neurosci 6:312–324

Lewis DA, Lieberman JA (2000) Catching Up on Schizophrenia. Neuron 28:325–334

Li HB, Matsumoto K, Yamamoto M, Watanabe H (1997) NMDA but not AMPA receptor antagonists impair the delay-interposed radial maze performance of rats. Pharmacol Biochem Behav 58:249–253

Light G a, Hsu JL, Hsieh MH, Meyer-Gomes K, Sprock J, Swerdlow NR, Braff DL (2006) Gamma band oscillations reveal neural network cortical coherence dysfunction in schizophrenia patients. Biol Psychiatry 60:1231–1240

Lim KO, Hedehus M, Moseley M, de Crespigny A, Sullivan E V, Pfefferbaum A (1999) Compromised white matter tract integrity in schizophrenia inferred from diffusion tensor imaging. Arch Gen Psychiatry 56:367–374

Linden RD, Campbell KB, Hamel G, Picton TW (1985) Human auditory steady state evoked potentials during sleep. Ear Hear 6:167–174

Lipska BK, Halim ND, Segal PN, Weinberger DR (2002) Effects of reversible inactivation of the neonatal ventral hippocampus on behavior in the adult rat. J Neurosci 22:2835–2842

Lipska BK, Swerdlow NR, Geyer MA, Jaskiw GE, Braff DL, Weinberger DR (1995) Neonatal excitotoxic hippocampal damage in rats causes post-pubertal changes in prepulse inhibition of startle and its disruption by apomorphine. Psychopharmacology (Berl) 122:35–43

Lodge DJ, Behrens MM, Grace AA (2009) A loss of parvalbumin-containing interneurons is associated with diminished oscillatory activity in an animal model of schizophrenia. J Neurosci 29:2344–2354

Luby ED, Cohen BD, Rosenbaum G, Gottlieb JS, Kelley R (1959) Study of a new schizophrenomimetic drug; sernyl. Arch Neurol Psychiatry 81:363–369

Luck SJ, Mathalon DH, O’Donnell BF, Hämäläinen MS, Spencer KM, Javitt DC, Uhlhaas PJ (2010) A Roadmap for the Development and Validation of Event-Related Potential Biomarkers in Schizophrenia Research. Biol Psychiatry

Lundgaard I, Luzhynskaya A, Stockley JH, Wang Z, Evans KA, Swire M, Volbracht K, Gautier HOB, Franklin RJM, Ffrench-Constant C, Attwell D, Káradóttir RT (2013) Neuregulin and BDNF Induce a Switch to NMDA Receptor-Dependent Myelination by Oligodendrocytes Barres BA, ed. PLoS Biol 11:e1001743

Ma J, Leung LS (2007) The supramammillo-septal-hippocampal pathway mediates sensorimotor gating impairment and hyperlocomotion induced by MK-801 and ketamine in rats. Psychopharmacology (Berl) 191:961–974

Ma J, Tai SK, Leung LS (2009) Ketamine-induced deficit of auditory gating in the hippocampus of rats is alleviated by medial septal inactivation and antipsychotic drugs. Psychopharmacology (Berl) 206:457–467

Malhotra AK, Pinals DA, Weingartner H, Sirocco K, Missar CD, Pickar D, Breier A (1996) NMDA receptor function and human cognition: the effects of ketamine in healthy volunteers. Neuropsychopharmacology 14:301–307

Manallack D, Lodge D, Beart P (1989) Subchronic administration of MK-801 in the rat decreases cortical binding of d-AP5, suggesting down-regulation of the cortical N-methyl-d-aspartate. Neuroscience

Mansbach RS, Geyer MA (1989) Effects of phencyclidine and phencyclidine biologs on sensorimotor gating in the rat. Neuropsychopharmacology 2:299–308

Markram H, Lübke J, Frotscher M, Sakmann B (1997) Regulation of synaptic efficacy by coincidence of postsynaptic APs and EPSPs. Science 275:213–215

Markram H, Toledo-Rodriguez M, Wang Y, Gupta A, Silberberg G, Wu C (2004) Interneurons of the neocortical inhibitory system. Nat Rev Neurosci 5:793–807

McCarley RW, Wible CG, Frumin M, Hirayasu Y, Levitt JJ, Fischer IA, Shenton ME (1999) MRI anatomy of schizophrenia. Biol Psychiatry 45:1099–1119

Miltner WH, Braun C, Arnold M, Witte H, Taub E (1999) Coherence of gamma-band EEG activity as a basis for associative learning. Nature 397:434–436

Miyamoto S, Leipzig JN, Lieberman JA, Duncan GE (2000) Effects of ketamine, MK-801, and amphetamine on regional brain 2-deoxyglucose uptake in freely moving mice. Neuropsychopharmacology 22:400–412

Mizuno Y, Suzuki T, Nakagawa A, Yoshida K, Mimura M, Fleischhacker WW, Uchida H (2014) Pharmacological Strategies to Counteract Antipsychotic-Induced Weight Gain and Metabolic Adverse Effects in Schizophrenia: A Systematic Review and Meta-analysis. Schizophr Bull

Moghaddam B, Adams B, Verma A, Daly D (1997) Activation of Glutamatergic Neurotransmission by Ketamine: A Novel Step in the Pathway from NMDA Receptor Blockade to Dopaminergic and Cognitive Disruptions Associated with the Prefrontal Cortex. J Neurosci 17:2921–2927

Moghaddam B, Adams BW (1998) Reversal of phencyclidine effects by a group II metabotropic glutamate receptor agonist in rats. Science 281:1349–1352

Monyer H, Burnashev N, Laurie DJ, Sakmann B, Seeburg PH (1994) Developmental and regional expression in the rat brain and functional properties of four NMDA receptors. Neuron 12:529–540

Moore THM, Zammit S, Lingford-Hughes A, Barnes TRE, Jones PB, Burke M, Lewis G (2007) Cannabis use and risk of psychotic or affective mental health outcomes: a systematic review. Lancet 370:319–328

Moran L V, Hong LE (2011) High vs Low Frequency Neural Oscillations in Schizophrenia. Schizophr Bull:1–5

Morgan CJA, Curran HV (2006) Acute and chronic effects of ketamine upon human memory: a review. Psychopharmacology (Berl) 188:408–424

Morgan CJA, Muetzelfeldt L, Curran HV (2009) Ketamine use, cognition and psychological wellbeing: a comparison of frequent, infrequent and ex-users with polydrug and non-using controls. Addiction 104:77–87

Morris HM, Hashimoto T, Lewis DA (2008) Alterations in somatostatin mRNA expression in the dorsolateral prefrontal cortex of subjects with schizophrenia or schizoaffective disorder. Cereb Cortex 18:1575–1587

Moussawi K, Pacchioni A, Moran M, Olive MF, Gass JT, Lavin A, Kalivas PW (2009) N-Acetylcysteine reverses cocaine-induced metaplasticity. Nat Neurosci 12:182–189.

Mulert C, Kirsch V, Pascual-Marqui R, McCarley RW, Spencer KM (2011) Long-range synchrony of γ oscillations and auditory hallucination symptoms in schizophrenia. Int J Psychophysiol 79:55–63

Müller A, Cadenas E, Graf P, Sies H (1984) A novel biologically active seleno-organic compound--I. Glutathione peroxidase-like activity in vitro and antioxidant capacity of PZ 51 (Ebselen). Biochem Pharmacol 33:3235–3239

Müller MM, Keil A, Gruber T, Elbert T (1999) Processing of affective pictures modulates right-hemispheric gamma band EEG activity. Clin Neurophysiol 110:1913–1920

Musall S, von Pföstl V, Rauch A, Logothetis NK, Whittingstall K (2014) Effects of neural synchrony on surface EEG. Cereb Cortex 24:1045–1053

Nagy Z, Westerberg H, Klingberg T (2004) Maturation of white matter is associated with the development of cognitive functions during childhood. J Cogn Neurosci 16:1227–1233

Nakazawa K, Zsiros V, Jiang Z, Nakao K, Kolata S, Zhang S, Belforte JE (2011) GABAergic interneuron origin of schizophrenia pathophysiology. Neuropharmacology

Niwa M, Kamiya A, Murai R, Kubo K, Gruber AJ, Tomita K, Lu L, Tomisato S, Jaaro-Peled H, Seshadri S, Hiyama H, Huang B, Kohda K, Noda Y, O'Donnell P, Nakajima K, Sawa A, Nabeshima T (2010) Knockdown of DISC1 by in utero gene transfer disturbs postnatal dopaminergic maturation in the frontal cortex and leads to adult behavioral deficits. Neuron 65:480–489

Nwokocha CR, Baker A, Douglas D, McCalla G, Nwokocha M, Brown PD (2013) Apocynin ameliorates cadmium-induced hypertension through elevation of endothelium nitric oxide synthase. Cardiovasc Toxicol 13:357–363

O'Donnell P (2011) Adolescent Onset of Cortical Disinhibition in Schizophrenia: Insights From Animal Models. Schizophr Bull 37:484–492

O'Donnell P (2012a) Cortical interneurons, immune factors and oxidative stress as early targets for schizophrenia. Eur J Neurosci 35:1866–1870

O'Donnell P (2012b) Cortical disinhibition in the neonatal ventral hippocampal lesion model of schizophrenia: new vistas on possible therapeutic approaches. Pharmacol Ther 133:19–25

O'Donnell P, Lewis BL, Weinberger DR, Lipska BK (2002) Neonatal hippocampal damage alters electrophysiological properties of prefrontal cortical neurons in adult rats. Cereb Cortex 12:975–982

Oranje B, Gispen-de Wied CC, Verbaten MN, Kahn RS (2002) Modulating sensory gating in healthy volunteers. Biol Psychiatry 52:887–895

Otte D-M, Sommersberg B, Kudin A, Guerrero C, Albayram O, Filiou MD, Frisch P, Yilmaz O, Drews E, Turck CW, Bilkei-Gorzó A, Kunz WS, Beck H, Zimmer A (2011) N-acetyl cysteine treatment rescues cognitive deficits induced by mitochondrial dysfunction in G72/G30 transgenic mice. Neuropsychopharmacology 36:2233–2243

Pacheco-López G, Giovanoli S, Langhans W, Meyer U (2013) Priming of metabolic dysfunctions by prenatal immune activation in mice: relevance to schizophrenia. Schizophr Bull 39:319–329

Patil ST, Zhang L, Martenyi F, Lowe SL, Jackson KA, Andreev B V, Avedisova AS, Bardenstein LM, Gurovich IY, Morozova MA, Mosolov SN, Neznanov NG, Reznik AM, Smulevich AB, Tochilov VA, Johnson BG, Monn JA, Schoepp DD (2007) Activation of mGlu2/3 receptors as a new approach to treat schizophrenia: a randomized Phase 2 clinical trial. Nat Med 13:1102–1107

Pawlas N, Małecki A (2007) Effects of ebselen on glutathione level in neurons exposed to arachidonic acid and 4-hydroxynonenal during simulated ischemia in vitro. Pharmacol Reports 59:708–714

Paxinos G, Watson C (1998) The Rat Brain in Stereotaxic Coordinates, Sixth Edition.

Pfeffer CK, Xue M, He M, Huang ZJ, Scanziani M (2013) Inhibition of inhibition in visual cortex: the logic of connections between molecularly distinct interneurons. Nat Neurosci 16:1068–1076

Phillips WA, Silverstein SM (2003) Convergence of biological and psychological perspectives on cognitive coordination in schizophrenia. Behav Brain Sci 26:65–82; discussion 82–137

Pinault D (2008) N-methyl d-aspartate receptor antagonists ketamine and MK-801 induce wake-related aberrant gamma oscillations in the rat neocortex. Biol Psychiatry 63:730–735

Plourde G (1996) The effects of propofol on the 40-Hz auditory steady-state response and on the electroencephalogram in humans. Anesth Analg 82:1015–1022

Plourde G, Baribeau J, Bonhomme V (1997) Ketamine increases the amplitude of the 40-Hz auditory steady-state response in humans. Br J Anaesth 78:524–529

Plourde G, Boylan JF (1991) The auditory steady state response during sufentanil anaesthesia. Br J Anaesth 66:683–691

Plourde G, Picton TW (1990) Human auditory steady-state response during general anesthesia. Anesth Analg 71:460–468

Radi R (2004) Nitric oxide, oxidants, and protein tyrosine nitration. Proc Natl Acad Sci 101:4003–4008

Raver SM, Haughwout SP, Keller A (2013) Adolescent cannabinoid exposure permanently suppresses cortical oscillations in adult mice. Neuropsychopharmacology 38:2338–2347

Rodriguez E, George N, Lachaux JP, Martinerie J, Renault B, Varela FJ (1999) Perception's shadow: long-distance synchronization of human brain activity. Nature 397:430–433

Roelfsema PR, Engel AK, König P, Singer W (1997) Visuomotor integration is associated with zero time-lag synchronization among cortical areas. Nature 385:157–161

Rojas DC, Maharajh K, Teale PD, Kleman MR, Benkers TL, Carlson JP, Reite ML (2006) Development of the 40Hz steady state auditory evoked magnetic field from ages 5 to 52. Clin Neurophysiol 117:110–117

Rotarska-Jagiela A, Schönmeyer R, Oertel V, Haenschel C, Vogeley K, Linden DEJ (2008) The corpus callosum in schizophrenia-volume and connectivity changes affect specific regions. Neuroimage 39:1522–1532

Rowland LM, Astur RS, Jung RE, Bustillo JR, Lauriello J, Yeo RA (2005a) Selective cognitive impairments associated with NMDA receptor blockade in humans. Neuropsychopharmacology 30:633–639

Rowland LM, Bustillo JR, Mullins PG, Jung RE, Lenroot R, Landgraf E, Barrow R, Yeo R, Lauriello J, Brooks WM (2005b) Effects of ketamine on anterior cingulate glutamate metabolism in healthy humans: a 4-T proton MRS study. Am J Psychiatry 162:394–396

Rutter L, Carver FW, Holroyd T, Nadar SR, Mitchell-Francis J, Apud J, Weinberger DR, Coppola R (2009) Magnetoencephalographic gamma power reduction in patients with schizophrenia during resting condition. Hum Brain Mapp 30:3254–3264

Salter MG, Fern R (2005) NMDA receptors are expressed in developing oligodendrocyte processes and mediate injury. Nature 438:1167–1171

Schall U, Catts S V., Karayanidis F, Ward PB (1999) Auditory event-related potential indices of fronto-temporal information processing in schizophrenia syndromes: valid outcome prediction of clozapine therapy in a three-year follow-up. Int J Neuropsychopharmacol 2:83–93

Schizophrenia Working Group of the Psychiatric Genomics Consortium (2014). Biological insights from 108 schizophrenia-associated gene loci. Nature 511:421-427.

Schmitz C, Hof PR (2005) Design-based stereology in neuroscience. Neuroscience 130:813–831

Sigurdsson T, Stark KL, Karayiorgou M, Gogos JA, Gordon JA (2010) Impaired hippocampal-prefrontal synchrony in a genetic mouse model of schizophrenia. Nature 464:763–767

Sivarao D V., Frenkel M, Chen P, Healy FL, Lodge NJ, Zaczek R (2013) MK-801 disrupts and nicotine augments 40 Hz auditory steady state responses in the auditory cortex of the urethane-anesthetized rat. Neuropharmacology 73:1–9

Smith JW, Gastambide F, Gilmour G, Dix S, Foss J, Lloyd K, Malik N, Tricklebank M (2011) A comparison of the effects of ketamine and phencyclidine with other antagonists of the NMDA receptor in rodent assays of attention and working memory. Psychopharmacology (Berl) 217:255–269

Sohal VS, Zhang F, Yizhar O, Deisseroth K (2009) Parvalbumin neurons and gamma rhythms enhance cortical circuit performance. Nature 459:698–702

Spencer KM, Nestor PG, Perlmutter R, Niznikiewicz MA, Klump MC, Frumin M, Shenton ME, McCarley RW (2004) Neural synchrony indexes disordered perception and cognition in schizophrenia. Proc Natl Acad Sci USA 101:17288–17293

Spencer KM, Niznikiewicz MA, Nestor PG, Shenton ME, McCarley RW (2009) Left auditory cortex gamma synchronization and auditory hallucination symptoms in schizophrenia. BMC Neurosci 10:85

Spencer KM, Salisbury DF, Shenton ME, McCarley RW (2008) Gamma-band auditory steady-state responses are impaired in first episode psychosis. Biol Psychiatry 64:369–375

Sponheim SR, Clementz BA, Iacono WG, Beiser M (1994) Resting EEG in first-episode and chronic schizophrenia. Psychophysiology 31:37–43

Stefani MR, Moghaddam B (2002) Effects of repeated treatment with amphetamine or phencyclidine on working memory in the rat. Behav Brain Res 134:267–274

Steinmetz PN, Roy A, Fitzgerald PJ, Hsiao SS, Johnson KO, Niebur E (2000) Attention modulates synchronized neuronal firing in primate somatosensory cortex. Nature 404:187–190

Stephan KE, Baldeweg T, Friston KJ (2006) Synaptic plasticity and dysconnection in schizophrenia. Biol Psychiatry 59:929–939

Steullet P, Cabungcal JH, Kulak A, Kraftsik R, Chen Y, Dalton TP, Cuenod M, Do KQ (2010) Redox dysregulation affects the ventral but not dorsal hippocampus: impairment of parvalbumin neurons, gamma oscillations, and related behaviors. J Neurosci 30:2547–2558

Steullet P, Neijt HC, Cuénod M, Do KQ (2006) Synaptic plasticity impairment and hypofunction of NMDA receptors induced by glutathione deficit: relevance to schizophrenia. Neuroscience 137:807–819

Stevens KE, Meltzer J, Rose GM (1995) Nicotinic cholinergic normalization of amphetamine-induced loss of auditory gating in freely moving rats. Psychopharmacology (Berl) 119:163–170

Stone JM, Davis JM, Leucht S, Pilowsky LS (2009) Cortical dopamine D2/D3 receptors are a common site of action for antipsychotic drugs--an original patient data meta-analysis of the SPECT and PET in vivo receptor imaging literature. Schizophr Bull 35:789–797

Stone JM, Dietrich C, Edden R, Mehta MA, De Simoni S, Reed LJ, Krystal JH, Nutt D, Barker GJ (2012) Ketamine effects on brain GABA and glutamate levels with 1H-MRS: relationship to ketamine-induced psychopathology. Mol Psychiatry 17:664–665

Strous RD, Cowan N, Ritter W, Javitt DC (1995) Auditory sensory (“echoic”) memory dysfunction in schizophrenia. Am J Psychiatry 152:1517–1519

Sweet RA, Henteleff RA, Zhang W, Sampson AR, Lewis DA (2009) Reduced dendritic spine density in auditory cortex of subjects with schizophrenia. Neuropsychopharmacology 34:374–389

Swerdlow NR, Geyer M a, Shoemaker JM, Light G a, Braff DL, Stevens KE, Sharp R, Breier M, Neary A, Auerbach PP (2006) Convergence and divergence in the neurochemical regulation of prepulse inhibition of startle and N40 suppression in rats. Neuropsychopharmacology 31:506–515

Symond MP, Symond MB, Harris AWF, Gordon E, Williams LM (2005) “Gamma synchrony” in first-episode schizophrenia: a disorder of temporal connectivity? Am J Psychiatry 162:459–465

Tamminga CA, Holcomb HH (2005) Phenotype of schizophrenia: a review and formulation. Mol Psychiatry 10:27–39

Tandon R (2011) Antipsychotics in the treatment of schizophrenia: an overview. J Clin Psychiatry 72 Suppl 1:4–8

Thomases DR, Cass DK, Tseng KY (2013) Periadolescent exposure to the NMDA receptor antagonist MK-801 impairs the functional maturation of local GABAergic circuits in the adult prefrontal cortex. J Neurosci 33:26–34

Tosic M, Ott J, Barral S, Bovet P, Deppen P, Gheorghita F, Matthey M-L, Parnas J, Preisig M, Saraga M, Solida A, Timm S, Wang AG, Werge T, Cuénod M, Do KQ (2006) Schizophrenia and oxidative stress: glutamate cysteine ligase modifier as a susceptibility gene. Am J Hum Genet 79:586–592

Tseng K, O’Donnell P (2007a) D2 dopamine receptors recruit a GABA component for their attenuation of excitatory synaptic transmission in the adult rat prefrontal cortex. Synapse 61:843–850

Tseng KY, Chambers RA, Lipska BK (2009) The neonatal ventral hippocampal lesion as a heuristic neurodevelopmental model of schizophrenia. Behav Brain Res 204:295–305

Tseng KY, Lewis BL, Hashimoto T, Sesack SR, Kloc M, Lewis DA, O'Donnell P (2008) A neonatal ventral hippocampal lesion causes functional deficits in adult prefrontal cortical interneurons. J Neurosci 28:12691–12699

Tseng K-Y, O'Donnell P (2007a) Dopamine modulation of prefrontal cortical interneurons changes during adolescence. Cereb Cortex 17:1235–1240

Tsuang M (2000) Schizophrenia: genes and environment. Biol Psychiatry 47:210–220

Tukker JJ, Fuentealba P, Hartwich K, Somogyi P, Klausberger T (2007) Cell type-specific tuning of hippocampal interneuron firing during gamma oscillations in vivo. J Neurosci 27:8184–8189

Turetsky BI, Bilker WB, Siegel SJ, Kohler CG, Gur RE (2009) Profile of auditory information-processing deficits in schizophrenia. Psychiatry Res 165:27–37

Turetsky BI, Calkins ME, Light G a, Olincy A, Radant AD, Swerdlow NR (2007) Neurophysiological endophenotypes of schizophrenia: the viability of selected candidate measures. Schizophr Bull 33:69–94

Uhlhaas PJ (2011) The Adolescent Brain: Implications for the Understanding, Pathophysiology, and Treatment of Schizophrenia. Schizophr Bull 37:480–483

Uhlhaas PJ, Linden DEJ, Singer W, Haenschel C, Lindner M, Maurer K, Rodriguez E (2006) Dysfunctional long-range coordination of neural activity during Gestalt perception in schizophrenia. J Neurosci 26:8168–8175

Uhlhaas PJ, Roux F, Rodriguez E, Rotarska-Jagiela A, Singer W (2010) Neural synchrony and the development of cortical networks. Trends Cogn Sci 14:72–80

Uhlhaas PJ, Roux F, Singer W, Haenschel C, Sireteanu R, Rodriguez E (2009) The development of neural synchrony reflects late maturation and restructuring of functional networks in humans. Proc Natl Acad Sci USA 106:9866–9871

Uhlhaas PJ, Singer W (2006) Neural synchrony in brain disorders: relevance for cognitive dysfunctions and pathophysiology. Neuron 52:155–168

Uhlhaas PJ, Singer W (2010) Abnormal neural oscillations and synchrony in schizophrenia. Nat Rev Neurosci 11:100–113

Uhlhaas PJ, Singer W (2011) The development of neural synchrony and large-scale cortical networks during adolescence: relevance for the pathophysiology of schizophrenia and neurodevelopmental hypothesis. Schizophr Bull 37:514–523

Umbricht D, Krljes S (2005) Mismatch negativity in schizophrenia: a meta-analysis. Schizophr Res 76:1–23

Umbricht D, Schmid L, Koller R, Vollenweider FX, Hell D, Javitt DC (2000) Ketamine-induced deficits in auditory and visual context-dependent processing in healthy volunteers: implications for models of cognitive deficits in schizophrenia. Arch Gen Psychiatry 57:1139–1147

Umbricht D, Vyssotki D, Latanov a, Nitsch R, Lipp H-P (2005) Deviance-related electrophysiological activity in mice: is there mismatch negativity in mice? Clin Neurophysiol 116:353–363

Van Berckel BN, Oranje B, van Ree JM, Verbaten MN, Kahn RS (1998) The effects of low dose ketamine on sensory gating, neuroendocrine secretion and behavior in healthy human subjects. Psychopharmacology (Berl) 137:271–281

Vohs JL, Chambers RA, Krishnan GP, Donnell BFO, Morzorati SL (2010) GABAergic modulation of 40hz auditory steady-state response in a rat model of schizophrenia. Int J Neuropshychopharmacology 13:487–497.

Vohs JL, Chambers RA, O’Donnell BF, Krishnan GP, Morzorati SL (2012) Auditory steady state responses in a schizophrenia rat model probed by excitatory/inhibitory receptor manipulation. Int J Psychophysiol

Vohs JLJL, Chambers RAA, Krishnan GPGP, O’Donnell BF, Hetrick WPWP, Kaiser STST, Berg S, Morzorati SLSL, O’Donnell BF (2009) Auditory sensory gating in the neonatal ventral hippocampal lesion model of schizophrenia. Neuropsychobiology 60:12–22

Vollenweider FX, Leenders KL, Scharfetter C, Antonini A, Maguire P, Missimer J, Angst J (1997) Metabolic hyperfrontality and psychopathology in the ketamine model of psychosis using positron emission tomography (PET) and [18F]fluorodeoxyglucose (FDG). Eur Neuropsychopharmacol 7:9–24

Von Stein A, Chiang C, König P (2000) Top-down processing mediated by interareal synchronization. Proc Natl Acad Sci USA 97:14748–14753

Wang C, McInnis J, Ross-Sanchez M, Shinnick-Gallagher P, Wiley JL, Johnson KM (2001) Long-term behavioral and neurodegenerative effects of perinatal phencyclidine administration: implications for schizophrenia. Neuroscience 107:535–550

Wang CZ, Johnson KM (2005) Differential effects of acute and subchronic administration on phencyclidine-induced neurodegeneration in the perinatal rat. J Neurosci Res 81:284–292

Wang CZ, Yang SF, Xia Y, Johnson KM (2008) Postnatal phencyclidine administration selectively reduces adult cortical parvalbumin-containing interneurons. Neuropsychopharmacology 33:2442–2455

Wang H-X, Gao W-J (2009) Cell type-specific development of NMDA receptors in the interneurons of rat prefrontal cortex. Neuropsychopharmacology 34:2028–2040

Weinberger DR (1987) Implications of normal brain development for the pathogenesis of schizophrenia. Arch Gen Psychiatry 44:660–669

Weinberger DR, Berman K (1988) Speculation on the meaning of cerebral metabolic hypofrontality in schizophrenia. Schizophr Bull 14:157–168

Wespatat V, Tennigkeit F, Singer W (2004) Phase sensitivity of synaptic modifications in oscillating cells of rat visual cortex. J Neurosci 24:9067–9075

Winterer G, Coppola R, Goldberg TE, Egan MF, Jones DW, Sanchez CE, Weinberger DR (2004) Prefrontal broadband noise, working memory, and genetic risk for schizophrenia. Am J Psychiatry 161:490–500

Woo T-UW, Crowell AL (2005) Targeting synapses and myelin in the prevention of schizophrenia. Schizophr Res 73:193–207

Wu JC, Buchsbaum MS, Bunney WE (1991) Positron emission tomography study of phencyclidine users as a possible drug model of schizophrenia. Yakubutsu Seishin Kodo 11:47–48

Yao JK, Keshavan MS (2011) Antioxidants, redox signaling, and pathophysiology in schizophrenia: an integrative view. Antioxid Redox Signal 15:2011–2035

Yao JK, Leonard S, Reddy RD (2004) Increased nitric oxide radicals in postmortem brain from patients with schizophrenia. Schizophr Bull 30:923–934

Yonezawa Y, Kuroki T, Kawahara T, Tashiro N, Uchimura H (1998) Involvement of gamma-aminobutyric acid neurotransmission in phencyclidine-induced dopamine release in the medial prefrontal cortex. Eur J Pharmacol 341:45–56

Zarate CA, Singh JB, Carlson PJ, Brutsche NE, Ameli R, Luckenbaugh DA, Charney DS, Manji HK (2006) A randomized trial of an N-methyl-D-aspartate antagonist in treatment-resistant major depression. Arch Gen Psychiatry 63:856–864